DIRECT MEASURMENT OF SULPHUR ISOTOPE COMPOSITION IN LICHENS BY CONTINUOUS FLOW-ISOTOPE RATIO MASS SPECTROMETRY (CF-IRMS)

MISUK YUN

DIRECT MEASUREMENT OF SULPHUR ISOTOPE COMPOSITION IN LICHENS BY CONTINUOUS FLOW-ISOTOPE RATIO MASS SPECTROMETRY (CF-IRMS)

by

Misuk Yun

A thesis submitted to the

School of Graduate Studies

in partial fulfilment of the

requirements for the degree of

Master of Science in Environmental Science

Environmental Science Program
Memorial University of Newfoundland

September 2000

St. John's Newfoundland

ABSTRACT

An on-line analytical method has been developed for the routine measurement of S isotopic composition in lichens using continuous flow-isotope ratio mass spectrometry (CF-IRMS). 15 mg (equivalent to about 9 μg S) of chemically-untreated lichen powder (*Alectoria sarmentosa*) together with V_2O_5 was weighed into 40 mg Sn capsules and then combusted directly in an oxidation-reduction reactor (packed with WO_3, pure Cu and quartz wool, heated to 1050°C) of an elemental analyzer, connected to the IRMS via an open-split interface. All combusted gases were carried in a stream of He gas (at 80 mL/min) through a trap (75% $Mg(ClO_4)_2$ + 25% quartz chips) to remove $H_2O_{(g)}$. A 1.2 m Teflon column (Poropak™ QS, heated to 75°C) was used to chromatographically separate SO_2 from CO_2 and N_2. The separated gases were transferred into the IRMS through the interface where excess CO_2 was diluted by the supply of He (set at 25 psi). Using these parameters over 150 samples can be analyzed successively, changing the H_2O trap and cleaning residual ash from the combustion reactor after every 40 samples.

Mean $\delta^{34}S_{CDT}$ values of +6.3 ± 0.4‰ (calibrated using sulphates) and +6.1 ± 0.3‰ (calibrated using sulphides) measured on a homogenized, composite lichen sample collected from the Botanical Garden of Memorial University of Newfoundland, show excellent agreement with those acquired by dual inlet (DI)-IRMS (+6.2 ± 0.2‰), and by on-line CF-IRMS in which samples are chemically pretreated to convert S to $BaSO_4$ (+5.9 ± 0.3‰).

Four different lichen samples with various S concentrations and $\delta^{34}S$ values collected from various locations in Newfoundland also show excellent accuracy and precision compared to DI technique. Lichen samples containing as little as 5-6 μg S (equivalent to about 9 mg lichen powder) produce valid isotopic measurements without a loss of precision. No memory effects were observed over a $\delta^{34}S_{CDT}$ value range of +6 to +16‰. Compared to DI-IRMS and CF-mineral methods, analytical time and reasonable S amount required per CF-lichen analysis are reduced greatly to 15 mins and 9 μg S, respectively.

The developed CF-lichen method was applied to young and old portions of single lichen strands (25-35 cm in length) collected from Come-By-Chance oil refinery area, eastern Newfoundland to investigate variations of S isotopic composition with time. There were systematic variations in S isotope signatures ($\delta^{34}S_{CDT}$) between old (+6.2 to +10.9‰) and young (+5.1 to +8.2‰) portions, suggesting that the old portions may preserve the S isotopic signatures before the refinery operation while those of the young portions show the present S isotopic signatures. This study demonstrates that the micro analytical capability of the developed CF-lichen method can successfully be applied to other studies which require very small amount of organic material with low S concentrations.

ACKNOWLEDGMENTS

I would like to dedicate my thesis to my father, Hungyun Yun, who has been struggling with cancer, and his precious life. I wish to express my love and appreciation to my parents who have been encouraging me all the time. I love you, Mom and Dad!

I would like to express my gratitude to my supervisor, Dr. Moire A. Wadleigh, for her inestimable advice, support, encouragement and generosity. She always showed me her patience and welcomed my endless questions with her big and friendly smile.

I would like to thank Alison Pye and Pam King for their support, advice and assistance in the labs. I am grateful to these undergraduate and graduate students who I have worked with in the labs: Alison Gollop, Lori Ennis, Christine Malloy, Michelle Miskell, Steve Emberley, Jocelyn Tucker and Renée Wiseman. They have all made this experience enjoyable and worthwhile.

The friendship, love and advice of my dearest friends, Nami Choe and the Serushago family, especially during the rough times, have been a source of motivation. I thank Mrs. Yangim Kim for her advice on life. I always love the humble conversation with her with cups of coffee. I also thank all my friends for their friendship and love.

I would like to thank my daughter, Injeong Yang, for her understanding and patience. She was always a big good girl to me. I love you, honey. Finally, I would like to express my immeasurable love and appreciation to my husband, Panseok Yang. Without his love,

unwavering support and encouragement, this thesis would have never been possible. Panseok, you have been there day in and day out always ready with a smile and a big hug.

TABLE OF CONTENTS

CHAPTER 2

SAMPLING AND ANALYTICAL METHODS

CHAPTER 3

DEVELOPMENT OF CF-LICHEN METHOD

CHAPTER 4

RESULTS AND DISCUSSION

CHAPTER 5

VARIATIONS OF S ISOTOPIC COMPOSITIONS IN A LICHEN STRAND

CHAPTER 6

CONCLUSIONS

LIST OF TABLES

LIST OF FIGURES

CHAPTER 1

INTRODUCTION

1.1 SCOPE AND OBJECTIVES

Atmospheric sulphur causes environmental problems such as acidification and climate change, which subsequently harm human and animal health, and lead to ecosystem damage. To better understand these impacts, S concentrations have been monitored in a wide variety of media. Precipitation, aerosols, lakewater, sediments and vegetation have all been used. In addition, sulphur stable isotopes have been used to distinguish anthropogenic from natural inputs by comparing the distinct isotopic signatures of various sulphur sources.

Such measurements are made by isotope ratio mass spectrometry (IRMS) whereby inorganic or organic samples experience chemical pretreatment in order to convert their S to a solid form such as silver sulphide (Ag_2S) or barium sulphate ($BaSO_4$), and then to the gaseous compound such as sulphur dioxide (SO_2) or sulphur hexafluoride (SF_6), suitable for introduction into the instrument. Such sample preparation procedures require relatively large amounts of original sample to obtain sufficient S (e.g. 3-7 mg of S) for analysis (Giesemann et al., 1994). They are also time-consuming (e.g. >18 hrs per analysis for sample preparation and IRMS analysis) and labor-intensive, and in some cases may be both difficult and expensive (Giesemann et al., 1994; Finnigan® MAT, 1997). Finally, they possess the potential for incomplete combustion and isotopic fractionation.

In order to minimize the problems associated with sample preparation, a new inlet system has been created by interfacing an elemental analyzer (EA) to an IRMS. In the on-line continuous-flow isotope ratio mass spectrometry (CF-IRMS), samples with no or reduced pretreatment are directly combusted in an EA, converted to SO_2, and then analyzed by an IRMS. In addition to minimizing the problems identified above, this automated on-line method yields better reproducibility by reducing human errors and increases laboratory productivity (Barrie and Prosser, 1996). For the past several years, significant improvements have been made to CF-IRMS techniques for S isotopic determinations in inorganic materials. S amount required for each analysis has been reduced to about 10 μg S and time for sample preparation and IRMS analysis to about 1 hour (Giesemann et al., 1994).

However, the application of this on-line technique to the direct determination of S isotopic compositions in organic materials has not been as successful, mainly because of extremely low S concentration of most organic materials (e.g. <0.06 wt% S in the lichen analyzed for this study) compared to inorganic materials (e.g. >50 wt% S in pyrite), requiring large amount of samples. Large sample size may lead to incomplete combustion and subsequent isotopic fractionation. In addition, the high C:S ratio of most organisms (e.g. >90% of the total combusted gases of the lichen analyzed for this study is CO_2) requires much higher oxygen demand for complete sulphur oxidation than mineral analysis.

The major objective of this study was to develop an on-line analytical method for the direct measurement of S isotopic composition in lichens, with no chemical pretreatment, using a CF-IRMS. Lichens were chosen for this study because of their widespread use as

an atmospheric S biomonitor. The quality of the developed analytical technique is evaluated by comparison with two existing, independent methods, off-line DI-IRMS and CF-IRMS with minerals. The method is then applied to old and young portions of single lichen strands to investigate the variation of S isotopic composition with time. It is believed that this study will become a cornerstone for the analysis of other organisms with low S concentrations by CF-IRMS.

1.2 SULPHUR

Sulphur is present in nearly all natural environments (Hoefs, 1997). It may be a major component in ore deposits and evaporites. It occurs as a minor component in igneous and metamorphic rocks, throughout the biosphere in organic substances, in marine sediments as both sulphide and sulphate, and in ocean water as sulphate (Ehleringer and Rundel, 1988; Hoefs, 1997).

1.2.1 Atmospheric sulphur cycle

Figure 1-1 illustrates the atmospheric sulphur cycle (Brimblecombe et al., 1989). Various sulphur compounds are emitted into the atmosphere, with a wide range of fluxes. These include hydrogen sulphide (H_2S), dimethyl sulphide (DMS, CH_3SCH_3), carbonyl sulphide (COS), carbon disulphide (CS_2), sulphur dioxide (SO_2) and sulphate (SO_4^{2-}). Table 1-1 summarizes natural and anthropogenic sources of atmospheric sulphur emission.

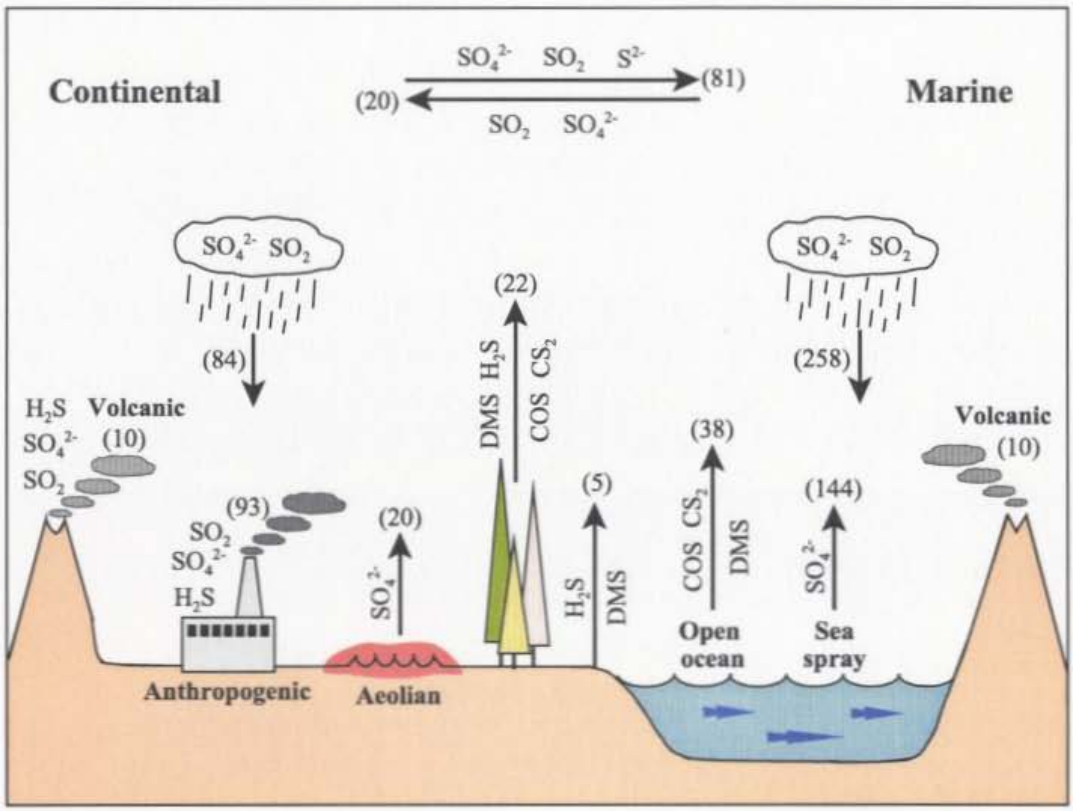

Figure 1-1. Atmospheric sulphur cycle (Jamieson, 1996 modified from Brimblecombe et al., 1989). All fluxes in Tg S/yr.

Table 1-1. Natural and anthropogenic sources of atmospheric sulphur (Ryaboshapko, 1983; Andreae, 1985; Brimblecombe et al., 1989; Charlson, et al., 1992).

Natural
• emission of sea salt sulphur from the ocean
• biogenic emission from coastal regions and the open ocean
• biogenic emission from land
• volcanic emissions of sulphur compounds
• aeolian weathering of sulphates in arid regions
Anthropogenic
• combustion of fossil fuels for the production of energy
• oil refining and treatment of oil products
• smelting of ferrous and non-ferrous ores

1.2.1.1 Sources

1.2.1.1.1 Natural

The direct source of particulate sulphur to the marine atmosphere is from the production of seasalt aerosol at the ocean surface (Andreae, 1985). The aerosol is produced from seawater droplets that form when air bubbles burst at the sea surface. Under very high wind conditions, droplets can also be formed when water is torn away from the crest of a wave (Andreae, 1985). The sulphate flux from the formation of seaspray aerosol is probably between 40 Tg S/yr and 300 Tg S/yr (Andreae, 1985). Brimblecombe et al. (1989) estimated it to be 144 Tg S/yr (Figure 1-1). Most seasalt entering the atmosphere is redeposited to the ocean surface (Andreae, 1985). However, as much as 10% of the total flux is carried over continents and deposited on land (Andreae, 1985).

From coastal regions and the open oceans, gaseous reduced sulphur compounds are emitted by phytoplankton (DMS) and various organic matter decomposition processes (H_2S) (Ryaboshapko, 1983). The most active reduction of sulphate occurs in periodically flooded and shallow parts of sea basins, especially in parts with considerable organic matter (Ryaboshapko, 1983). Areas of high primary productivity are important for DMS emissions. Estimates of the ocean and continental biogenic sulphur flux into the atmosphere vary from 34 Tg S/yr (Granat et al., 1976) to 267 Tg S/yr (Eriksson, 1963).

Formation of biogenic volatile sulphur compounds, mainly H_2S along with COS, CS and DMS, occurs in continental areas under the anaerobic conditions found in marshes and microorganisms play a leading role in this process (Ryaboshapko, 1983). Emissions are

likely to vary, therefore, with the temperature and moisture status of the environment and with the availability of nutrients (Ryaboshapko, 1983). Also, the direct estimation of the biogenic flux from land is rather difficult since its value may vary in space and time (Ryaboshapko, 1983). Considering the uncertainty of the estimate of reduced sulphur with short residence time in this reservoir, the flux may be within the range 3.5-30 Tg S/yr (Ryaboshapko, 1983).

Volcanoes and geothermal areas emit a number of sulphur gases as well as other sulphur species, including H_2S, COS and sulphate aerosol, during both eruptive and non-eruptive phases (Andreae, 1985). Based on the results of field measurements from volcanoes throughout the world by Berresheim and Jaeschke (1983), SO_2 emissions during non-eruptive phases (8 Tg S/yr) are considerably larger than those during eruptive periods (1 Tg S/yr).

Estimates of dust emissions from arid regions (about 10% of the earth's land) vary between 200 Tg/yr and 3,000 Tg/yr (Ryaboshapko, 1983). Depending on the assumed values for both the total dust mobilization and the sulphur content of the dust, source estimates proposed are between 3 Tg and 30 Tg S/yr (Ryaboshapko, 1983). Substantial amounts of this dust can be transported over more than 1,000 km and can be of great importance to regional sulphur cycling (Ryaboshapko, 1983).

1.2.1.1.2 Anthropogenic

The anthropogenic flux of sulphur to the atmosphere results from the utilization in

industry of sulphur compounds themselves and from the utilization of other materials that contain sulphur as an unwanted or unavoidable by-product (Table 1-1). Emissions of anthropogenic sulphur to the atmosphere are almost entirely in the form of sulphur dioxide. Combustion of fossil fuels accounts for 80 to 85% of the total, with the remainder coming from the smelting of ores and other industrial processes and burning (Whelpdale, 1992). The total flux of anthropogenic sulphur to the atmosphere is estimated to be 80 Tg S/yr by Ivanov (1983) and 93 Tg S/yr by Brimblecombe et al. (1989).

In coal, sulphur exits as organic compounds, pyrites and sulphate (Ryaboshapko, 1983). During the combustion processes, organic sulphur and pyrite are oxidized to SO_2 and partially SO_3 which, together with flue gases, are released to the atmosphere (Ryaboshapko, 1983). On combustion, 95% of the sulphur in fuel is released to the atmosphere (Kellogg et al., 1972).

In natural oils, sulphur exists as hydrogen sulphide and organic compounds (Ryaboshapko, 1983). Typically, the content of sulphur in oil is about 2% (Brimblecombe et al., 1989). The bulk of this sulphur (80%) remains in oil products. About 8% of the sulphur is released from the refinery into the atmosphere as the dioxide. The remaining 12% is partly utilized for other products.

In ores of non-ferrous metals, sulphur exits in the sulphide form (pyrites). The sulphur concentration in some pyrites reaches 45% (dry weight) (Ryaboshapko, 1983). Sulphur from sulphide ore is emitted as sulphate directly formed in high-temperature processes or as sulphur dioxide which can be oxidized further to sulphate during its

atmospheric residence (Thode, 1991). During smelting of copper, zinc, lead and nickel, sulphide sulphur is oxidized to SO_2, which is emitted into the atmosphere, unless otherwise used (Ryaboshapko, 1983).

1.2.1.2 Transformations

Most reduced sulphur compounds emitted to the atmosphere are quickly (<1 day) oxidized to SO_2 and eventually most of this is oxidized to SO_4, by gas-phase (homogeneous) or aqueous-phase (heterogeneous) processes (Newman et al., 1991). For gas-phase processes, H_2S, for example, is oxidized by the reaction with free radical (OH) (Newman et al., 1991):

$$OH + H_2S \text{ -----> } HS + H_2O \qquad (1.1)$$

$$HS + 2O_2 \text{ -----> } HSO_4 \qquad (1.2)$$

$$HSO_4 \text{ -----> } OH + SO_3 \qquad (1.3)$$

$$SO_3 + H_2O \text{ -----> } H_2SO_4 \qquad (1.4)$$

Since most of the anthropogenic emissions are in the form of SO_2, and since biogenic sulphides are oxidized to SO_2, the chemistry of SO_2 in the atmosphere is of major importance (Newman et al., 1991). The summary of homogeneous and heterogeneous oxidation processes of SO_2 can be written as follows (Newman et al., 1991):

Homogeneous oxidation:

$$SO_{2(g)} + OH \text{ -----> } HOSO_2 \qquad (1.5)$$

$$HOSO_2 + O_2 \text{ -----> } SO_{3(g)} + HO_2 \qquad (1.6)$$

$$SO_{3(g)} + H_2O \text{ -----> } H_2SO_{4(l)} \qquad (1.7)$$

Heterogeneous oxidation

$$SO_{2(g)} + H_2O_{(l,\,g)} \text{ -----> } SO_2{\cdot}H_2O \qquad (1.8)$$

$$SO_2{\cdot}H_2O \text{ ------> } HSO_3^-{}_{(aq)} + H^+ \qquad (1.9)$$

$$HSO_3^-{}_{(aq)} \text{ -----> } HSO_4^-{}_{(aq)} \qquad (1.10)$$

1.2.1.3 Deposition

Chemical constituents in the atmosphere can be brought to the surface by a variety of processes. The deposition processes which do not involve precipitation are collectively termed dry deposition (Figure 1-2a) (Whelpdale, 1992). Particles larger than about 10 μm in diameter may be removed by gravitational sedimentation (Whelpdale, 1992). However, smaller particles and gases are more efficiently brought to the near-surface region by turbulent atmospheric motions, where they may be subsequently be brought into contact with surface elements by molecular-scale processes (Whelpdale, 1992). Actual uptake is accomplished by chemical reaction, dissolution and adsorption (Whelpdale, 1992). Sulphur dioxide is dry deposited more efficiently than particulate sulphate because it is more readily taken up at the surface (Whelpdale, 1992).

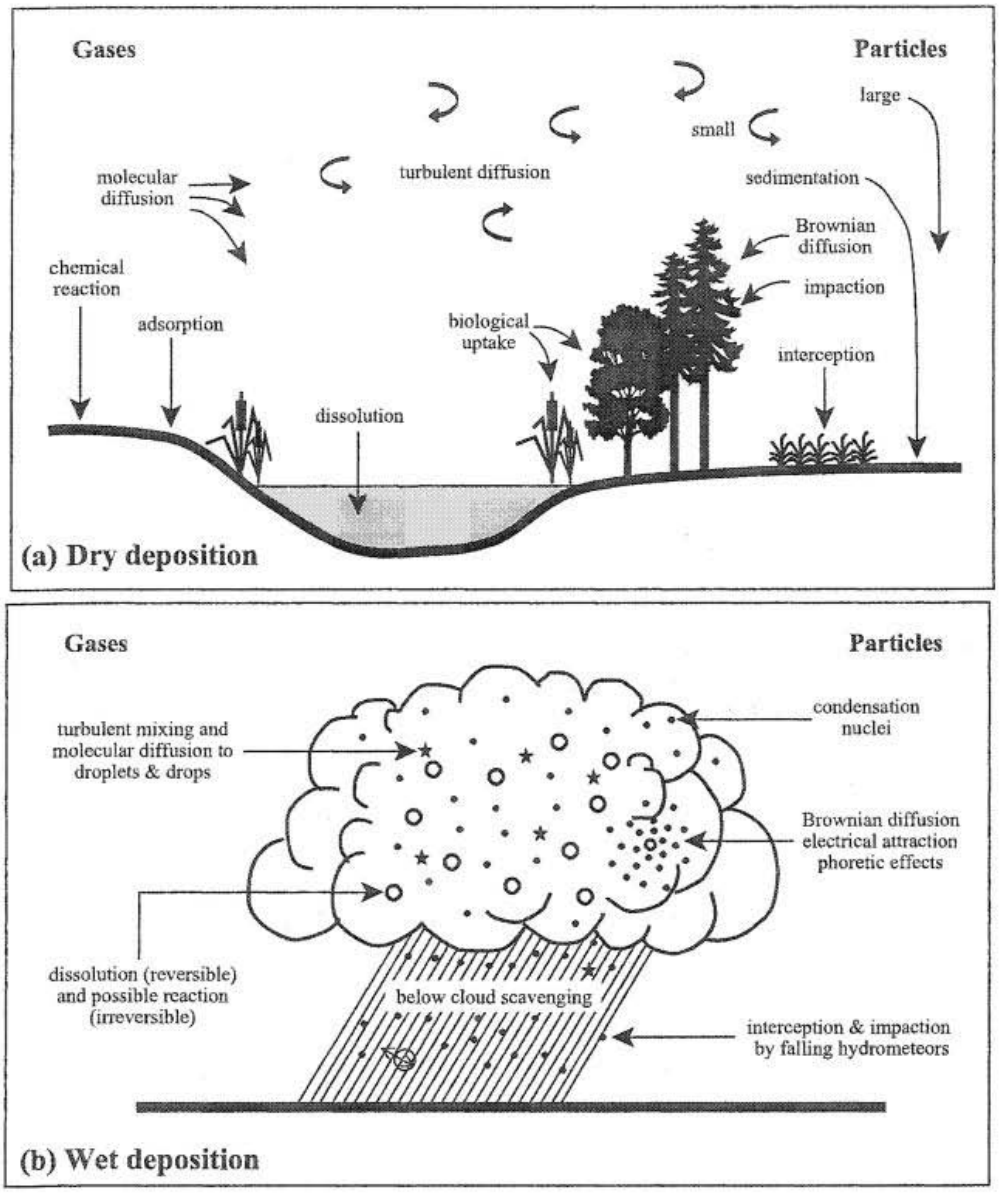

Figure 1-2. Schematic representation of the deposition processes: (a) dry deposition and (b) wet deposition (Whelpdale, 1992).

Those processes for which precipitation is the delivery mechanism are termed wet deposition (Figure 1-2b). Gases, such as sulphur dioxide, can dissolve in cloud and rain drops or adsorb on to frozen precipitation elements (Whelpdale, 1992). Sulphate particles are efficient condensation nuclei and are incorporated into precipitation by nucleation or as a result of scavenging by cloud droplets and falling drops (Whelpdale, 1992).

Finally, the third deposition process includes mass transfer to the surface by impaction of fog or cloud droplets, and by riming. In high-elevation forested ecosystems or in areas with frequent fog, they can be very efficient (Whelpdale, 1992). This is not usually included as wet or dry deposition.

1.2.2 Sulphur stable isotopes

Sulphur has four stable isotopes, ^{32}S, ^{33}S, ^{34}S and ^{36}S, occurring with natural abundances of 95.02, 0.75, 4.21 and 0.02%, respectively (Krouse, 1980; Mitchell et al., 1998). ^{32}S and ^{34}S are the ones most frequently used in stable isotope studies because of their higher abundances and the extensive use of SO_2 gas for mass spectrometric determinations (Krouse, 1980; Trust and Fry, 1992). In general, isotopic compositions are reported using relative units (per mille (‰), on the delta (δ) scale). Natural abundance measurements are always made relative to a known standard reference material because absolute measurements are technically more difficult to achieve on a routine basis (McKinney et al., 1950). $\delta^{34}S$ is defined as:

$$\delta^{34}S\ (‰) = [\frac{(^{34}S/^{32}S)_{sample}}{(^{34}S/^{32}S)_{standard}} - 1] \times 10^{3} \qquad (1.11)$$

where $^{34}S/^{32}S$ is the ratio of the number of ^{34}S atoms to the number of ^{32}S atoms in the sample or the standard (Krouse, 1988; Thode, 1991; Mitchell et al., 1998). In addition, δ-notation represents a convenient means for expressing the small differences in isotope ratios measured at natural abundance without the redundancy of carrying multiple preceding zeros. The standard for sulphur used internationally is Cañon Diablo troilite (CDT, $^{34}S/^{32}S = 449.94 \times 10^{-4}$), which is an iron sulphide (FeS) from the Cañon Diablo meteorite (Krouse, 1988; Trust and Fry, 1992; Mitchell et al., 1998).

1.2.2.1 Fractionation mechanisms

Certain natural processes lead to isotopic fractionation which alters the ratio of $^{34}S/^{32}S$ in various compounds. Isotopic fractionation occurs because of the mass differences between isotopes. Heavier isotopes have lower zero-point energies which means that they tend to be bonded more strongly, and thus react less readily, than lighter isotopes (Hoefs, 1997). Fractionation is represented by the symbol alpha (α) which can be written as:

$$\alpha_{A-B} = \frac{R_A}{R_B} \qquad (1.12)$$

where R_A and R_B are the ratios of isotopes (e.g. $^{34}S/^{32}S$) in substances A and B, respectively.

Two main phenomena produce isotope fractionation: (i) equilibrium isotope effect and (ii) kinetic isotope effect (Thode, 1991; Hoefs, 1997). Equilibrium isotope effects involve the exchange of isotopes between substances, phases or molecules in a system at chemical equilibrium (Hoefs, 1997). Isotope exchange between hydrogen sulphide (H_2S) and SO_2 is an example (Thode, 1991). The overall exchange reaction is:

$$H_2{}^{34}S + {}^{32}SO_2 \text{ <----------> } H_2{}^{32}S + {}^{34}SO_2 \qquad (1.13)$$

The equilibrium constant K may be expressed as below:

$$K = \frac{[{}^{34}SO_2]/[{}^{32}SO_2]}{[H_2{}^{34}S]/H_2{}^{32}S]} \qquad (1.14)$$

This expression shows that when K is not unity the ratio $^{34}S/^{32}S$ will not be the same in the two equilibrium phases (Thode, 1991). Therefore, the extent to which K differs from unity is a measure of the equilibrium isotope effect (Thode, 1991). For the H_2S and SO_2 system above, the equilibrium constant K is 1.0064 at 800 K. Therefore, at 800 K under equilibrium conditions, SO_2 will be 6.4‰ enriched in ^{34}S compared to H_2S (Thode, 1991).

Kinetic isotope effects occur during incomplete and unidirectional reactions such as evaporation, dissociation reactions, biologically mediated reactions and diffusion (Hoefs, 1997). Since lighter isotopes react more quickly, these reactions tend to give products

depleted in the heavier isotopes (Hoefs, 1997). Fractionation factors for kinetic reactions can be calculated from reaction rate constants (k). As an example, the reduction of SO_4 to H_2S can be represented by two reactions:

$$^{32}SO_4 \text{ <----------> } H_2{}^{32}S \qquad k_{32} \qquad (1.15)$$

$$^{34}SO_4 \text{ <----------> } H_2{}^{34}S \qquad k_{34} \qquad (1.16)$$

The ratio of rate constants k_{32}/k_{34} for the above reactions is ~1.022 at room temperature (Thode, 1991). Since the $^{32}SO_4^{2-}$ species reacts 1.022 times faster than the $^{34}SO_4^{2-}$, the H_2S produced at any instant is depleted in ^{34}S by about 22‰ relative to the remaining SO_4^{2-} (Thode, 1991).

1.2.2.2 Usefulness of sulphur stable isotopes in atmospheric studies

The combination of equilibrium and kinetic effects results in distinct isotopic signatures for various sulphur sources. Figure 1-3 illustrates the variations of sulphur isotopic signatures for different natural as well as anthropogenic sources of atmospheric sulphur compounds (Newman et al., 1991). This makes the stable isotope technique a powerful tool to identify sources of anthropogenic sulphur and trace its pathway in the atmospheric environment.

In particular, isotope techniques work best if the isotopic value of anthropogenic sulphur is quite different from that of natural background or other sources. Such is the case

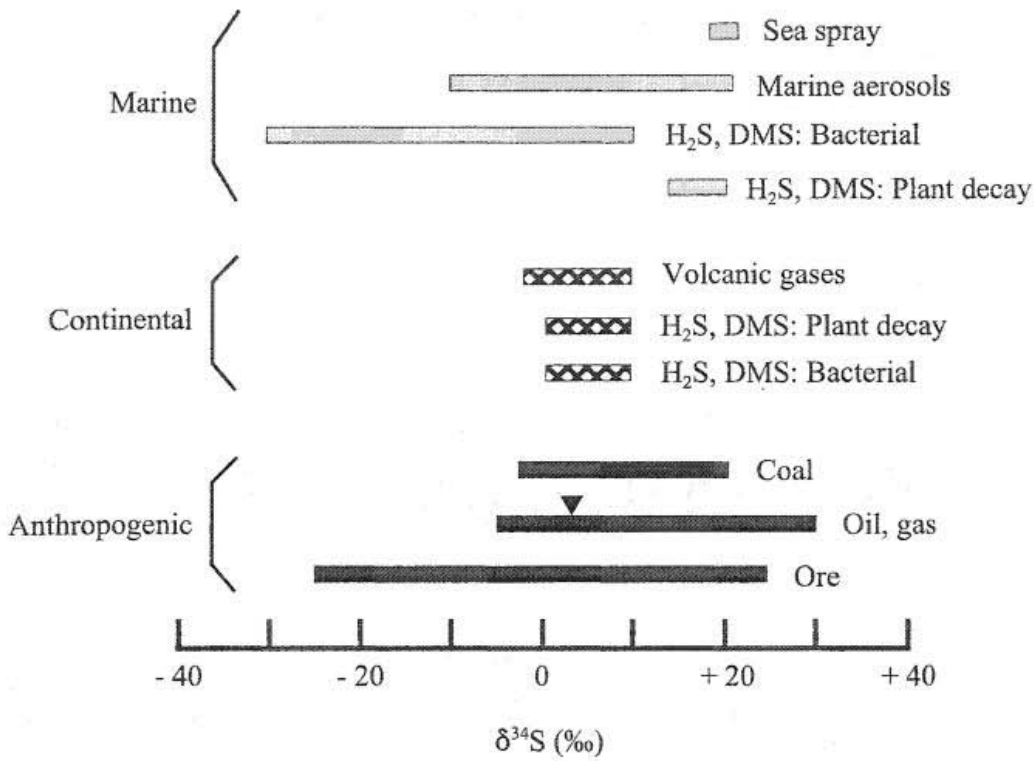

Figure 1-3. Variation of $\delta^{34}S$ values for different sources of atmospheric sulphur compounds (modified from Newman et al., 1991). ▾ is average $\delta^{34}S$ of oil and gas from northeastern America.

for emissions from sour gas processing in Alberta, Canada, where the isotopic differences ($\delta^{34}S$ values) between emitters and natural background range from +20 to +50‰ (Krouse, 1991). A number of studies have been reported in which isotopes have been successfully employed to determine source contributions and to elucidate atmospheric processes (Jensen and Nakai, 1961; Cortecci and Longinelli, 1970; Dequasi and Grey, 1970; Holt et al., 1972; Grey and Jensen, 1972; Castleman et al., 1974; Ludwig, 1976; Krouse, 1977; Nriagu, et al., 1991; Wadleigh et al., 1994; Jamieson, 1996; Wadleigh et al., 1996).

1.3 LICHENS

1.3.1 Biological background on lichens

1.3.1.1 Lichens and their nutrients

Lichens are symbiotic organisms composed of a fungal component (mycobiont) and an algal component (photobiont) (Ahmadjian, 1967; Hale, 1974; Hawksworth and Rose, 1976; Richardson, 1992). In the relationship, the algal component usually suffers no appreciable harm, and actually receives some benefits; it is shielded from excessive sunlight, desiccation and mechanical injury, and receives inorganic substances from its fungal component. In return, the fungus receives nutrients from the photosynthetic algae (Hawksworth and Rose, 1976; Richardson, 1992).

Lichens take nutrients from the environment in which they live: (1) they have active uptake systems for anions like nitrates and sulphates within the cell, (2) they adsorb metal ions such as Ca^{2+} through an ion exchange mechanism and (3) they can trap tiny particles

within their structure (Richardson, 1992). Some of the metabolites produced by lichens can break down such particles, releasing nutrients which may then be taken into the cells of lichens (Richardson, 1992).

The fact that lichens do not possess roots, the efficient nutrient absorption system for higher plants, has led to major dependence on atmospheric sources of nutrients (Nieboer et al., 1978; Nash III, 1996), although some lichens take nutrients from soil and rock substrates (Nash III, 1996). The processes of nutrient uptake from the atmosphere include wet deposition such rainfall, snow, fog and dew and dry deposition such as sedimentation of large aerosols (greater than 2-10 μm in diameter), impaction of smaller aerosols and gaseous uptake (Nash III, 1996). These nutrient supplies are very dependent on water because the nutrients are dissolved in water and adsorbed over the surface of the lichen thallus (Blum, 1973; Hawksworth and Rose, 1976; Richardson, 1992).

1.3.1.2 Groups and structure

Lichens can be divided, according to their thallus growth forms into three groups, crustose, foliose and fruticose (Figure 1-4) (Ahmadjian, 1967; Hale, 1974; Hawksworth and Rose, 1976; Richardson and Nieboer, 1981; Richardson, 1992). The crustose lichens (Figure 1-4a) are closely attached or embedded in their substrates, and the foliose ones (Figure 1-4b) are usually flat, circular or lobed and grow loosely, or only centrally, attached to their substrates. The fruticose lichens (Figure 1-4c) are hair-like, shrubby or finger-like. *Alectoria sarmentosa,* the species used for this study, is a common fruticose lichen.

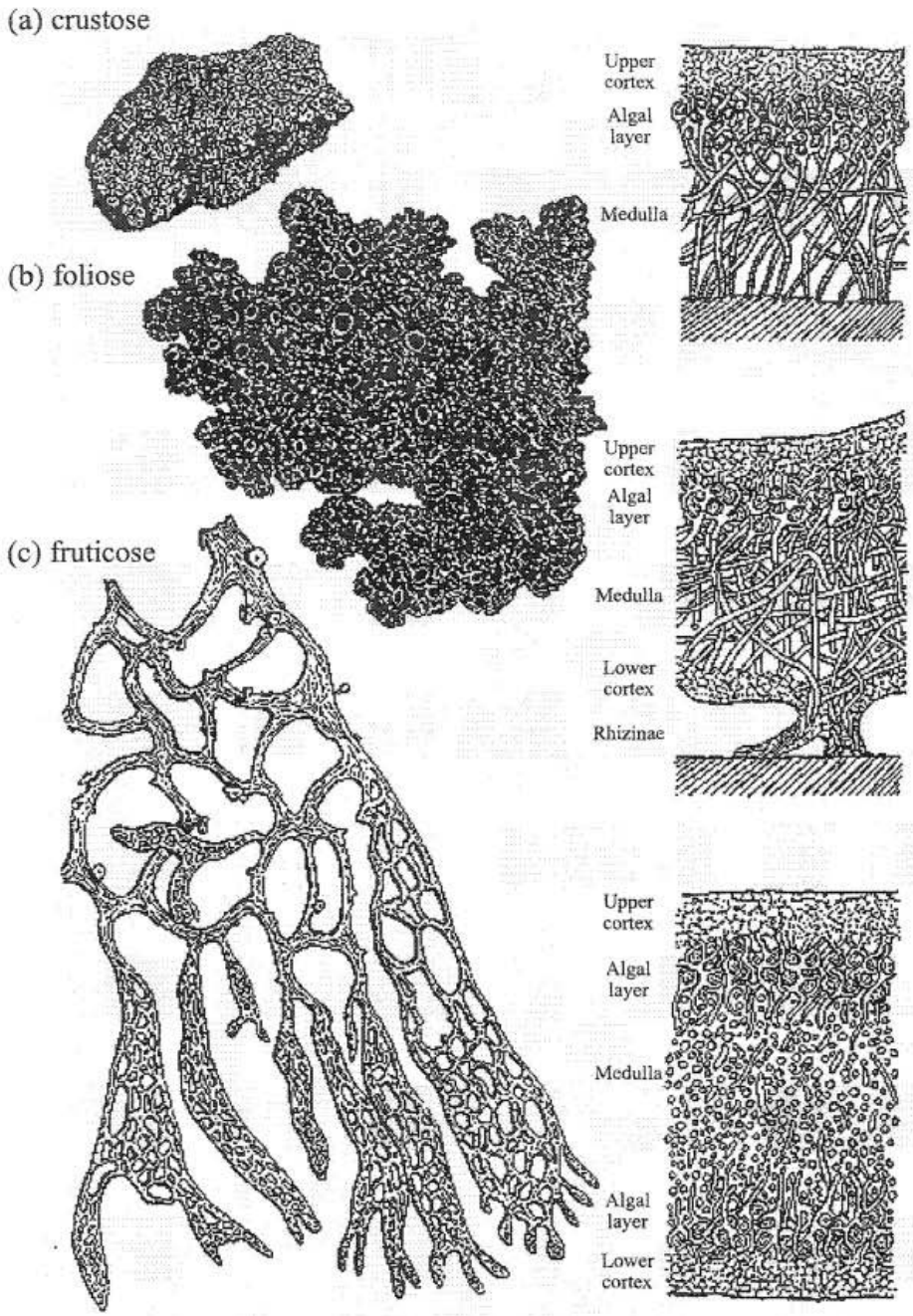

Figure 1-4. Three groups of lichens and their structures: (a) crustose, (b) foliose and (c) fruticose lichens (Ahmadjian, 1967).

Fruticose lichens may be round or flattened, unbranched or richly branched and can range from 1 mm to 5 m in length. The internal structure is radial with a dense outer cortex, a medulla and a thin algal layer (Figure 1-4). The cortex serves as a protective covering over the thallus. It is composed of more or less compressed, heavily gelatinized hyphae (fungal threads), firmly cemented together. The medulla consists of loosely interwoven fungal strands. The medulla may be as much as 500 μm thick. The medulla has a greater water-holding capacity than any of the other tissues and is a region of nutrients. Within the algal layer, positioned between the cortex and the medulla, lichen algae are completely surrounded by fungal tissues. The algal layer is about 7% of the total thallus volume and its thickness varies in different lichen genera. The structure of the lichen thallus shows considerable variation in different genera (Ahmadjian, 1967; Hale, 1974; Hawksworth and Rose, 1976; Richardson and Nieboer, 1981).

1.3.2 Importance of lichens as biomonitors of air pollution

Since the last 19th century, lichens have been used as biomonitors of atmospheric pollution (Richardson, 1992). Several properties of lichens make them useful biomonitors of atmospheric pollution (Ahmadjian, 1967; Hale, 1974; Hawksworth and Rose, 1976; Richardson and Nieboer, 1981; Richardson, 1992; Gries, 1996). Firstly, lichens are abundant and have a wide range of habitats. They can be found from extreme low tide level on the sea shore to the tops of high mountains and from arctic to tropical regions. Secondly, lichens take and accumulate materials mainly from the atmosphere. The accumulation may result

by active uptake of ions from precipitation, passive adsorption of ions by ion exchange, or direct incorporation of particulate materials into lichen tissues. Thirdly, lichens cannot regulate the amount of uptake from the atmosphere because they do not possess specialized protective structures such as a cuticle or stomates, which are found in higher plants. Fourthly, lichens are slow growing and long-lived so they can be used in long term monitoring. Growth rates vary from year to year and between habitats and may vary with age of lichen. In general, the fruticose species are the fastest growing at between 1.6 mm to 10 mm annually, followed by the foliose (0.01 mm/year to 4 mm/year) and crustose (0.25 mm/year to 1 mm/year) lichens. The longevity of lichens may be tens or hundreds of years or more. In most cases the life of a lichen is determined by the longevity of its substrate.

1.3.3 Atmospheric sulphur biomonitoring with lichens

Sulphur is an essential nutrient for lichens. However, the uncontrolled accumulation of sulphur can disrupt the metabolic processes in lichens such as photosynthesis and respiration. Also, the growth rate can be reduced, the size of lichen thallus decreased and the color of thallus changed (Hawksworth and Rose, 1976).

Lichens are especially sensitive to sulphur dioxide (SO_2), a major component of urban and industrial air pollution (Hawksworth and Rose, 1976; Richardson, 1992). Sulphur dioxide (1) may be adsorbed on a thallus and then absorbed when the thallus is wetted by dew or rain, (2) may be absorbed by surface moisture and then taken up by the lichens, or

(3) may be dissolved in rainwater as sulphuric acid prior to deposition on the lichen (Hawksworth and Rose, 1976; Richardson, 1992; Ahmadjian, 1993). Several factors can be correlated with the sensitivity of lichens to sulphur dioxide; (1) the concentration of sulphur dioxide in the atmosphere, (2) exposure time to sulphur dioxide, (3) wind speed, (4) water content, (5) morphology, (6) physiology and (7) structure of the lichen species (Richardson and Nieboer, 1981; Ahmadjian, 1993).

1.3.3.1 Fractionation of sulphur stable isotopes during lichen metabolism

Various sulphur compounds in the atmosphere may be deposited on vegetation, including lichens. Most of these compounds are oxidized when they encounter water on the thallus and form sulphate, which then enters the cells where it is reduced to sulphide and incorporated into useful organic compounds (Taiz and Zeiger, 1991; Trust and Fry, 1992). This biochemical process, called assimilatory sulphate reduction, is summarized in Figure 1-5 (Taiz and Zeiger, 1991; Trust and Fry, 1992).

Sulphate from the external environment begins activation reactions with adenosine triphosphate (ATP). The activated sulphate is transferred to a carrier (CarSH) and reduced to sulphite, followed by a further reduction to sulphide (Figure 1-5). The reduction of sulphite may involve either free sulphite, to form free sulphide, or carrier-bound sulphite, which is reduced to carrier-bound sulphide.

With respect to isotopic fractionation of sulphur, very small isotope fractionations are expected during the steps of the uptake of sulphate by the cell, the activation involving

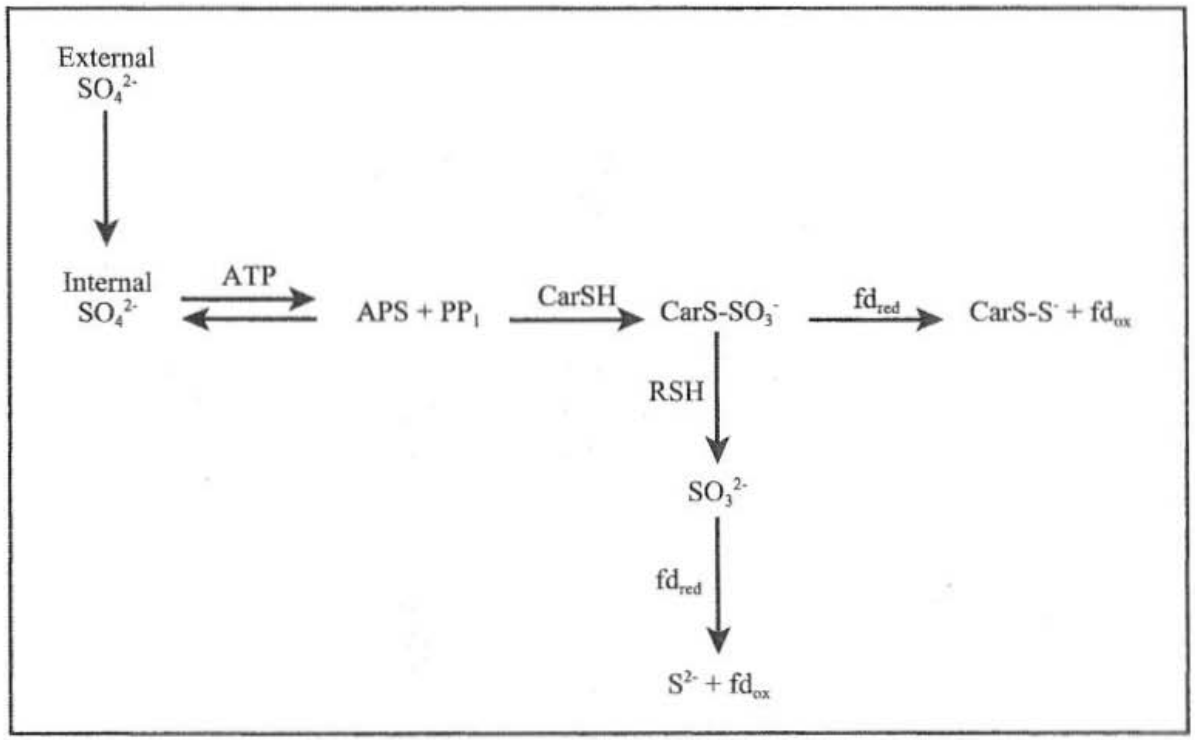

Figure 1-5. Reaction sequence of the assimilatory pathway of sulphate reduction by higher plants. APS = adenosine-5'-phosphosulphate; ATP = adenosine triphosphate; CarSH = unidentified carrier molecule; CarS-S^- = carrier-bound sulphide; CarS- SO_3^- = carrier-bound sulphite; fd_{red} = reduced ferredoxin; fd_{ox} = oxidized ferredoxin; PP_i = inorganic pyrophophate; RSH = a thiol molecule (Trust and Fry, 1992).

ATP and the transferring of sulphate to a carrier (Trust and Fry, 1992). However, there is the potential to produce large fractionations due to the actual reduction steps in which sulphur-oxygen bonds are broken (Rees, 1973; Winner et al., 1981). Since the overall fractionations that are observed during the assimilatory reduction of sulphate are small, the rate of sulphate reduction in plants must be controlled either by the uptake or activation of sulphate (Trust and Fry, 1992). Otherwise, if the reaction was limited by one of the reduction steps, larger fractionations during the assimilatory reduction of sulphate by plants would be observed (Trust and Fry, 1992). Many studies have reported that large fractionations do not occur during sulphur metabolism by vegetation, including lichens.

The study of Krouse et al. (1984) is an example. The objective of this study was to investigate how sulphur-gas emissions from the Amoco Canada Petroleum Company Limited West Whitecourt Sulphur Recovery Gas Plant affected the boreal forest ecosystem including air, water, soil and vegetation (Krouse et al., 1984). A large difference in isotopic composition was observed between sulphur gas emissions (~ +22‰) and the pre-industrial soil at a depth of 60 cm (0‰), representing the natural environmental background (Krouse et al., 1984). Interestingly the vegetation (jack pine needles and moss) showed slightly lower isotopic values than the sulphur gas emissions, demonstrating the vegetation was receiving sulphur from the atmosphere as well as inputs from the root system. Figure 1-6 is an illustration of portions of the moss, *Polytrichum juniperinum*, showing the difference of sulphur isotopic values in each portion. The upper portion of the moss has $\delta^{34}S$ values near +20‰, showing the direct influence of sulphur gas emissions, and the humus surrounding

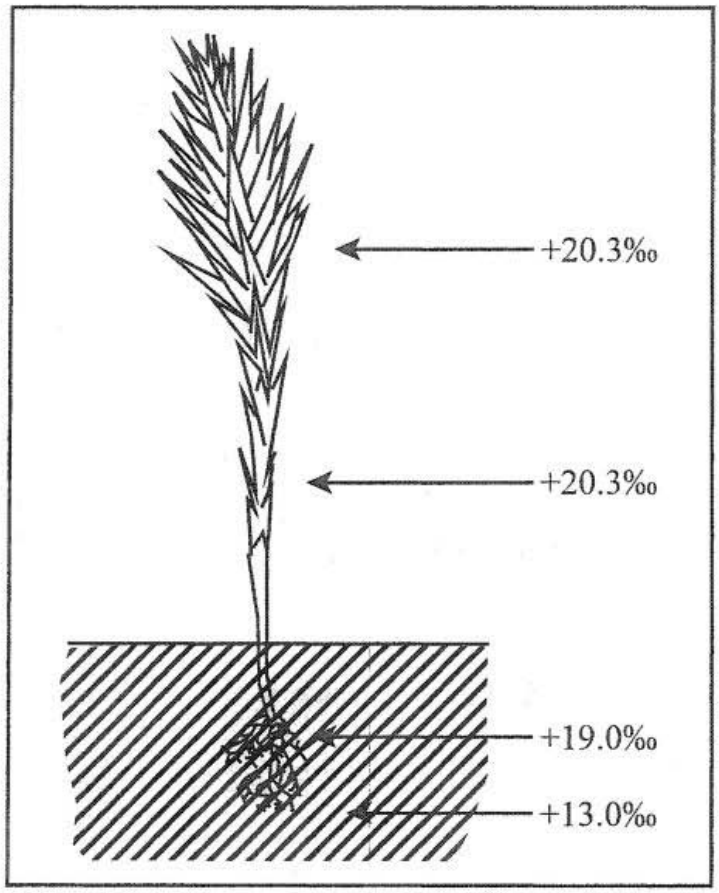

Figure 1-6. $\delta^{34}S$ values for different portions of a moss, *Polytrichum juniperinum* (Krouse et al., 1984).

the rhizoids was at about +13‰. The rhizoids, +19‰, were intermediate between the two. This study shows that the isotopic value of each portion of the plant represents that of the surrounding environment and that sulphur stable isotope fractionation is very limited during the assimilation and reduction of sulphate in vegetation.

In 1977, Krouse applied sulphur stable isotopes to *Usnea sp.*, a fruticose lichen species in Alberta, Canada. The sulphur isotope composition of the lichen species coincided closely with the average isotopic composition of the air around the region (Figure 1-7) (Krouse, 1977). However, the sulphur isotope composition of the pine needles, *Pinus contorta*, from the region were approximately 10‰ lighter compared with those of air and lichens (Figure 1-7) (Krouse, 1977). This result indicates that the lichens absorb a much higher proportion of their sulphur content from the air or rain than do coniferous trees, for which soil is the primary source for sulphur. Thus, intermediate isotopic values were obtained for the pine needles.

A similar result was found in the study of Case and Krouse (1980). They investigated variations in sulphur isotopic composition and content of vegetation near a SO_2 source at Fox Creek, Alberta, Canada. Lichen species, *Usnea scabrata*, derived most of their sulphur from the air while pine needles derived sulphur from both air and soil. Also, in this study, it was found that the $^{34}S/^{32}S$ ratio in the lichen species decreased with increasing distance from the emitter, while pine needles did not show this trend.

A series of studies in Newfoundland, Canada, has shown that the lichen species, *Alectoria sarmentosa,* influenced by sulphur from anthropogenic and sea spray sources

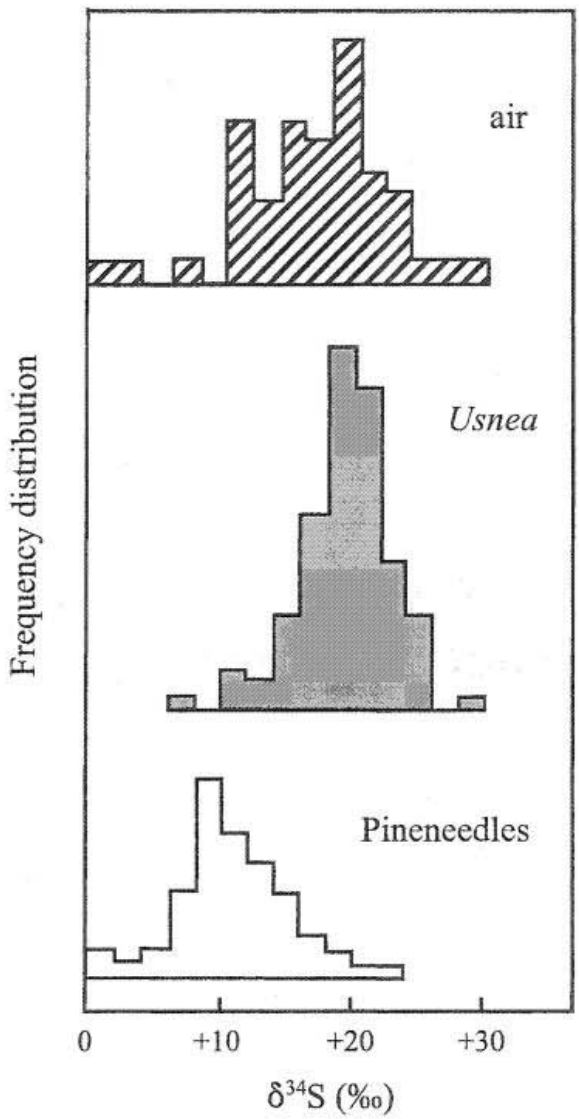

Figure 1-7. $\delta^{34}S$ values for atmospheric SO_2, lichen and pineneedles, Ram River Area, Alberta (Krouse, 1977).

showed lower and higher sulphur isotopic compositions, respectively (Evans, 1996; Blake, 1998; Gollop, 1998; Nowotczynski, 1998; Wadleigh and Blake, 1999). For example, the lichens sampled around the Come-By-Chance oil refinery portrayed very low (~ +4‰) sulphur isotopic data, indicating that this area is polluted by anthropogenic sulphur. On the other hand, the lichen samples collected from along the coastline displayed very high (~+18‰) sulphur isotopic data, leading to the conclusion that the sulphur in the atmosphere along the coastline is mainly from a natural source, sea salt.

1.4 ISOTOPE RATIO MASS SPECTROMETRY

IRMS consists of four essential components: (1) ion source, (2) mass analyzer, (3) detector and (4) inlet system (Figure 1-8). IRMS ionizes gaseous molecules and separates the ions into a spectrum according to their mass-to-charge ratio using electric and magnetic fields. The relative abundances of molecules of different mass-to-charge ratio are then found by measuring the currents generated by these separated ion beams (Figure 1-8). Detailed reviews of IRMS are provided by White and Wood (1986), Potts (1987), Barrie and Prosser (1996), Brenna et al. (1997), Hoefs (1997), and Kendall and Caldwell (1998).

A good vacuum system ($< 10^{-8}$ mbar) is required for IRMS for two reasons; first, the trajectory of ions will be modified resulting peak broadening if the ions collide with any residual gas molecules and second, residual gases in the ionizing chamber are also ionized together with the sample material giving rise to an instrument background.

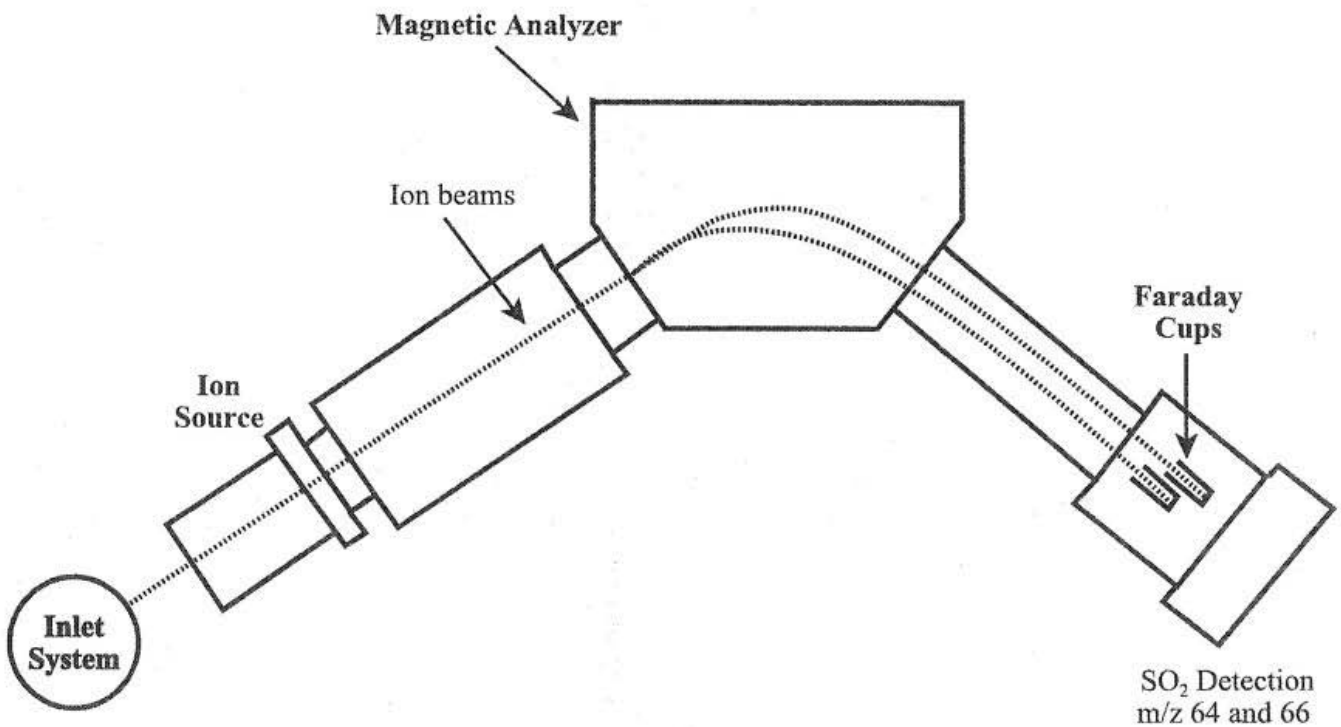

Figure 1-8. Simplified diagram of IRMS principles (modified from Caimi, 1995).

1.4.1 Inlet systems

The dual inlet is the most conventional inlet system of IRMS. It alternatively admits sample and reference gases into the mass spectrometer, perhaps six to ten times each over 10 mins, to give the effect of simultaneous measurement of the isotope ratio under identical conditions (Figure 1-9) (Barrie and Prosser, 1996; Kendall and Caldwell, 1998). Since the original design of Nier-McKinney in 1950, significant improvements have been made on dual inlet systems with respect to electronics, vacuum technology and computer control, resulting in the automation of the system control and of data processing, and in more stable electronics.

However, as mentioned earlier in Section 1.1, for solid and liquid samples, this inlet system requires lengthy, multiple-step, labor-intensive, difficult and expensive, off-line chemical pretreatments before isotopic determination. On-line sample preparation, which will be discussed in the next section, allows rapid analysis, and is easy-to-use.

1.4.1.1 Continuous-flow inlet system and interface

In CF-IRMS, sample chemistry and gas purification take place in an atmosphere of He and pulses of sample-derived gases (i.e., N_2, CO_2, N_2O or SO_2) flow directly into the ion source (Barrie and Prosser, 1996). There are two branches of CF-IRMS. In EA-IRMS, a sample is combusted and the reaction products separated by gas chromatograph (GC) with pulses of pure sample gases directed to the IRMS (Barrie and Prosser, 1996; Kendall and Caldwell, 1998). In GC-IRMS, the compounds of interest in the mixture are first separated

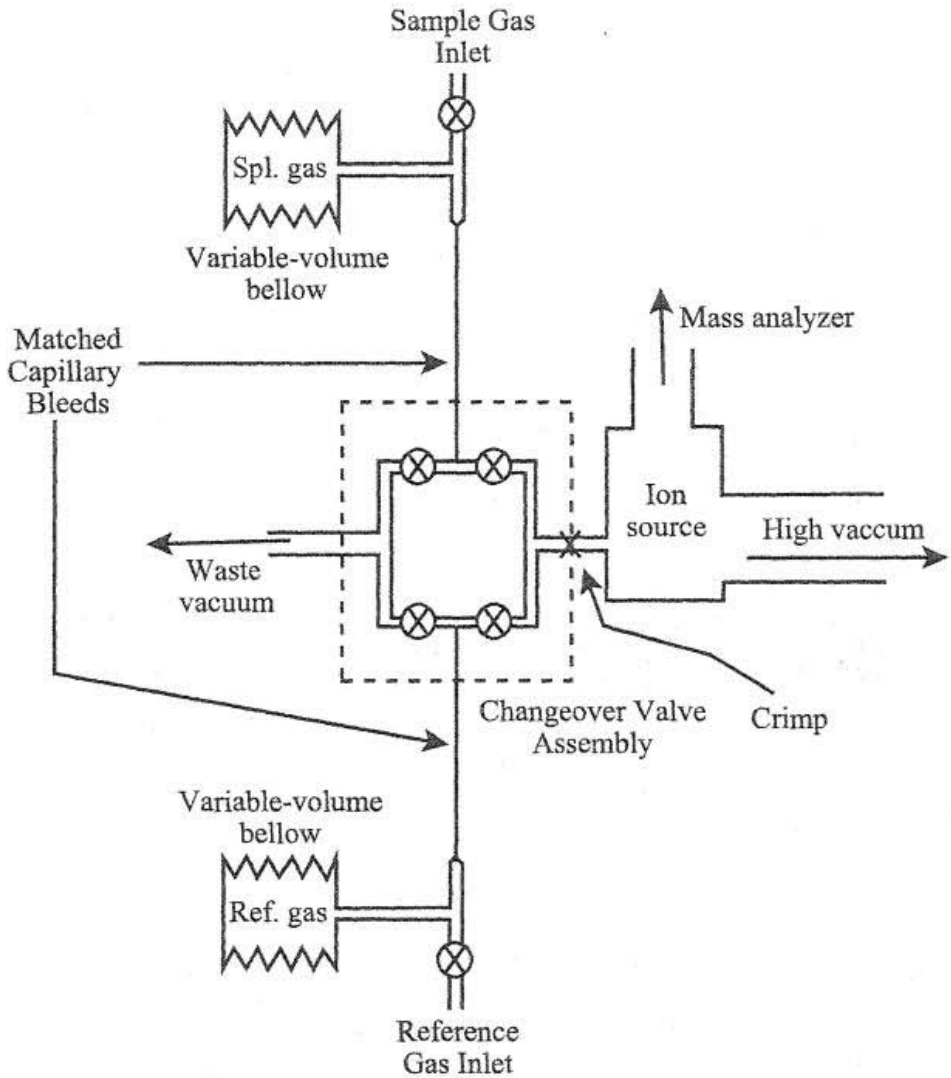

Figure 1-9. Schematic diagram of DI-IRMS principles (Barrie and Prosser, 1996).

by GC and then these compounds enter a reaction interface where they are oxidized, pyrolized or reduced to pulses of suitable gases for analysis (Barrie and Prosser, 1996). The first method is utilized for sulphur isotopic analysis and is discussed in more detail below. Detailed reviews of GC-IRMS can be found elsewhere: Barrie and Prosser, 1996; Krouse et al., 1996; Brenna, 1997; Kendall and Caldwell, 1998.

The general operation of EA-IRMS is illustrated in Figure 1-10. Solid and liquid samples are sealed into tin (Sn) capsules and loaded into an autosampler. The samples are purged of air by a flow of He in the autosampler. They are dropped into the vertical combustion tube as a pulse of O_2 temporarily replaces the He carrier gas. The combustion (oxidation) and reduction tubes are packed with various chemicals, depending on the isotope analysis of interest. For example, for ^{15}N and ^{13}C analysis, the packing consists of an oxidation catalyst Cr_2O_3 granules and chopped CuO wire to oxidize hydrocarbons, and Ag wool to trap S and halogens. Combustion products are swept into the reduction tube (Cu wires) where NO_x are reduced to N_2, and excess O_2 is removed. For ^{34}S analysis, The combustion and reduction takes places in a single tube packed with WO_3 and Cu wires. A desiccant trap removes water. If only ^{15}N is being analyzed, then another suitable alkaline trap is used to remove CO_2. He carrier gas sweeps the all combusted gases through a GC column that separates the sample gas of interest from others.

The sample gas is then swept in the He gas stream into the ion source via an open-split interface (Figure 1-10). In addition to the efficient transfer of gases from the EA into the ion source, the interface can be adjusted to reflect the relative abundance of different

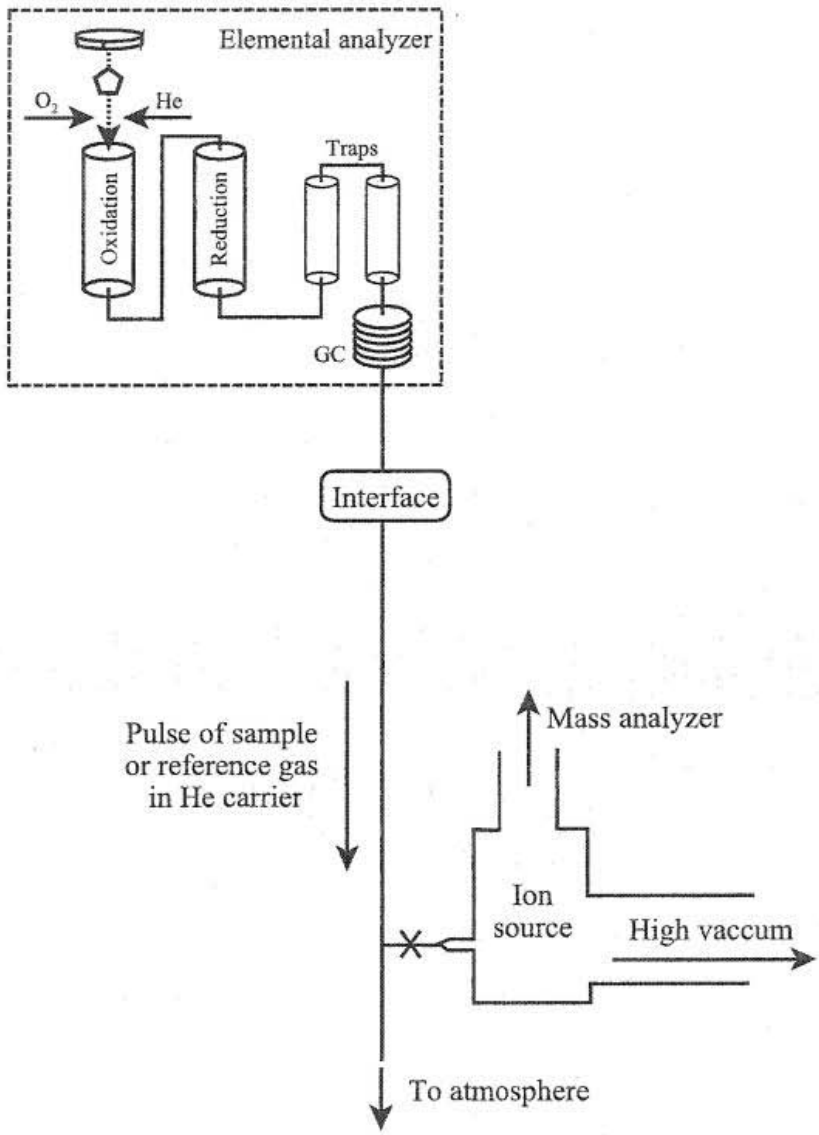

Figure 1-10. Simplified diagram of CF-IRMS principles (modified from Barrie and Prosser, 1996).

elements in one sample and to allow independent isotope ratio calibration for up to two elements (Finnigan® MAT, 1996).

Of the most interest among the researchers using stable isotope techniques are the type of sample analyzed, the amount of sample available, the number of samples to be analyzed and the precision of measurement required. With on-line CF-IRMS, samples can be accepted in their natural state, or with minimal sample preparation and the amount of sample has been reduced significantly, for example, from 3-7 mg S for DI-IRMS to 20 μg S for CF-IRMS method with minerals (Giesemann et al., 1994). On-line techniques have increased productivity more than 5-10-fold over DI-IRMS techniques and reduced the cost of analysis, enabling both larger-scale and more rapid experiments (Barrie and Prosser, 1996). Generally, the analytical precision available for CF-IRMS is slightly poorer than with the conventional DI-IRMS methods, but this will be improved in the next few years (Kendall and Caldwell, 1998).

CHAPTER 2

SAMPLING AND ANALYTICAL METHODS

2.1 SAMPLING

2.1.1 Sampling description

The species of lichen chosen for this study was *Alectoria sarmentosa*, which is common in Newfoundland. This species, known locally as Old Man's Beard, is yellow-green in color, and hair-like and bushy in appearance (Figure 2-1). It is classified as epiphytic and fruticose. The samples were taken from Balsam Fir, which is one of the most common trees in Newfoundland and a common substrate for this lichen species.

The Memorial University of Newfoundland (MUN) Botanical Garden is located in Pippy Park in St. John's, Newfoundland (Figure 2-2). Sampling was conducted on May 8, 1998. The weather was moderately sunny, temperature 15-20 °C and wind less than 10 km/hr.

Samples were collected from three different sites, A, B and C (Figure 2-2), along the trails of the Botanical Garden. These sites were selected because of the abundance of the lichen species and accessibility. All of the sampling sites were located more than 250 meters from the main road.

To avoid any contamination during sample collection, new unpowdered vinyl gloves and sampling bags (Kraft paper) were used for each site. Lichens were taken only from the tree branches, at a distance of 20-25 cm from the trunks. The trees were approximately

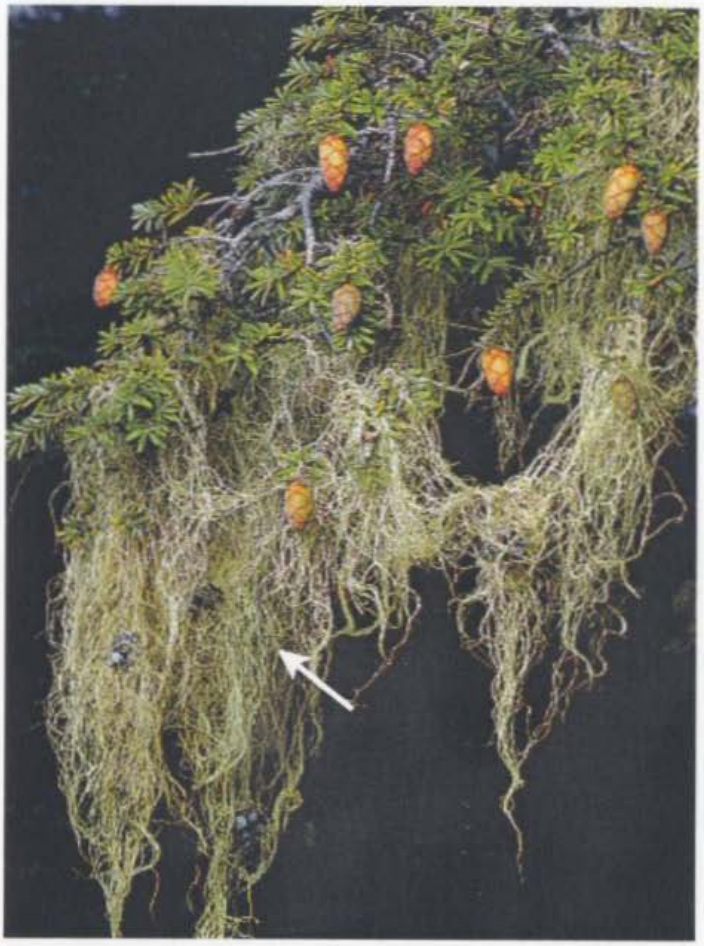

Figure 2-1. Photograph of *Alectoria sarmentosa* (arrow).

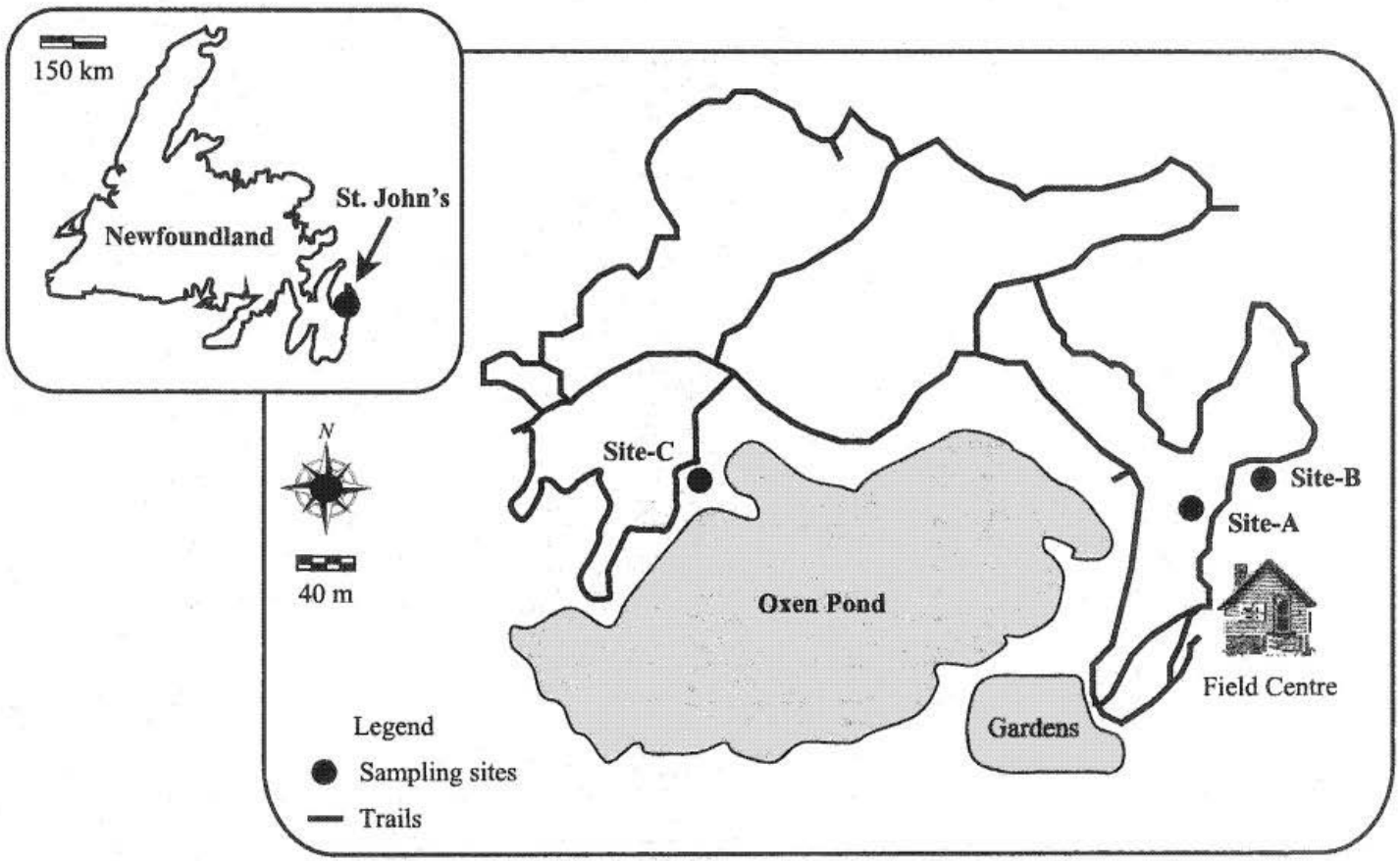

Figure 2-2. Map showing three sampling sites along the trails of the Botanical Garden, MUN (modified from the pamphlet of the Botanical Garden, MUN, used with permission).

10-15 cm in diameter. Samples were collected from all sides of each tree. From site-A, approximately 55 g of lichens were collected, and from sites-B and -C, about 48 g and 110 g were collected, respectively. The sample paper bags from each site were stored in Ziploc™ bags and labeled.

2.1.2 Sample preparation

Samples collected from the field underwent a series of physical pretreatments such as air-drying, cleaning, grinding and sieving, and homogenizing. The composite lichen powder was then processed independently by each of three techniques as summarized in Figure 2-3: CF-IRMS analysis of chemically-untreated lichen powder (henceforth referred to as *CF-lichen*); conversion to $BaSO_4$ and analysis by CF-IRMS (henceforth *CF-$BaSO_4$*); and the conventional chemical treatment and analysis by dual inlet-IRMS (henceforth *DI*).

2.1.2.1 Physical pretreatments

All lichen samples were air dried in a clean room in the Department of Earth Sciences, MUN, for 2-5 days. To avoid any contamination during the drying, the lichen samples were covered with Kimwipe™ towels. The dried lichen samples were then cleaned by removing foreign materials such as twigs and other lichen species, using clean stainless steel tweezers and unpowdered vinyl gloves. The dried and cleaned samples were crushed into a fine powder using a tungsten carbide puck mill for 1-2 minutes, sieved to -60 mesh, and then placed in a labeled glass vial. Before storing the lichen sample powder, the glass

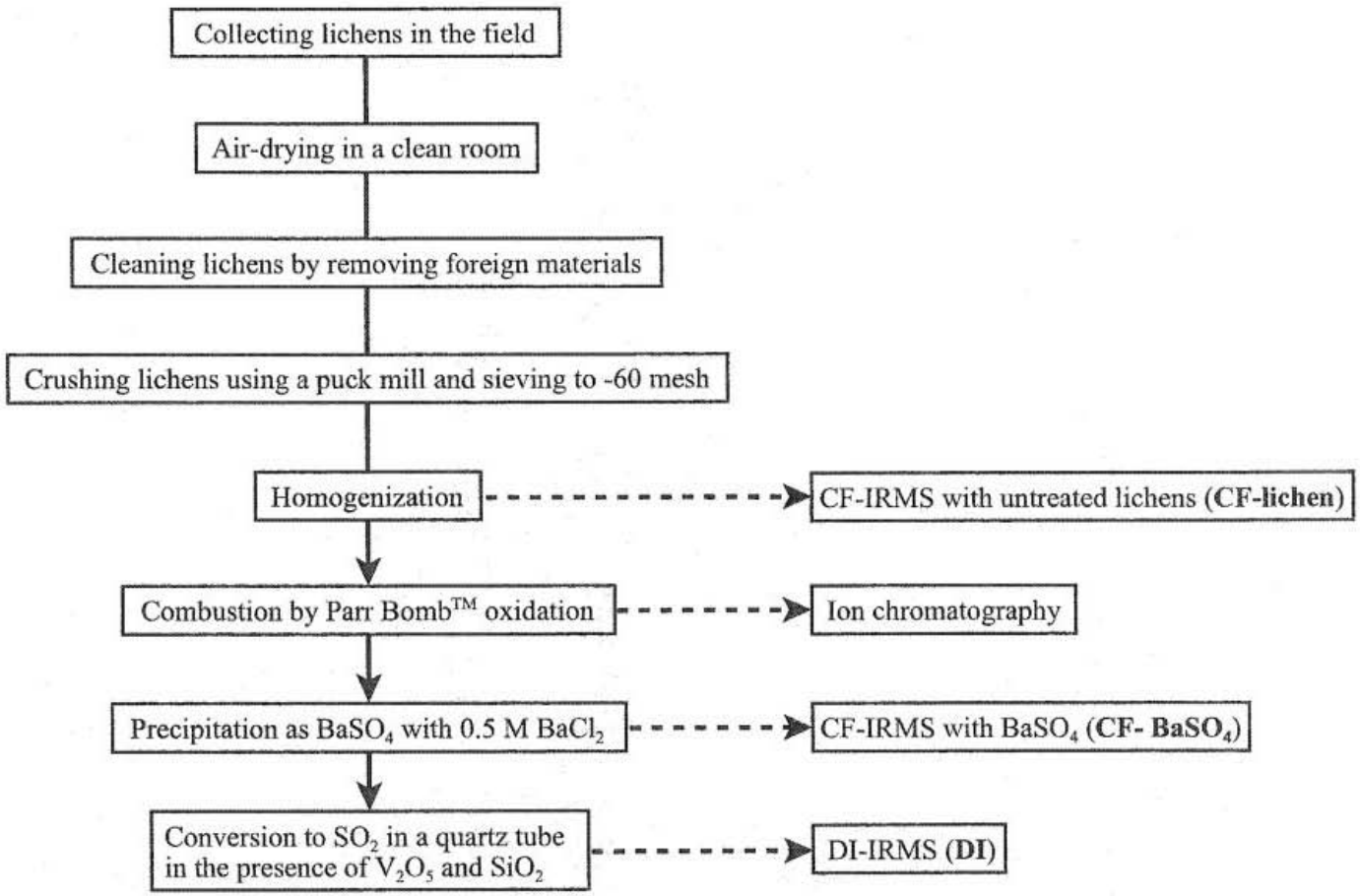

Figure 2-3. Sample preparation steps for three isotope analysis methods (CF-lichen, CF-$BaSO_4$ and DI) and ion chromatography analysis.

vial was soaked in 1.5 N HNO_3 for at least one day, rinsed with deionized water several times, and air dried for one day.

The glass vial containing the sample powder was then rolled on a rolling machine for over 20 minutes to ensure homogenization. In order to enhance homogenization, 6 glass beads (cleaned in the same way as the glass vial) were rolled together with the lichen powder in the glass vial. Between usages, the glass vial was kept in the refrigerator. This lichen powder was used in all subsequent analyses (Figure 2-3).

2.1.2.2 Parr Bomb™ oxidation

For CF-$BaSO_4$ and DI methods, $BaSO_4$ was obtained from the homogenized lichen sample powder by Parr Bomb™ oxidation. The Parr Bomb™ is a stainless steel container that can withstand high temperatures and pressures. It converts all forms of sulphur in the sample to sulphate.

Approximately 0.7-1.0 g of lichen powder was accurately weighed into a cleaned combustion capsule. 10 cm of nickel (Ni) or platinum (Pt) alloy fuse wire (45C10) was attached to the electrodes on the lid of the bomb. The capsule was then placed into the ring holder, making sure that the fuse wire was positioned just above (1-2 mm) the top of the lichen powder in the capsule, as illustrated in Figure 2-4. 10 ml deionized water and 5-7 drops of 50% hydrogen peroxide (H_2O_2) were poured into the bottom of the bomb (Figure 2-4). The bomb was sealed very carefully and 30 atmospheres of O_2 was pumped into it.

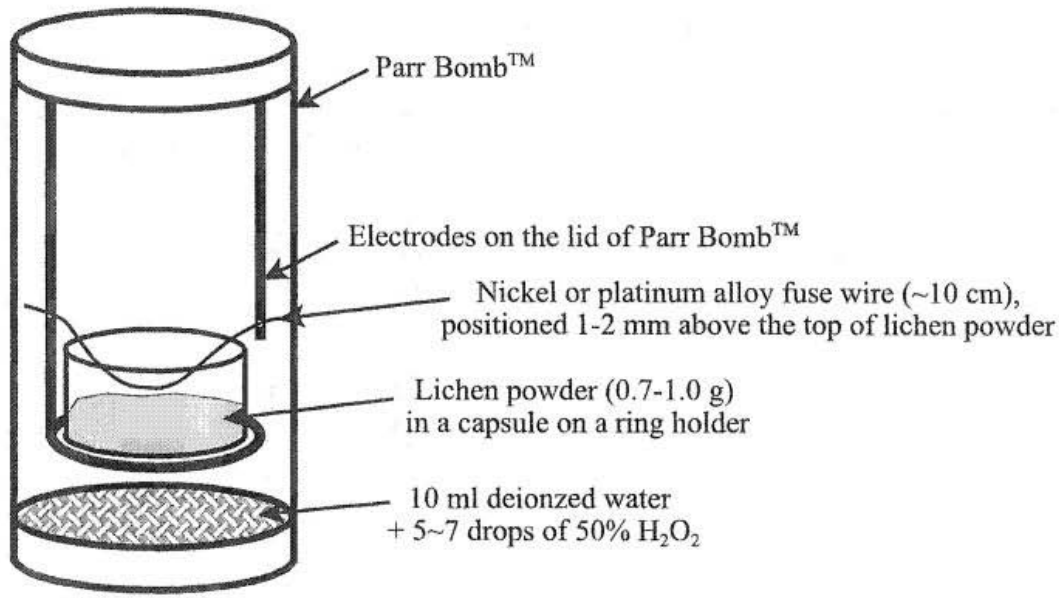

Figure 2-4. Illustration of Parr Bomb™ setting.

The bomb was placed into a cold water bath in a fume hood and checked for leaks. The sample was then ignited by the alloy fuse wire. After 15-20 minutes, the bomb was removed from the cold water bath. The pressure of the bomb was slowly released. When the bomb was at atmospheric pressure, it was opened and the inside of the bomb, capsule, lid and electrodes were rinsed several times with deionized water and collected in a cleaned beaker.

The collected sample solution was filtered through a cellulose nitrate membrane filter paper into an Erlenmeyer™ flask under vacuum. The filtered solution was diluted to make 500 mL with deionized water and a 10 mL aliquot was taken to measure S concentration of the lichen sample by ion chromatography (Figure 2-3). The remaining sample solution, returned to a clean beaker, was heated on a hot plate. The solution was acidified to pH 4 with few drops of 8 N HNO_3. When the sample solution was boiling, 10 mL of 0.5M $BaCl_2$ was added to precipitate sulphate to the form of $BaSO_4$, and the temperature was reduced. The solution was then left to digest for over 2 hours (up to 24 hours) to precipitate $BaSO_4$. The $BaSO_4$ solution was filtered twice through Fisherbrand ashless filter papers under vacuum, rinsing the beaker with warmed deionized water. The filter papers were dried in a clean oven at around 70 °C for several hours and then combusted in a clean Vitrosil crucible over a bunsen burner, leaving $BaSO_4$ in the crucible. The crucible with $BaSO_4$ was placed in a desiccator until cool. The extracted $BaSO_4$ was weighed, and stored and labeled in a clean vial. This $BaSO_4$ was used for CF-$BaSO_4$ and DI methods (Figure 2-3).

2.1.2.3 Sulphur dioxide extraction line

The $BaSO_4$ extracted by the Parr Bomb™ oxidation was used to obtain SO_2 based on the method of Yanagisawa and Sakai (1983), Ueda and Krouse (1986), and Wadleigh and Blake (1999). A schematic of the SO_2 extraction line is shown in Figure 2-5.

Approximately 5 mg of $BaSO_4$ was thoroughly mixed with 50 mg each of vanadium pentoxide (V_2O_5) and silica (SiO_2) in an agate mortar and pestle. V_2O_5 and SiO_2 contribute oxygen for the reaction to produce SO_2. The ratio of $BaSO_4$:V_2O_5:SiO_2 is maintained close to 1:10:10 to ensure that the oxygen isotopic composition of the SO_2 is completely controlled by these components and is independent of the original oxygen isotopic composition of the $BaSO_4$.

The mixed sample powder was placed in the bottom of a 9 mm (outer diameter (o.d.)) quartz combustion tube. A small wad of quartz wool was placed on top of the reaction mixture. Another small wad of quartz wool was placed about 2 cm above the first wad. About 5-6 cm of copper turnings, used to reduce SO_3 to SO_2, were then placed on top of the quartz wool. Figure 2-6 illustrates the packing of the combustion tube.

The prepared sample tube was connected to a vacuum line by a Cajon Ultra-Torr union (Figure 2-5). A thermocouple was set into the combustion furnace, along with the combustion tube. After evacuating the combustion tube for 3-5 minutes (valve-A), the copper turnings were flamed to remove any oxide coating. In order to remove any water and volatile organics that might be in the reaction mixture, the combustion tube was heated, to 250 °C for 10 minutes, and then increased to 350 °C for 20 minutes, with evacuation (valve-

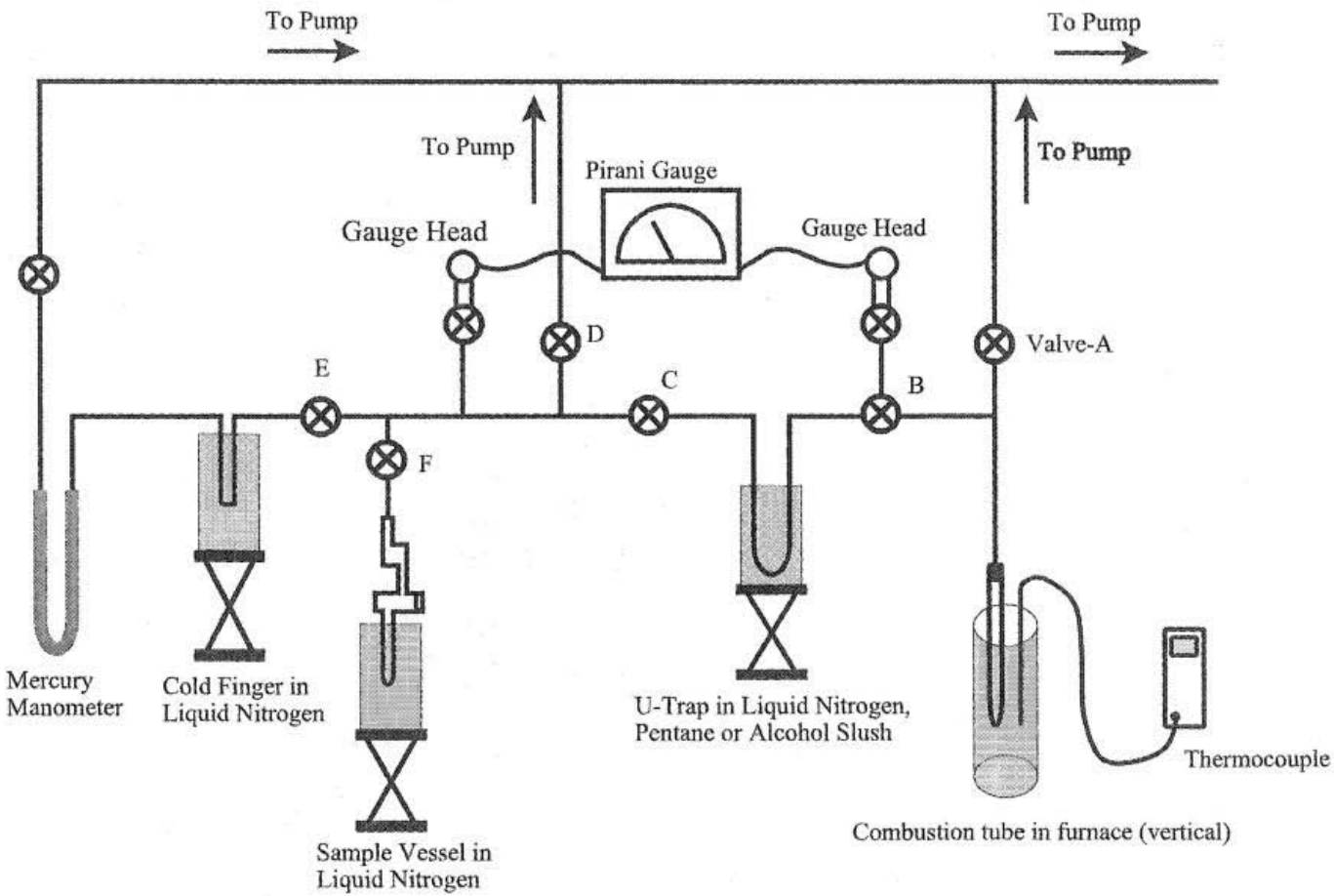

Figure 2-5. Sulphur dioxide extraction line.

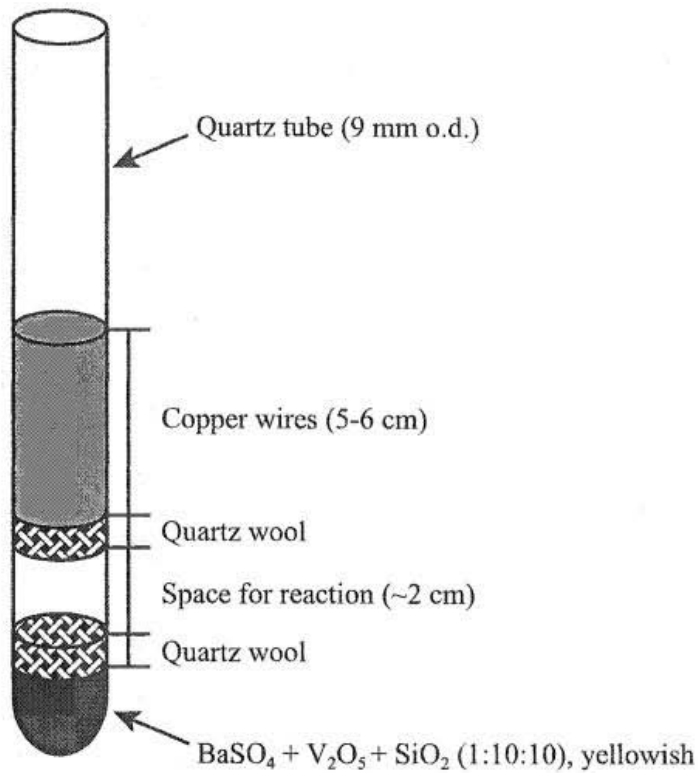

Figure 2-6. Packing of sample combustion tube for sulphur dioxide extraction line.

A) continuing until outgassing ceased.

The sample mixture was then heated to 950 °C during which the reaction occurred, producing SO_2, CO_2, $H_2O_{(g)}$ and O_2. The temperature was raised slowly, 1-2 °C rise/sec, in order to prevent bumping of the mixture, to ensure the consistency of the oxygen isotope ratio of the evolved SO_2, and to achieve complete reduction of SO_3 by the copper. The sample mixture was combusted 20-30 minutes after the temperature reached 950 °C. SO_2, CO_2 and $H_2O_{(g)}$ were frozen in the U-trap by liquid N_2, while O_2 was released through valves-C and -D to the pump. The temperature must not exceed 1040 °C because this can lead to reaction between copper and oxygen, causing incomplete SO_2 formation due to the lack of oxygen.

Slushes of different temperatures were then used to cryogenically separate and purify the SO_2. A pentane and liquid N_2 slush (-128 °C) was used to freeze SO_2 and $H_2O_{(g)}$ while liberating CO_2. An alcohol and liquid N_2 slush (-80 to -90 °C) was used to freeze $H_2O_{(g)}$ releasing SO_2. The SO_2 was then collected, through the valves-C and -E, into the cold finger of a yield manometer in a liquid N_2 bath. After recording the yield, SO_2 was transferred, through valve-F, into a sample vessel in a liquid N_2 bath. Throughout the procedure, the movement of gases was observed by a Pirani gauge. The extracted SO_2 gas was used for DI method (Figure 2-3).

2.1.3 Sample selection methods

Figure 2-7 summarizes the sample selection for the three analytical methods used in

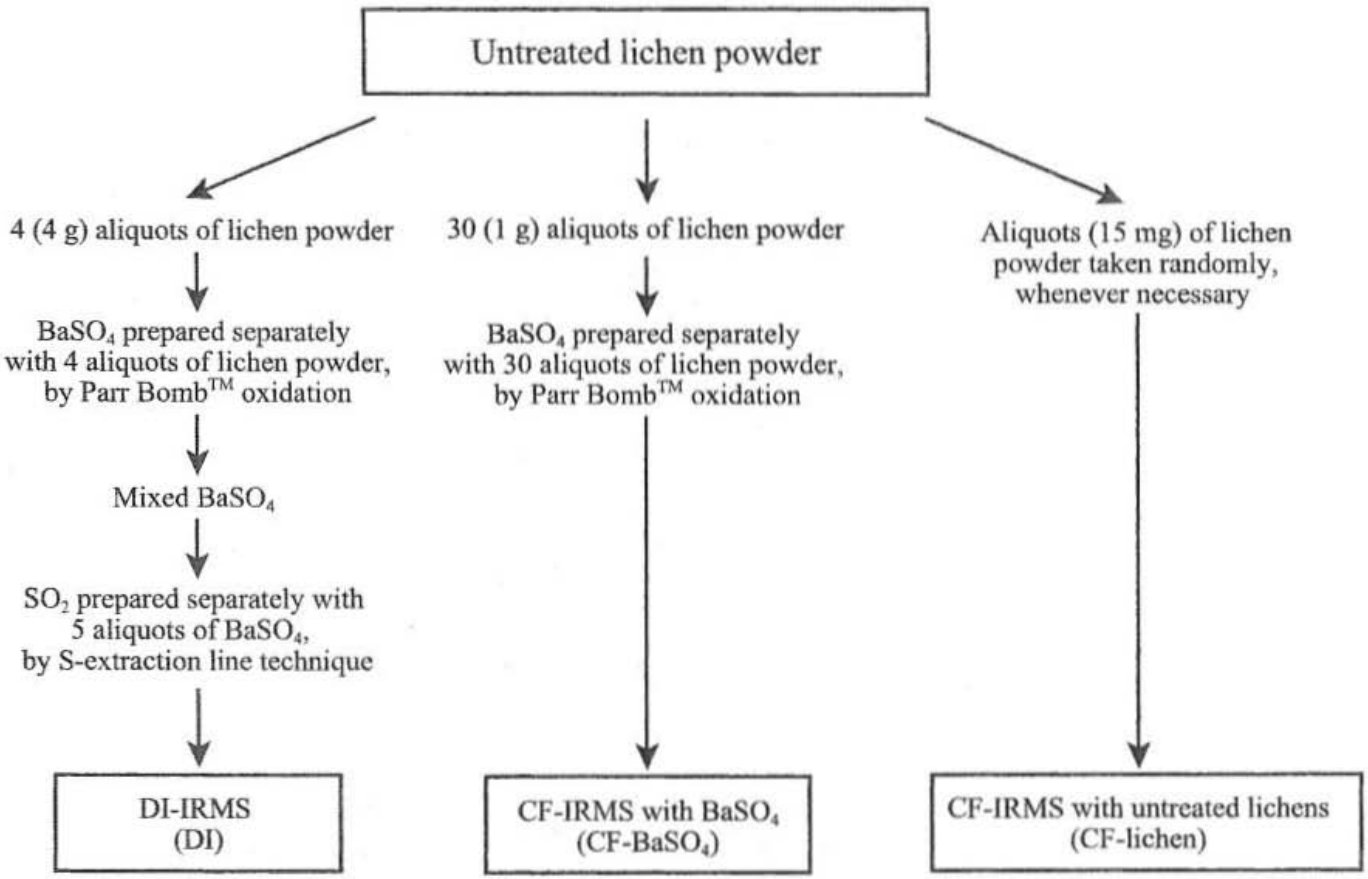

Figure 2-7. Summary of sample selection methods for DI- and CF-IRMS analyses.

this study. For DI method, four 4 g aliquots of lichen powder were taken from the original composite sample. These aliquots were used to prepare four separate $BaSO_4$ precipitates by Parr Bomb™ oxidation. The precipitates were then combined in a single vial. Five aliquots of this mixed $BaSO_4$ were converted separately to SO_2 for IRMS analysis. For CF-$BaSO_4$ method, thirty 1 g aliquots of lichen powder were converted separately to $BaSO_4$ for IRMS analysis. For CF-lichen method, 15 mg aliquots of lichen powder were taken randomly from the lichen powder, whenever necessary, for IRMS analysis.

2.2 ANALYTICAL METHODS

2.2.1 Ion chromatography

Ion chromatography involves ion exchange separation of species, such as Cl^-, PO_4^{3-}, NO_3^- and SO_4^{2-} (in the case of S), in solution followed by conductivity detection. The chromatograph was calibrated using solutions of different concentrations prepared from National Institute of Standards and Technology (NIST) standards. For the lichen samples, an aliquot of bomb washings (see Section 2.1.2.2) was analyzed using a Dionex DX-100 Ion Chromatograph at the Department of Earth Sciences, MUN, to obtain sulphate concentration in the samples. S concentration was then calculated from the sulphate concentration by multiplication of the raw sulphate concentration determined from ion chromatography analysis by the fraction of S in sulphate ion. The detailed calculation procedure is illustrated with an example in Appendix I.

2.2.2 DI-IRMS analysis

SO_2 sample gas prepared by SO_2 extraction line (Section 2.1.2.3) was introduced into the IRMS (Finnigan® MAT 252) through a dual inlet system. SO_2 reference gas was also prepared from an independently analyzed pyrite (MUN-Py, FeS_2, $\delta^{34}S_{CDT}$ = 1.26‰). The sample and reference gases were alternately introduced to the ion source via a changeover valve and the ion currents of masses 66 and 64 of the sample were compared to those of the reference gas. Ten cycles were averaged for each determination. To check accuracy of the analysis, MUN-Py and the international NIST standard, NBS-127 (barium sulphate, $BaSO_4$) were used. Replicate analyses yielded $\delta^{34}S_{CDT}$ = +1.3 ± 0.5‰ and +20.3 ± 0.4‰, respectively.

2.2.3 CF-IRMS analysis with $BaSO_4$

The experimental procedure and parameters of on-line $BaSO_4$ analysis were adopted mostly from the Instruction Manual of NA 1500, Carlo Erba® instruments and Giesemann et al. (1994). The detailed analytical parameters used are given in Table 2-1. With these parameters, more than 200 $BaSO_4$ samples could be analyzed with a single combustion reactor packing, cleaning the residual ash from the combustion reactor after every 40 samples. The calibration method for on-line methods (CF-$BaSO_4$ and CF-lichen) in this study can be found in Section 3.4.

Table 2-1. Analytical parameters for CF-$BaSO_4$ method.

- $BaSO_4$ (mg): 0.20-0.30
- Sn capsule (mg): 30
- Combustion reactor (°C): 1050
- Combustion reactor packing: WO_3, pure Cu & quartz wool
- O_2 supply (mL/min): 25-27
- O_2 loop (mL): 10
- Flow rate of He carrier (mL/min): 80
- H_2O trap: $Mg(ClO_4)_2$
- Length of GC column (m): 2.0
- GC oven (°C): 90

CHAPTER 3

DEVELOPMENT OF CF-LICHEN METHOD

The developed on-line method with untreated lichens is highlighted in detail in Chapter 3, by addressing the problems encountered during the development and discussing their improvement. The main obstacle in the early stages of development was low S concentration (~600 ppm) in the lichen samples, which meant a large amount of sample was required for each analysis. This set the direction for subsequent method development. Therefore, the following sections centre around combustion of large quantities of lichen (several mg).

3.1 EXPERIMENTAL PROCEDURES

Samples of the lichen (*Alectoria sarmentosa*), initially used for development of this analytical method, were collected from various locations in Newfoundland by Blake (1998). Based on the tests of minimum S amount reported by Giesemann et al. (1994), 10 μg of S was considered to be the lower limit of S amount. Therefore, about 20-23 mg samples (containing about 12-14 μg S) of untreated lichen powder were used for the early trials. Figure 3-1 shows the schematic diagram of CF-IRMS used for this study, consisting of an elemental analyzer (Carlo Erba® NA 1500), an open-split interface (Finnigan® MAT ConFlo II) and an IRMS (Finnigan® MAT 252). The analytical parameters used in the early stages of the development are summarized in Table 3-1 and were adopted mostly from the

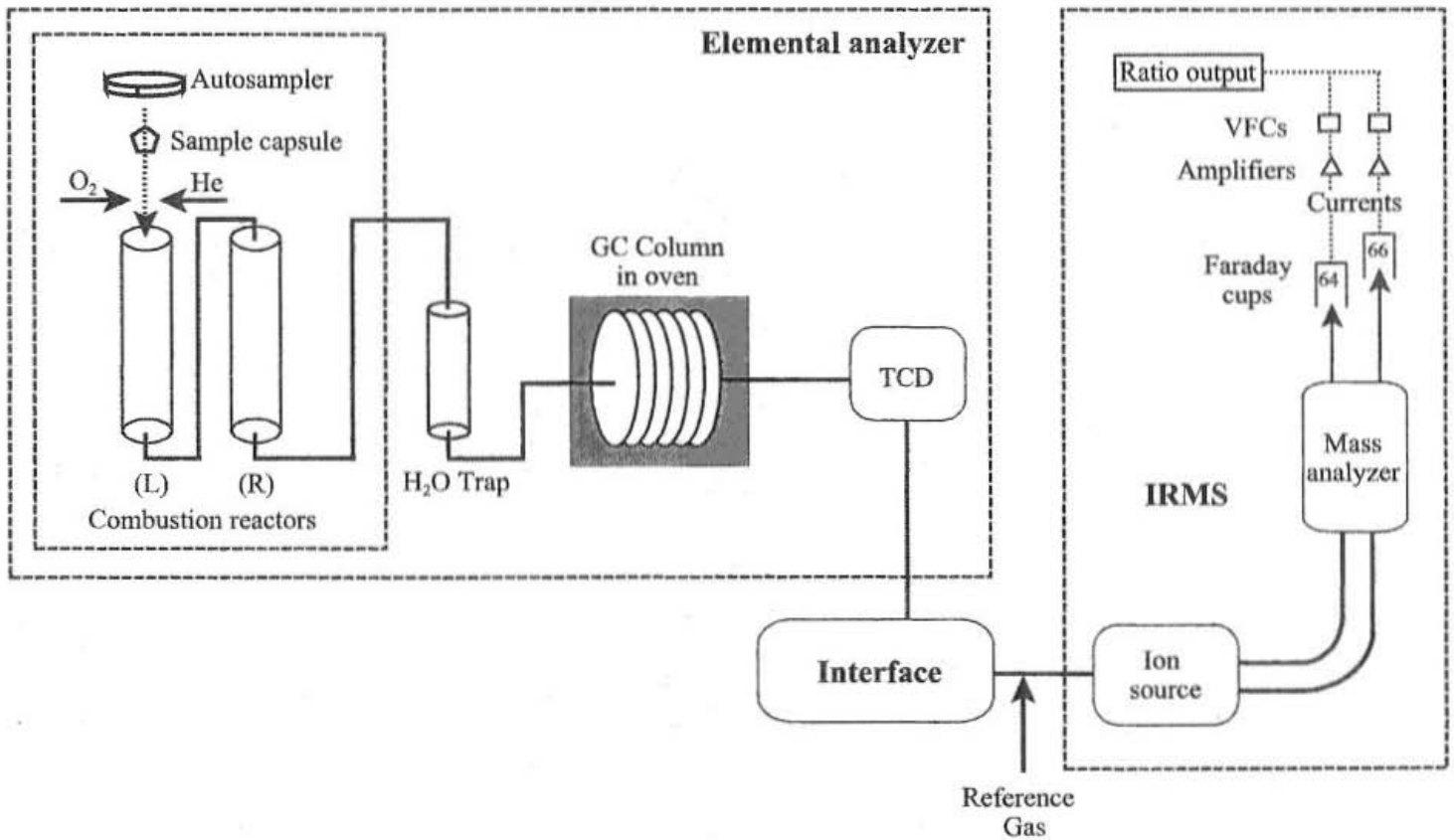

Figure 3-1. Schematic diagram of the CF-IRMS system in the Department of Earth Sciences, MUN, consisting of an elemental analyzer (Carlo Erba® NA 1500), an open-split interface (Finnigan® MAT ConFlo II) and an IRMS (Finnigan® MAT 252). TCD and VFCs represent thermal conductivity detector and voltage to frequency converter, respectively.

Table 3-1. Initial and final analytical parameters for CF-lichen method.

Parameters	Initial[1]	Final
Lichen (mg)	20-23[2]	15[3]
Sn capsule (mg)	60	40
Combustion reactor (°C)	1050	1050
Combustion reactor	WO_3, pure Cu & Quartz wool	WO_3, pure Cu & Quartz wool
O_2 supply (mL/min)	25-27	25-27
O_2 loop (mL)	10	10
Flow rate of He carrier (mL/min)	80	80
H_2O trap	$Mg(ClO_4)_2$	75% $Mg(ClO_4)_2$ & 25% Quartz chips
Length of GC column (m)	2.0	1.2
GC oven (°C)	90	75
He for CO_2 dilution (psi)	25	25

Note:

1 Initial analytical parameters were adopted mostly from the Instruction Manual of NA 1500, Carlo Erba® Instruments and Giesemann et al. (1994).

2 Lichen samples collected from various locations in Newfoundland by Blake (1998).

3 Lichen samples collected from the Botanical Garden, MUN.

Instruction Manual of NA 1500, Carlo Erba® Instruments and Giesemann et al. (1994).

Chemically-untreated lichen samples were wrapped together with V_2O_5 in Sn capsules (10 × 10 × 10 mm^3, 60 mg). The sample capsules were introduced from an autosampler into the EA. In the EA, there are two furnaces. A transparent quartz combustion reactor (45 cm in length, 1.5 cm in inner diameter (i. d.) and 0.1 cm in thickness) was located inside the left furnace set at 1050°C (Figure 3-1). The right furnace was not used in this study, however, the temperature was set at 750°C to ensure thermal equilibrium with the left combustion furnace. The combustion reactor, composed of both oxidation and reduction parts, was packed with tungstic oxide (WO_3), pure Cu wire and very fine quartz wool (Figure 3-2). WO_3 was used as a combustion catalyst. It is known that WO_3 does not react with the quartz combustion tube even after prolonged periods of heating and also does not stop the flow of sulphur oxides (Rittner and Culmo, 1966). Pure Cu wire was used to reduce any trace SO_3 to SO_2 and NO_X to N_2, and to trap surplus O_2. The quartz wool was used as a baffle and provided additional high temperature surface for complete combustion of any stray fragments of the sample (Dugan, 1977). On top of this packing, a tube made of quartz (22 cm in length, 1.1 cm i.d. and 0.1 cm in thickness) with quartz wool (~1 cm) at its bottom was installed to collect residual ash after combustion of samples (Figure 3-2).

O_2 was supplied from a 10 mL loop at a rate of 25-27 mL/min by He carrier gas. To achieve complete combustion, it is important to introduce the sample into the reactor when O_2 is enriched in the combustion zone. This was accomplished by adjusting the sample inlet time to about 2 seconds before the flash of combustion (Instruction Manual of NA 1500,

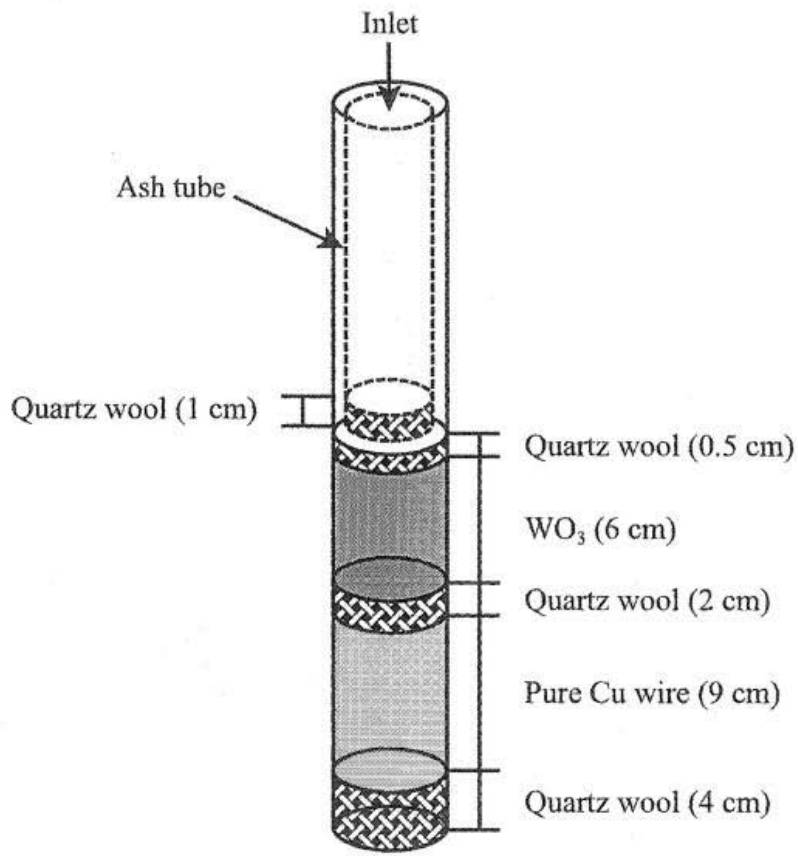

Figure 3-2. Configuration of combustion reactor for CF-IRMS method.

Carlo Erba® Instruments). Gaseous combustion products, SO_2, CO_2, N_2 and $H_2O_{(g)}$, were carried in a stream of He gas (at a rate of 80 mL/min) through a trap to remove $H_2O_{(g)}$. The trap was filled with anhydrous magnesium perchlorate ($Mg(ClO_4)_2$) and quartz wool (Figure 3-3). The remaining gases, SO_2, CO_2 and N_2, passed through a 2.0 m-long GC column (Porapak™ QS, Teflon), heated to 90°C, where CO_2 and N_2 were separated from the sample gas, SO_2 (Figure 3-1)

The separated gases were transferred into the ion source of the IRMS through an open-split interface (Figure 3-4). The excess CO_2 was diluted by He supply (set to 25 psi) in the interface so that the dynamic range of the IRMS was not exceeded. He was supplied through a movable capillary (Figure 3-4) controlled automatically by computer. As SO_2 is the only gas of interest for this study, the capillary of the reference gas of CO_2 was not used.

SO_2 reference gas supplied from a separate bellow attached to one of the dual inlets (Figure 3-1) was also measured for a certain time interval (20 sec) when the sample gas was not being measured. The Finnigan® MAT ISODAT software then integrated the areas underneath the peaks (of masses 64 and 66) of sample and reference gases to determine the raw delta value ($\delta^{34}S_{raw}$) by the equation:

$$\delta^{34}S_{raw}(‰) = \left[\frac{A^{66}_{spl}/A^{64}_{spl}}{A^{66}_{ref}/A^{64}_{ref}} - 1\right] \times 1000 \qquad (3.1)$$

where A represents peak area, and spl and ref stand for sample and reference gases, respectively.

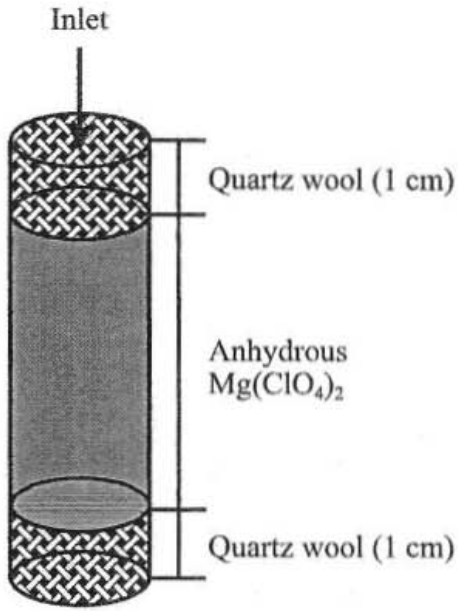

Figure 3-3. H_2O trap used in the early stages of development of CF-lichen method.

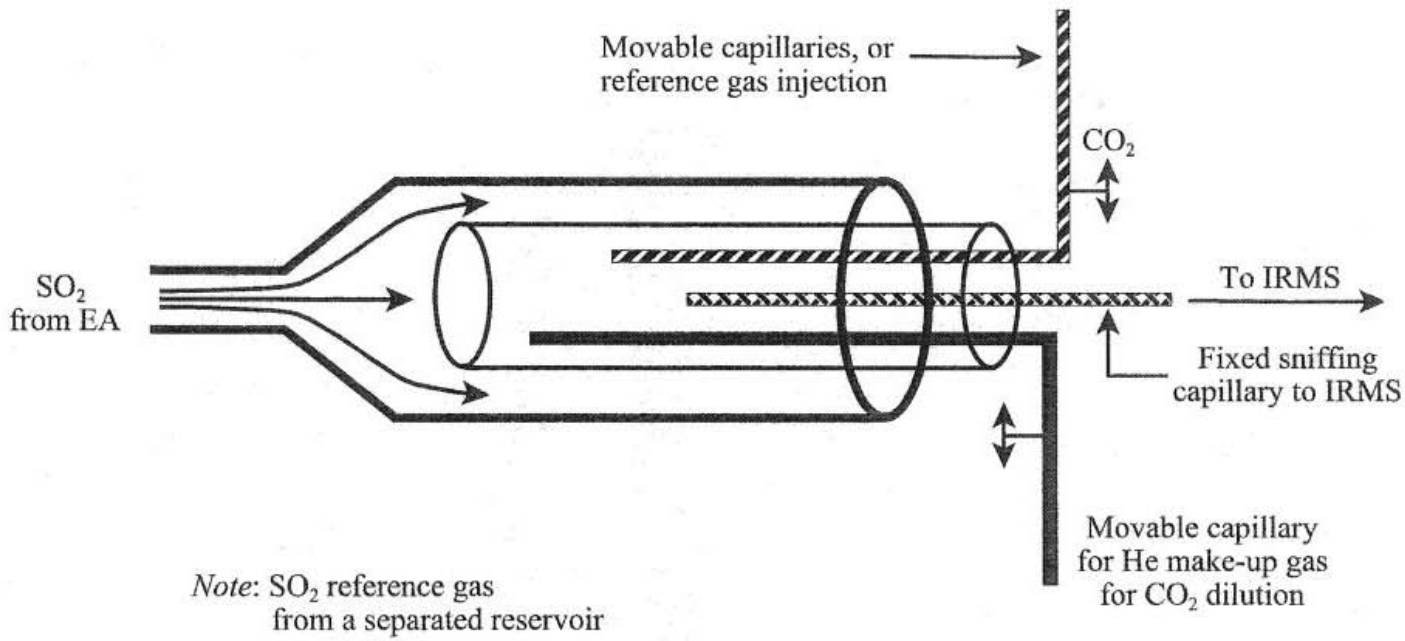

Figure 3-4. Schematic view of an open-split interface (Finnigan® MAT ConFlo II) (modified from Finnigan® MAT 252 Operator Course Note, 1997).

Figure 3-5 shows the typical peak traces of untreated lichens, minerals and reference gases. Since the sample gases pass through the GC column before IRMS analysis, the peak shapes of both masses 64 and 66 are sigmoidal (Figures 3-5a, b). Unlike the peaks of minerals, lichen peak shapes are lower in amplitude and greater in width (Figure 3-5a) because of low S concentration. Also, the peak tails of lichens are longer than those of minerals. Reference gas is introduced into the IRMS as a pulse directly from a bellow of dual-inlet system. Hence the peaks are more rectangular in shape (Figure 3-5c).

3.2 OBSERVED PROBLEMS

Several analytical problems were observed in the early stages of method development with untreated lichens. They included: (1) decreasing peak size (amplitude and area) and delayed peak start time after only a few analyses; (2) decreasing flow rate of He carrier gas; (3) no combustion flash; (4) discoloration of WO_3 and decreasing porosity in the WO_3 packing; (5) excessive water in the $Mg(ClO_4)_2$ trap and (6) the appearance of an unidentified peak.

(1) Decreasing peak size and delayed peak start time

Figure 3-6 illustrates a typical series of sample traces. Both peak amplitudes and areas (both mass 64 and 66/64 ratio) decreased significantly over the course of these analyses. By the 10^{th} analysis, the peak was no longer detected. Decreased peak was accompanied by a delay in peak start time, from 347.1 sec for the 2^{nd} analysis to about

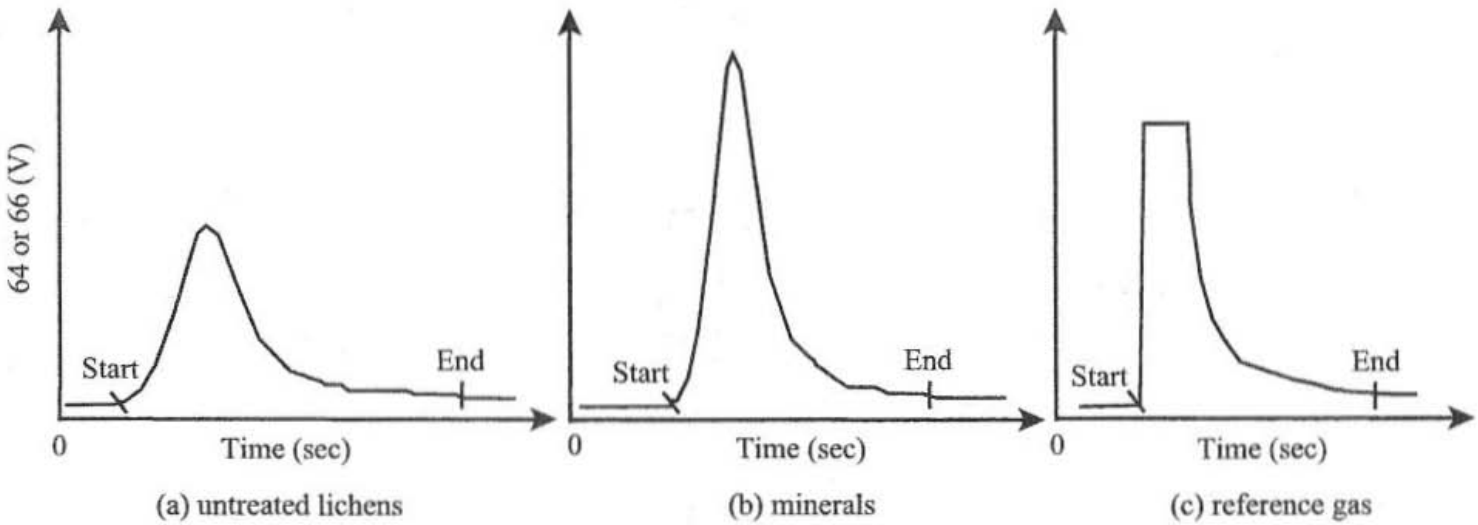

Figure 3-5. Compilation of typical traces; (a) untreated lichens, (b) minerals and (c) reference gas.

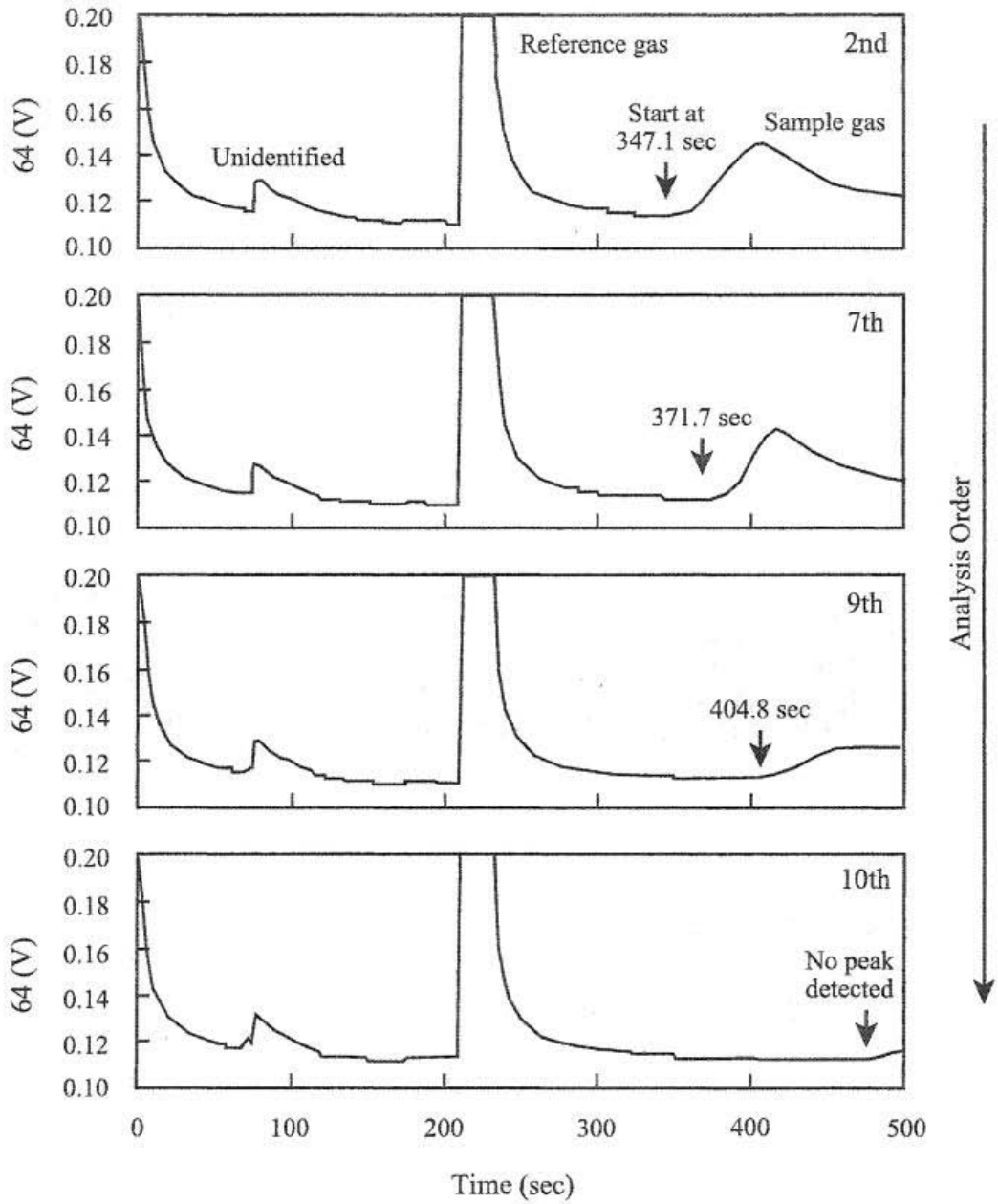

Figure 3-6. An example of typical series of peaks in the early stages of development of CF-lichen method, showing decreasing peak size (amplitue and area) and delayed peak start time with analysis, and an unidentified peak.

475 sec for the 10th.

(2) Decreasing flow rate of He carrier

The flow rate of He carrier gas was set to 80 mL/min using a bubble flowmeter (Hewlett Packard®) at the beginning of lichen analysis. Over the course of the lichen analyses illustrated in Figure 3-6, the flow rate gradually decreased eventually becoming zero. The decreasing flow rate of He carrier gas with analysis was necessarily accompanied by a decrease of flow rate of sample gas.

(3) No combustion flash

The combustion flash for each sample can be viewed through the window of the autosampler. Frequently, no flash was observed for lichen samples while a very bright flash could be seen for mineral analyses. This was interpreted as incomplete combustion for the lichen samples.

(4) Alteration of the properties of WO_3

(4.a) Discoloration of WO_3

Fresh WO_3 granules are bright yellow. After a series of mineral analyses, it was observed that the color changed to bright yellowish green. However, after several lichen analyses, it turned completely black. Removal of oxygen from WO_3 crystals darkens them first through green, then blue-green and finally black (Parker, 1993). This indicates clearly

that the combustion zone for lichen analysis was under a reducing environment, causing the extraction of oxygen from WO_3 crystals.

(4.b) Decreasing porosity in WO_3 packing

Typically, after a series of mineral analyses, no change in packing of WO_3 is observed. The original, irregular shapes and the amount of porosity are retained. However, after analysis of several lichen samples, a significant reduction in porosity was observed in the upper half of the WO_3 packing (Figure 3-7a) while the lower half preserved the original shapes of WO_3 granules and the initial porosity in the packing. The upper half also showed a difference in the shapes of WO_3 granules (Figure 3-7a). Figures 3-7 (b) and (c) show SEM (Scanning Electron Microscopy) images of the upper half. Numerous needle-shaped crystals were also observed, filling the interstitial spaces among WO_3 granules. These crystals were not observed on fresh WO_3 granules or after mineral analyses. Although the composition of the needle-shaped crystals was not identified, the crystals were considered as a by-product of incomplete combustion of lichen analyses.

(5) Excessive H_2O in $Mg(ClO_4)_2$ trap

After fewer than ten successive lichen analyses, it was observed that sufficient water had condensed at the top of H_2O trap to prevent the flow of gases. In order to measure the approximate water content, lichen samples were oven-dried (GCA Precision Scientific®) at 100°C for about 60 hours. This resulted in ~10 wt% loss. The lichen samples used in the

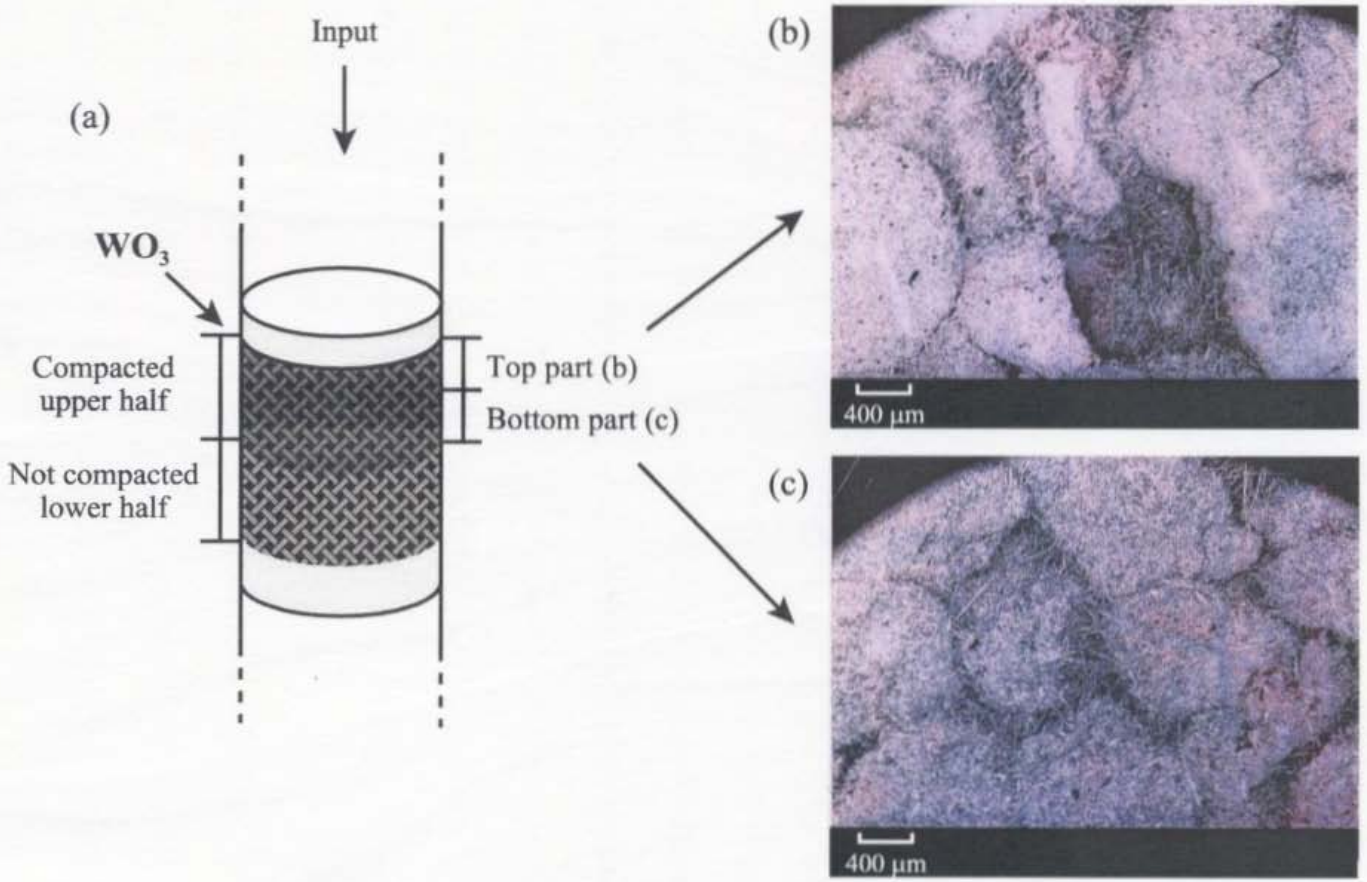

Figure 3-7. Magnified WO_3 packing after the analysis of about ten lichen samples (a) and SEM images of WO_3 granules of the top (b) and the bottom (c) parts of the compacted upper half.

initial stage of method development were not oven-dried. Thus, the high water content of the lichen samples was possibly enough to saturate the top of the H_2O trap.

Observations (1) to (5) can be attributed to incomplete combustion and subsequent blocking of gas flow, possibly due to (i) low combustion temperature, (ii) O_2 deficiency and (iii) high water content of the lichen. Complete combustion is highly important for quantitative conversion to SO_2, especially for organic samples with low S concentration (high C:S ratio). Dugan (1977) suggested that optimum O_2 and temperature conditions are important in order to achieve the dynamic conditions of flash combustion, especially for samples that are difficult to combust. Since the actual combustion temperature is provided by Sn, which locally raises the temperature to around 1700°C, ensuring complete oxidation (Barrie and Prosser, 1996), steps were taken to eliminate conditions that might contribute to a reduction in the actual combustion temperature, such as O_2 deficiency and high water content of the lichen. Dugan (1977) suggested that the results of S analysis, in particular, are poor if the sample is O_2 starved, while other elements such as C and N may still have acceptable results because the thermodynamics of the combustion reaction favour the formation of CO_2, N_2 and $H_2O_{(g)}$ ahead of SO_2. The situation is further complicated when other O_2 accepting elements such as Cl and P are present in a sample (Dugan, 1977), as is the case with lichen. In addition, lower O_2 pressure makes the combustion proceed slowly and the slow stream of SO_2 through the system causes adsorption of the gas on the walls of internal surfaces (Eriksen, 1996).

(6) Unidentified peak

An unidentified peak was observed during lichen analysis (Figure 3-6) which was not observed for the analysis of mineral. This peak always appeared abruptly at about 75 sec. However, its size varied with sample size. For example, the size of the unknown peak obtained from analysis of a 15 mg-lichen sample (containing 9 μg S) was approximately double that of a 6 mg-lichen sample (containing 3-4 μg S). A similar peak was observed during analysis of another organic material, BBOT ($C_{26}H_{26}N_2O_2S$). However, the peak size for BBOT was 7-8 times smaller than for lichen (even though the BBOT contained more S). The constant peak start time, the peak shape, and variation in size with sample amount suggest that it may related to isotopic interference composed of elements such as C and N, which exist in organics and which are separated earlier than S. However, more work is needed to explain the occurrence of these unidentified peaks.

3.3 IMPROVEMENT AND SOLUTION

(1) Drying of untreated lichens

To reduce the water content, lichen samples were oven-dried at 60°C for 15 hours. This resulted in 5~6 wt% loss. However, this oven-drying treatment did not reduce the amount of water condensing at the top of H_2O trap, nor did it improve the combustion flash or the color of WO_3, indicating that the combustion was still incomplete.

In order to reduce the water content as much as possible without isotopic fractionation, the temperature was increased to 80°C and samples were dried for the same

length of time. This yielded 9~10 wt% loss. The water loss at 80°C was almost same as that (~10 wt%) at 100°C for 60 hours, indicating almost complete drying.

The composition of the H_2O trap was also changed from $Mg(ClO_4)_2$ only, to a mixture of 75% $Mg(ClO_4)_2$ and 25% quartz chips (0.9-1.7 mm in diameter) in order to facilitate the flow of gases (Figure 3-8). With these modifications, condensation was reduced significantly, and about 40 lichen samples could be analyzed without changing the H_2O trap.

(2) Increasing O_2

To solve the problem of O_2 deficiency, two changes were made. The first was the reduction in weight of the Sn capsules used. The capsules are oxidized to SnOx by the combustion reaction and hence consume some of the O_2 needed to combust the lichen. The weight was reduced from 60 to 40 mg with no change of the volume of capsule ($10 \times 10 \times 10\ mm^3$), resulting in theoretically 0.33 times reduction in O_2 consumption for Sn oxidation. The second change was in the amount of lichen used per analysis. Sample size was reduced from 20-23 mg (12-14 μg S) to 15 mg (9 μg S), corresponding to a decrease of O_2 consumption by about 0.70 times.

These modifications, including oven-drying treatment of lichen samples, produced clear improvement as represented by; (i) bright combustion flash, (ii) consistent flow of He carrier gas throughout the life-time of the combustion reactor, (iii) bright green WO_3, (iv) no blocking in WO_3 packing and (v) improved analytical signals in terms of peak size and consistency from sample to sample.

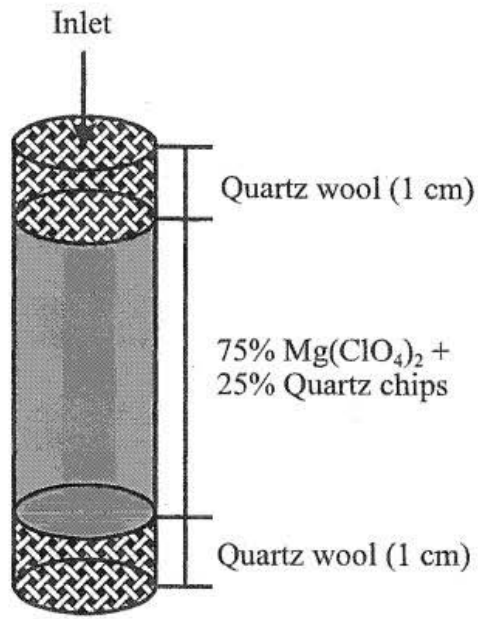

Figure 3-8. H_2O trap modified for CF-lichen method.

(3) Shorter GC column and lower GC oven temperature

To further improve the analytical signals of untreated lichen analysis, the length of GC column was shortened, from 2.0 to 1.2 m. This was done in order to decrease the retention time of SO_2 in the column and thereby increase peak resolution. This improved sensitivity by increasing the efficiency of delivering the sample gas to IRMS. However, the temperature of GC oven had to be reduced from 90 to 75 °C to prevent the overlapping of the sample peak with the unidentified peak (see Observation (6) of Section 3.2).

Table 3-1 summarizes the final analytical parameters for the analysis of untreated lichens. With the adopted analytical parameters, about 150 lichen samples (15 mg per analysis) could be analyzed with cleaning ash tube and changing the top of H_2O trap, after every 40 samples. After about 150 lichen sample analyses, the peaks became elongated with long peak tail, finally not enough to be detected, and the precision of $\delta^{34}S$ values became poorer. Figure 3-9 shows an example of improved peaks of the lichen samples. Note the constant peak size (amplitude and area) and peak start time for each analysis.

3.4 CALIBRATION PROCEDURE

Raw delta ($\delta^{34}S_{raw}$) values determined by IRMS analyses (see Eq. 3.1) are typically converted to $\delta^{34}S_{CDT}$ values by comparison with an internal reference gas whose isotopic composition has been calibrated to the internationally defined standard, CDT (Cañon Diablo Troilite, $^{34}S/^{32}S = 449.94 \times 10^{-4}$). For CF method, the conversion of $\delta^{34}S_{raw}$ to $\delta^{34}S_{CDT}$ of the sample was achieved by analyzing a set of mineral calibration standards at the beginning,

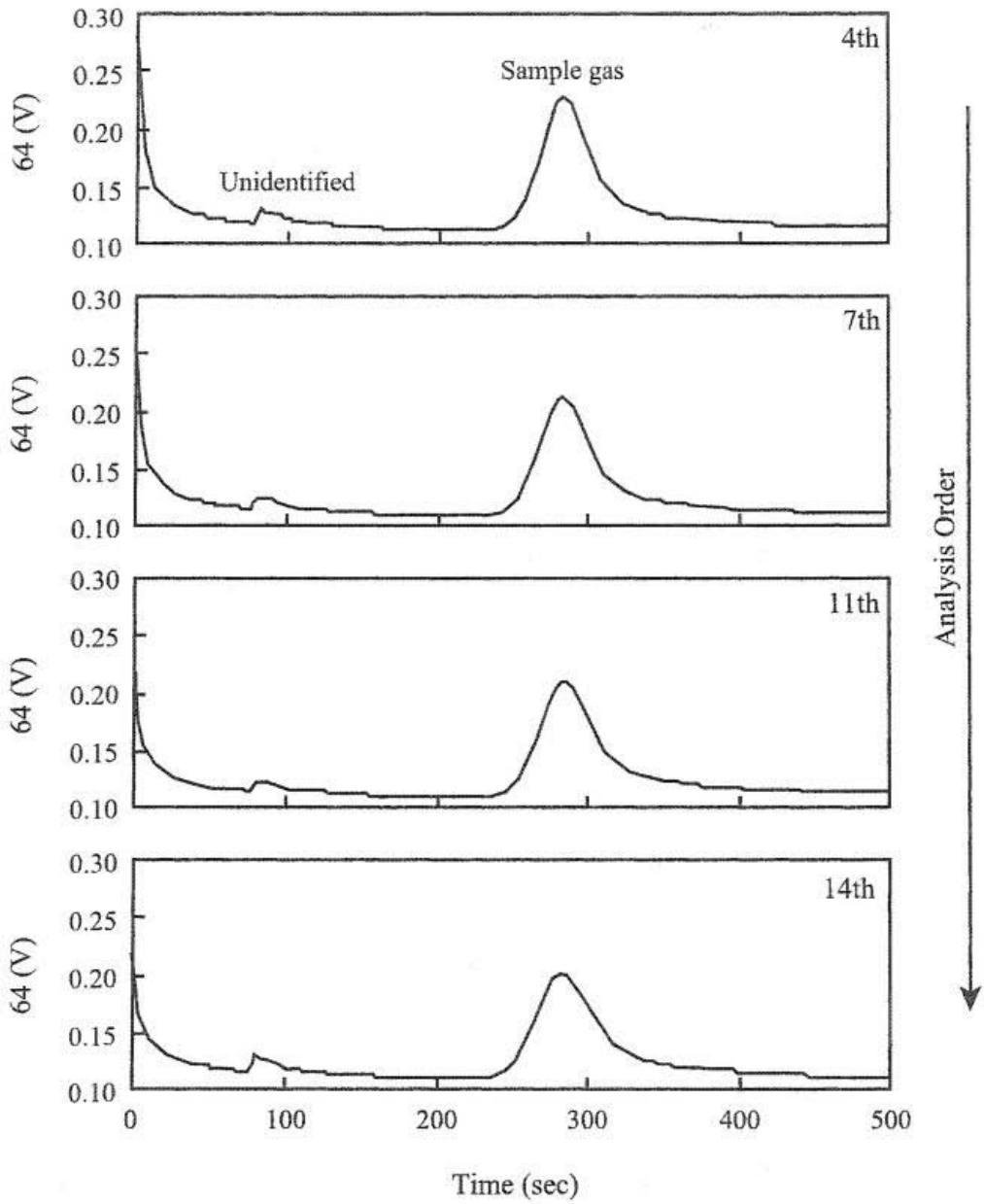

Figure 3-9. An example of typical series of peaks after the development of CF-lichen method, showing consistent peak size (amplitude and area) and peak start time. The peak of SO_2 reference gas started later than 500 sec.

middle and end of each run. A calibration line was calculated by performing least squares linear regression using the known $\delta^{34}S_{CDT}$ values and the measured $\delta^{34}S_{raw}$ values of the calibration standards. This procedure produces lines of slightly varying slope and intercept for each analysis run. This is due to differences in composition between samples, the condition of capillary tubes in the system with analysis and the degree of consumption of chemicals (i.e. Cu wire) in the combustion tube. Measured $\delta^{34}S_{raw}$ values from unknown samples are converted to $\delta^{34}S_{CDT}$ values using the calibration line calculated for that analysis run. An example of the calibration procedure is provided in Appendix II. Table 3-2 summarizes the five mineral calibration standards used for this study.

Table 3-2. Mineral calibration standards used in this study.

Standards	Composition	$\delta^{34}S_{CDT}$ (‰)	Distributors
NBS-127	barium sulphate	+20.32 ± 0.36	NIST
NBS-123	sphalerite	+17.09 ± 0.31	NIST
MUN-Py*[1]	pyrite	+1.26 ± 0.40	MUN
$BaSO_4$ #10*[2]	barium sulphate	+2.07 ± 0.40	MUN
CdS	cadmium sulphide	+11.00	Finnigan® MAT

Note:

* Made in the Department of Earth Sciences, MUN, and analyzed by other laboratories in Canada to obtain their isotopic compositions.

1 Made from a large cube of pyrite which was crushed, sieved and X-rayed for purity. Calibrated against NBS-123.

2 Made from reagent grade Na_2SO_4 and $BaCl_2$ by dissolving a known amount of the sulphate and then precipitating it as $BaSO_4$. Calibrated against MUN-Py.

CHAPTER 4

RESULTS AND DISCUSSION

Samples of the lichen *Alectoria sarmentosa* collected from the Botanical Garden, MUN, were analyzed by the developed CF-lichen method. The S concentration of this lichen averages 606 ± 93 ppm (n=4), measured by ion chromatography. Several tests were carried out to evaluate the developed CF-lichen method (Table 4-1), and the following sections describe the various features of the tests, the results and a discussion of their relative merits. The detailed results of individual analyses are provided in Appendix III.

4.1 EFFECTS OF V_2O_5

V_2O_5 has been widely used as a combustion/oxidation catalyst for S isotope analysis (Dugan, 1977; Eriksen and Johansen, 1994; Giesemann et al., 1994; Fry et al., 1996; Micromass®, 1996). However, the effects of V_2O_5 on S analysis have not been well established. In this study, the effects of V_2O_5 on the combustion reactions of minerals and lichens were investigated and Table 4-2 shows the summary of results.

4.1.1 Effects of V_2O_5 on mineral analysis

To test the effects of V_2O_5 on mineral combustion, three sets of NBS-127 analyses were performed (Table 4-2). Each set consisted of 6 replicates, having the same amount of

Table 4-1. Tests conducted to evaluate both CF-mineral and CF-lichen methods

- V_2O_5 effects
- Selection of calibration standards
- Accuracy and precision
- Minimum S amount
- Memory effects

Table 4-2. Results of V_2O_5 effect test.

Sample	V_2O_5 (mg)	Calibration standards	n	$\delta^{34}S_{CDT}$ (‰)
NBS-127*	No	NBS-123, MUN-Py	6	+20.5 ± 0.5
	0.10	NBS-123, MUN-Py	6	+20.0 ± 0.3
	0.20	NBS-123, MUN-Py	6	+20.2 ± 0.1
Lichen#	No	NBS-127, $BaSO_4$ #10	6	+6.6 ± 0.5
	0.20	NBS-127, $BaSO_4$ #10	6	+6.8 ± 0.3

Note:

* A mineral standard. Sample amount per analysis for three NBS-127 sets is approximately 0.26 mg.

\# Sample amount per analysis for two lichen sets is approximately 15.0 mg.

n Number of replicates.

Analytical errors are based on standard deviations (1σ).

$BaSO_4$ (0.26 mg), but differing in amount of V_2O_5 added. The first set had no V_2O_5 added. The second and third sets had 0.10 and 0.20 mg of V_2O_5 added, respectively. The calibration standards used were NBS-123 and MUN-Py. The same amount of V_2O_5 added to the samples was added to the calibration standards.

The measured $\delta^{34}S_{CDT}$ values are plotted in Figure 4-1. Mean values are +20.5 ± 0.5‰ for the set with no V_2O_5, and +20.0 ± 0.3‰ and +20.2 ± 0.1‰ for the sets with 0.10 and 0.20 mg V_2O_5, respectively (Table 4-2). These three values are not significantly different from one another at the 95% and 99% confidence levels (Duncan and Cochran tests, respectively). However, as can be seen in Figure 4-1, the set with 0.20 mg of V_2O_5 produced better precision than the other two. In general, standard deviation decreases with increasing amount of V_2O_5, at least up to 0.20 mg.

The areas, widths and amplitudes of the mass 64 peaks for each of the three NBS-127 sets described above are plotted in Figure 4-2. The reason for the wide variation in peak area for the first analysis is not known. The peak areas for the 0.20 mg V_2O_5 set do not vary greatly with analysis, while the other two sets show slightly decreasing trends with analysis (Figure 4-2a). In addition, the widths and amplitudes for the set with 0.20 mg of V_2O_5 are consistently lower and higher, respectively, compared to those of two other sets (Figures 4-2b, c). The above two facts indicate that the combustion of minerals with 0.20 mg of V_2O_5 is more consistent, more complete and faster than those with no and 0.10 mg of V_2O_5. Dugan (1977) also suggested, for more complete combustion of inorganic materials, that

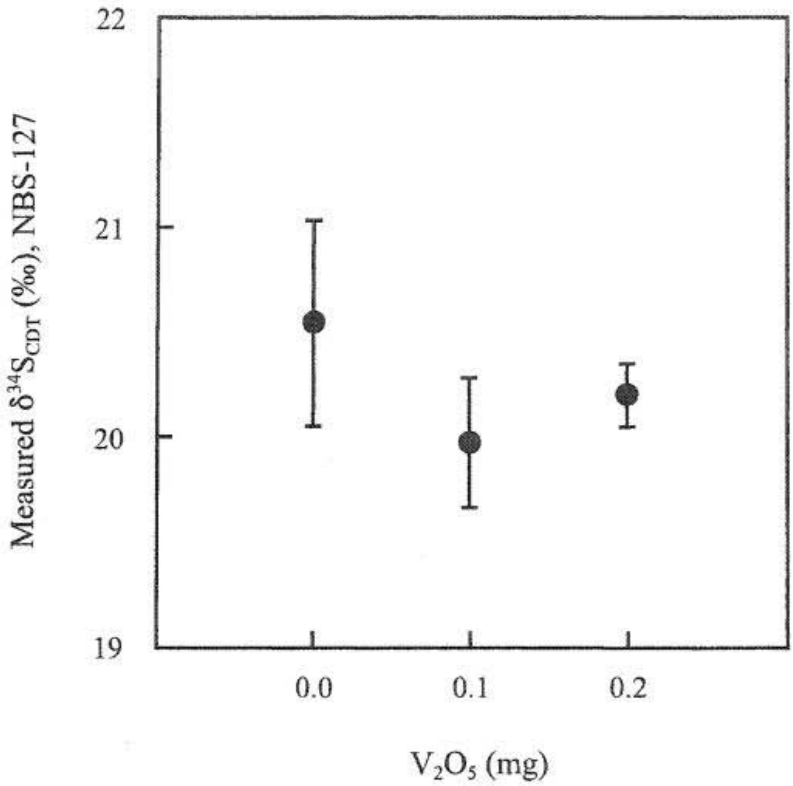

Figure 4-1. V_2O_5 effects on the $\delta^{34}S_{CDT}$ determination of NBS-127. Error bars are based on standard deviations (1σ).

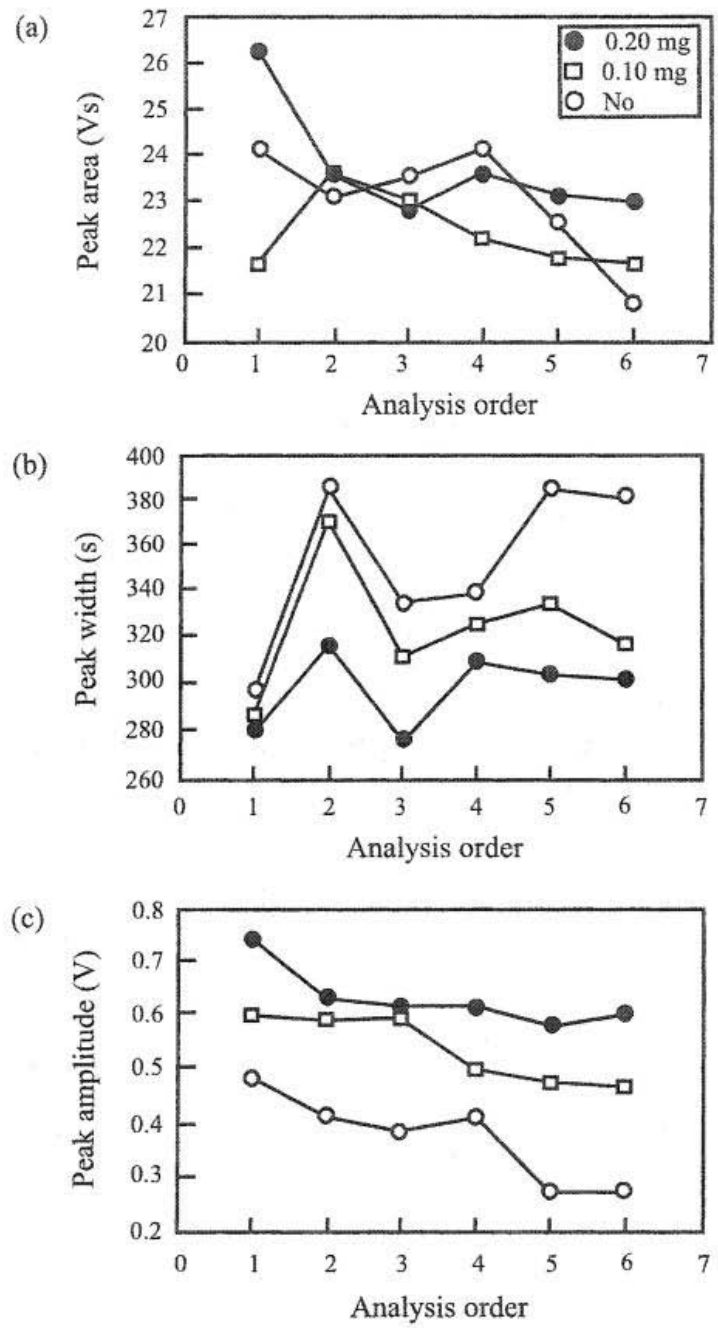

Figure 4-2. Areas, widths and amplitudes of peaks (mass 64) of NBS-127 with no (open circles), 0.10 mg (open squares) and 0.20 mg (solid circles) of V_2O_5. Each data point represents single analysis.

V_2O_5 should be included as an oxidation catalyst in an amount at least as great as the sample size. In conclusion, the addition of V_2O_5 yields better reproducibility and peak shape. Kendall (personal communication) found the same result that the addition of V_2O_5 did improve the precision although the accuracy of δ-values did not change. For this reason, in this study, about 0.20 mg of V_2O_5 was added to all minerals (0.10-0.20 mg) analyzed.

4.1.2 Effects of V_2O_5 on lichen analysis

In order to test the effects of V_2O_5 on combustion reactions of untreated lichens, two sets of lichen samples were analyzed with different amount of V_2O_5; one with no V_2O_5 and the other with 0.20 mg V_2O_5 (Table 4-2). Each set consisted of 6 replicates, containing similar amounts of lichen (15 mg, containing 9 μg S). NBS-127 and $BaSO_4$ #10 were used as calibration standards. On the basis of V_2O_5 effects on mineral analysis reported in Section 4.1.1, about 0.20 mg of V_2O_5 was added to the two calibration mineral standards.

Figure 4-3 shows the $\delta^{34}S_{CDT}$ values obtained for each set. Means are +6.6 ± 0.5‰ for the set with no V_2O_5, and +6.8 ± 0.3‰ for the set with 0.20 mg V_2O_5. These two values are not significantly different from each other in mean or in standard deviation (1σ) at the 95% confidence level (T and F tests). In addition, the areas, widths and amplitudes of peaks (mass 64) of the two sets are not greatly different except for the fifth analysis with no V_2O_5 added, the reason for which is not known (Figure 4-4). The apparent absence of V_2O_5 effects on the combustion of lichens may indicate that the amount of V_2O_5 (~0.20 mg) added was

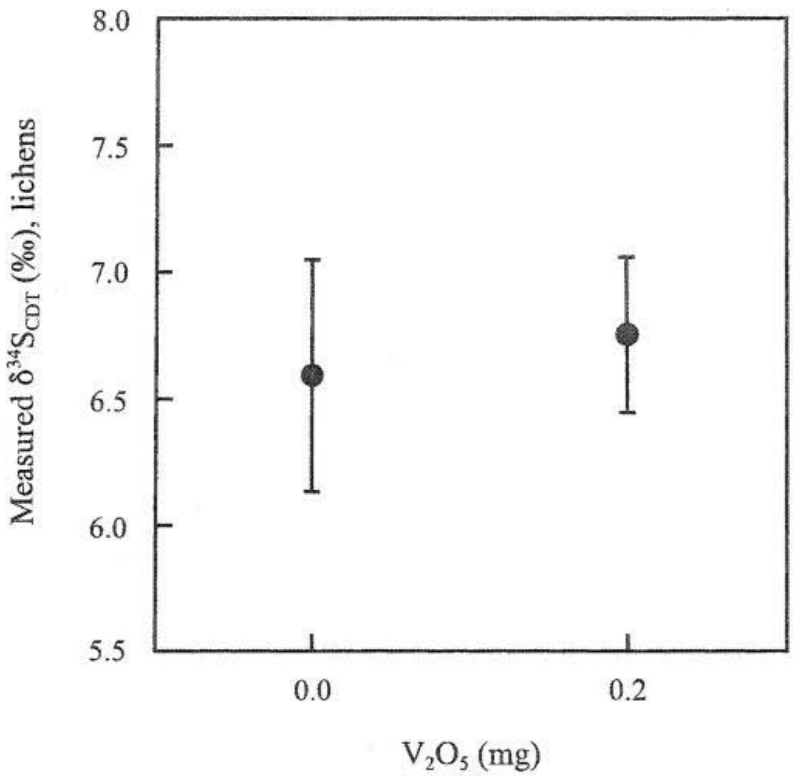

Figure 4-3. V_2O_5 effects on the $\delta^{34}S_{CDT}$ determination of lichens. Error bars are based on standard deviations (1σ).

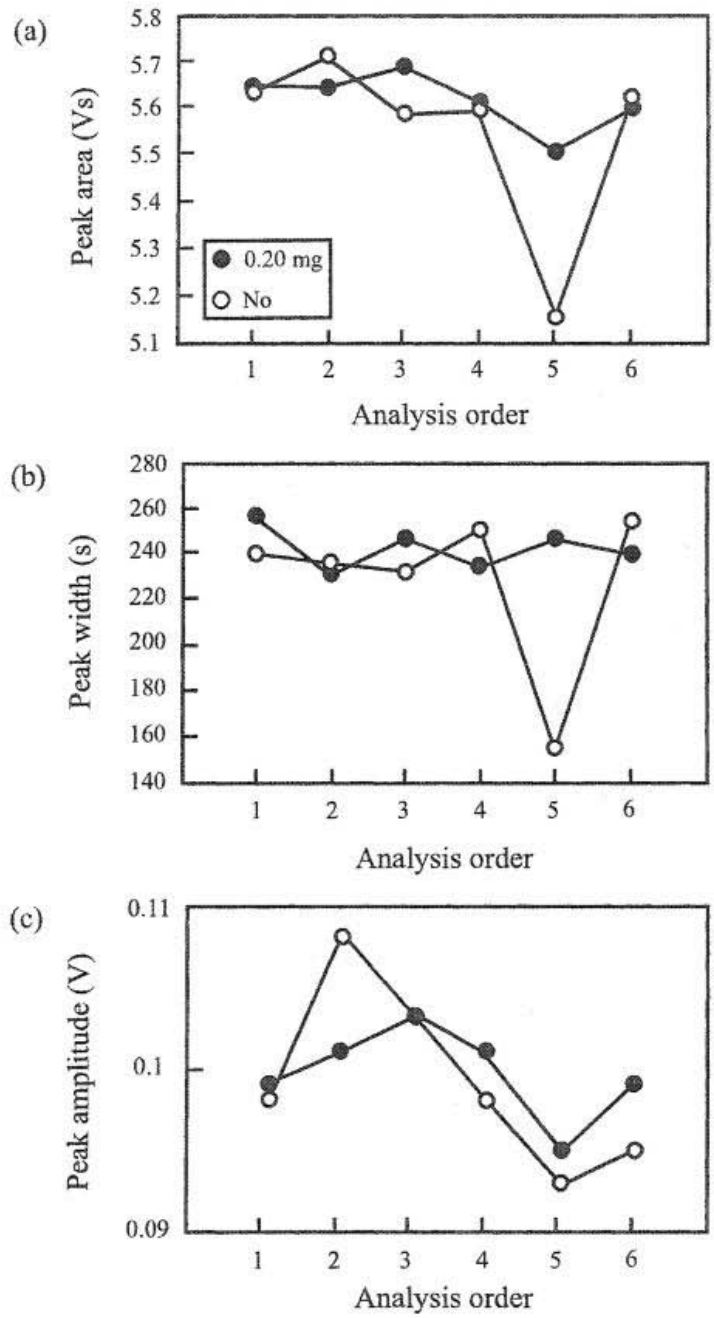

Figure 4-4. Areas, widths and amplitudes of peaks (mass 64) of lichens with no (open circles) and 0.20 mg (solid circles) of V_2O_5. Each data point represents single analysis.

not large enough to make significant differences. Since the addition of V_2O_5 amount similar with the sample amount produces more reproducible delta values and peaks in mineral analyses in Section 4.1.1, it was assumed that similar amount of V_2O_5 with the amount of lichen samples should be added. Although, there was no difference with the addition of V_2O_5, about 0.20 mg of V_2O_5 was added to all lichen samples analyzed in this study in order to make conditions of combustion as similar as possible to the mineral standards.

4.2 SELECTION OF CALIBRATION STANDARDS

As mentioned earlier in Section 3.4, raw delta values ($\delta^{34}S_{raw}$) determined by IRMS analysis are converted to $\delta^{34}S_{CDT}$ using mineral standards with known $\delta^{34}S_{CDT}$ values. However, it is desirable to investigate differences in calibration using different mineral types. In this study both sulphates and sulphides were tested as calibration standards since the oxygen in the sulphates may be another source of oxygen to alter the measured $\delta^{34}S$.

The $\delta^{34}S_{raw}$ values of duplicates or triplicates of the five mineral standards (NBS-127, $BaSO_4$ #10, CdS, MUN-Py and NBS-123) measured by CF-IRMS are plotted against their known $\delta^{34}S_{CDT}$ values in Figure 4-5. The linear correlation between the measured $\delta^{34}S_{raw}$ and their known $\delta^{34}S_{CDT}$ values (Known $\delta^{34}S_{CDT}$ = 1.186 (±0.009) × $\delta^{34}S_{raw}$ + 1.625 (±0.218), r^2 = 0.999) indicates that there is no difference between sulphate and sulphide standards as well as among all of the standards. Thus, in this study, for any given run, any combination of the five mineral standards may have been used.

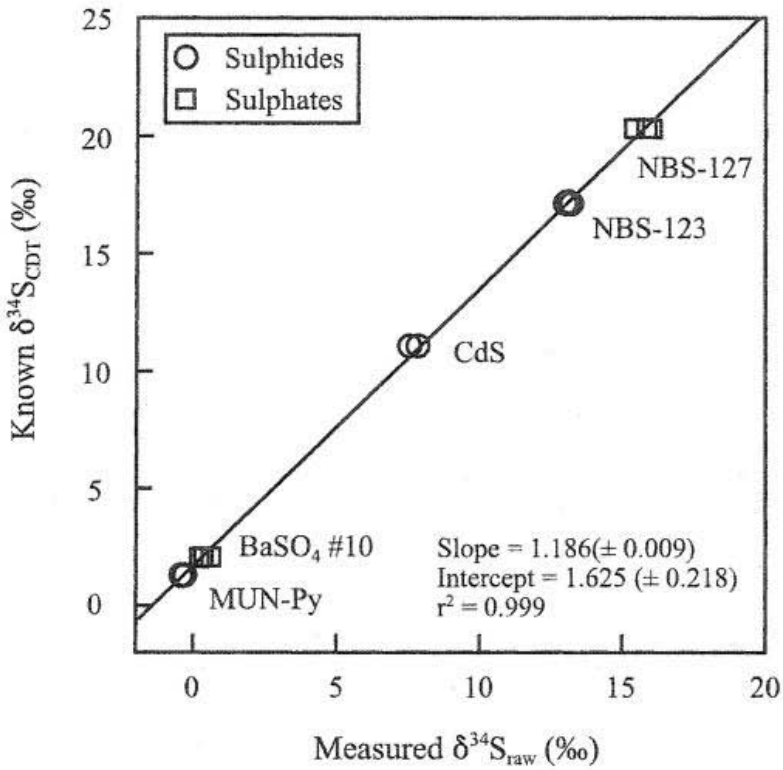

Figure 4-5. Measured $\delta^{34}S_{raw}$ values vs. corresponding known $\delta^{34}S_{CDT}$ values of five mineral calibration standards. Each data point represents single analysis.

4.3 ACCURACY AND PRECISION

The accuracy of an analytical method is typically estimated by comparing the measured value to the known value. This was the approach used for mineral analysis. Unfortunately, there are no lichen standards with accepted S-isotopic compositions. This problem can be overcome, however, by comparing the values obtained using the new method with those determined by one or more independent methods. For untreated lichen analysis by CF-IRMS in this study, this was the approach used to estimate the accuracy. Mineral analysis was also evaluated in this was.

The precision of an analytical method can be classified into two types; internal and external (Barrie and Prosser, 1996). Internal precision includes errors resulting from the performance of the instrument itself. For example, repeated analyses of the same aliquot of SO_2 gas by IRMS may represent internal precision. External precision represents errors involved in the entire analytical processes. For example, in this study, these would include errors caused during the conversion of S in lichen to SO_2 gas, transferring the gas through the inlet system, and measurement by IRMS. For DI-IRMS technique, it is possible to evaluate the two different types of precision separately. However, for the CF-IRMS method, only external precision can be estimated because it integrates the sample preparation with the analysis.

4.3.1 Accuracy and precision of mineral analysis

To evaluate the accuracy and precision for CF-mineral analysis, the mean $\delta^{34}S_{CDT}$ value obtained with $BaSO_4$ by this method (+5.9 ± 0.3‰, n=30) was compared to that measured by the DI method (+6.2 ± 0.2‰, n=5) (Table 4-3 and Figure 4-6). The accuracy and precision of the two methods are not significantly different at the 99% and 95% confidence levels (T and F tests, respectively), demonstrating that no significant isotopic fractionation occurred during the entire analytical processes.

The accuracy of CF-mineral analysis can also be evaluated by comparing the $\delta^{34}S_{CDT}$ values of five mineral calibration standards measured by the CF-mineral method in Section 4.2 to their known $\delta^{34}S_{CDT}$ values. The results are summarized in Table 4-4 and plotted in Figure 4-7. Three sulphide standards (NBS-123, MUN-Py and CdS) were analyzed as samples using two sulphate standards (NBS-127 and $BaSO_4$ #10) as calibration standards. The values of $\delta^{34}S_{CDT}$ are plotted against their known $\delta^{34}S_{CDT}$ values in Figure 4-7a. The slope (0.990 ± 0.009) and intercept (0.169 ± 0.173) of the regression line passing through the origin imply an excellent accuracy for the analysis of three sulphide minerals by CF-IRMS. The same method was applied to the two sulphates using the three sulphides as calibration standards. Similar accuracy is achieved for the sulphate analyses as sulphide analyses, with the slope of 1.010 ± 0.013 and the intercept of -0.171 ± 0.296 of the regression line (Figure 4-7b). These two comparisons demonstrate that accurate measurement of $\delta^{34}S_{CDT}$ can be obtained on minerals by on-line method, with $\delta^{34}S$ values ranging from +1 to

Table 4-3. Comparison of $\delta^{34}S_{CDT}$ values of the lichen samples, measured by the three isotope analysis methods.

Methods	Calibration standards	n	$\delta^{34}S_{CDT}$ (‰)
DI	-	5	+6.2 ± 0.2
CF-$BaSO_4$	NBS-127, $BaSO_4$ #10	30	+5.9 ± 0.3
CF-lichen	NBS-123, MUN-Py	15	+6.1 ± 0.3
	NBS-127, $BaSO_4$ #10	15	+6.3 ± 0.4

Note:
n Number of replicates.
Analytical errors are based on standard deviations (1σ).

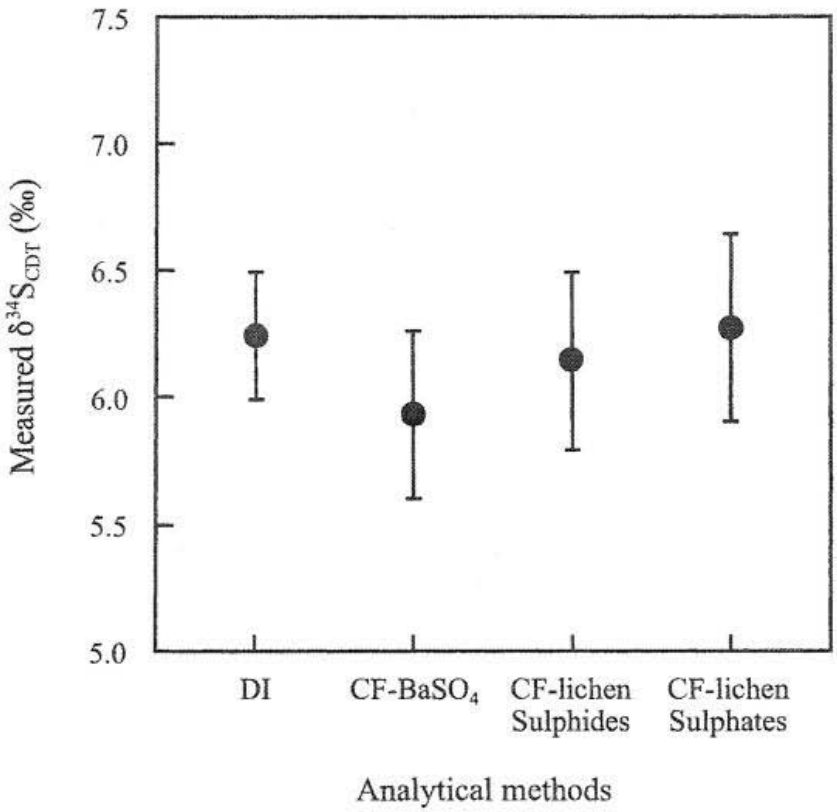

Figure 4-6. $\delta^{34}S_{CDT}$ values measured by three isotope analysis methods; DI, CF-$BaSO_4$ and CF-lichen. Two sets of CF-lichen analysis were calibrated by sulphides and sulphates, respectively. Error bars are based on standard deviations (1σ).

Table 4-4. Results of CF-mineral analyses for the mineral calibration standards.

Samples		Known $\delta^{34}S_{CDT}$ (‰)	Measured $\delta^{34}S_{CDT}$ (‰)	n	Calibration standards
Sulphides	NBS-123	+17.09 ± 0.31	+17.2 ± 0.1	3	NBS-127, $BaSO_4$ #10
	MUN-Py	+1.26 ± 0.40	+1.2 ± 0.1	3	
	CdS	+11.00	+10.7	2	
Sulphates	NBS-127	+20.32 ± 0.36	+20.3 ± 0.4	3	NBS-123, MUN-Py, CdS
	$BaSO_4$ #10	+2.07 ± 0.40	+2.2 ± 0.2	3	

Note:
n Number of replicates.
Analytical errors are based on standard deviations (1σ).

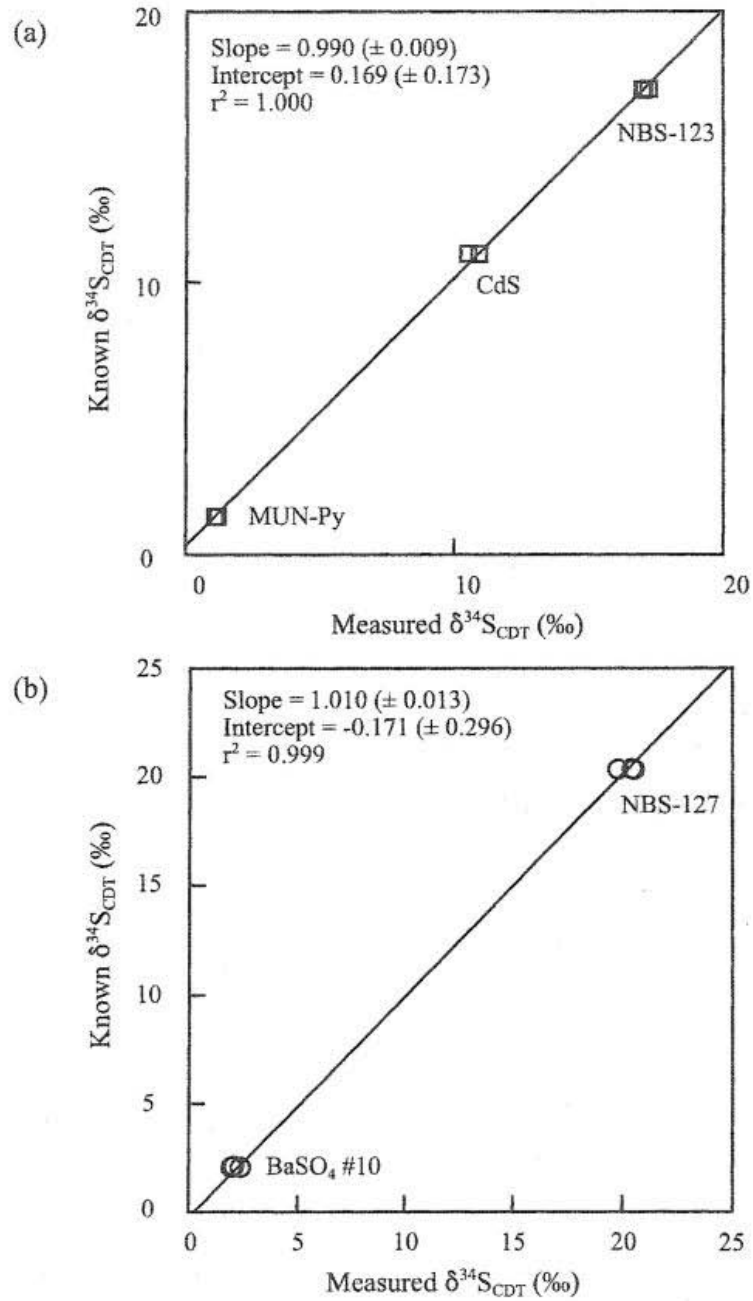

Figure 4-7. Comparison of $\delta^{34}S_{CDT}$ values measured by CF-mineral analyses for mineral calibration standards with their known $\delta^{34}S_{CDT}$ values; (a) sulphides calibrated by sulphates and (b) sulphates calibrated by sulphides. Each data point represents single analysis.

+20‰.

The standard deviations(1σ) of four calibration standards(NBS-123, MUN-Py, NBS-127 and $BaSO_4$ #10) were compared to their published precisions (Table 4-4). CdS was not included in this comparison because of insufficient replicates (n=2). For all of the standards analyzed, the measured standard deviations by on-line method are smaller than their published precisions.

4.3.2 Accuracy and precision of lichen analysis

In order to evaluate the accuracy and precision for CF-lichen analysis, the mean $\delta^{34}S_{CDT}$ value of the lichen samples obtained by this method was compared to those measured by two other independent methods, DI and CF-$BaSO_4$. Two different sets of the same lichen were analyzed by CF-lichen method; one set was calibrated using sulphides (NBS-123 and MUN-Py) and the other set using sulphates (NBS-127 and $BaSO_4$ #10). Each set consisted of fifteen lichen samples (15 mg/analysis, containing 9 μg S).

The mean $\delta^{34}S_{CDT}$ values achieved by the three different methods are given in Table 4-3 and compared in Figure 4-6. Similar means between CF-lichen analyses calibrated by sulphides (+6.1 ± 0.3‰) and sulphates (+6.3 ± 0.4‰) demonstrate that the effects of employing different types of calibration standard are negligible. The mean $\delta^{34}S_{CDT}$ values achieved by DI (+6.2 ± 0.2‰) and CF-$BaSO_4$ (+5.9 ± 0.3‰) analyses are not significantly different from those by CF-lichen analyses at the 95 or 99% confidence level (T test),

demonstrating that no significant isotopic fractionation occurred during the entire analytical processes including combustion. It is surprising that lichen with S concentration as low as 9 μg can be analyzed by CF method with an accuracy which is comparable to that obtained by DI and CF-$BaSO_4$.

In order to test the dependence of the accuracy of CF-lichen analysis on S concentration, lichens with various S concentrations were analyzed by this method and the results are compared to those obtained by the DI method. Four different lichen samples (MS-PN-09 and MS-BG: *Alectoria sarmentosa;* AG-214 and AG-017: *Cladonia sp.*) were selected for the test (Table 4-5). These samples were collected from various locations in Newfoundland, and have a relatively wide range of S concentrations (374 to 606 ppm S) and S isotopic compositions (+4 to +16‰, determined by DI analyses) (Table 4-5). NBS-127 and $BaSO_4$ #10 were used as calibration standards for CF-lichen analyses.

The mean $\delta^{34}S_{CDT}$ values of the lichen samples measured by CF-lichen and DI methods are summarized in Table 4-5 and are compared in Figure 4-8. In Figure 4-8, the solid line represents the linear regression of the four lichen samples and the shaded area represents the 95% confidence interval of the regression. The slope (1.071 ± 0.062) and intercept (-1.022 ± 0.639) of the regression line demonstrate again that within acceptable error limits, the CF-lichen method has an excellent accuracy for the tested range of S amount (5.8 to 9.5 μg) per analysis and $\delta^{34}S_{CDT}$ value (+4 to +16‰).

Table 4-5. Analytical results of four different lichen samples obtained by CF-lichen and DI methods.

Samples	Species	Sampling sites	S (ppm)[1]	S (μg)[2]	CF, $\delta^{34}S_{CDT}$ (‰)[3]	DI, $\delta^{34}S_{CDT}$ (‰)[3]
MS-PN-09[#]	*Alectoria sarmentosa*	Burin Peninsula	464	6.9	+15.9 ± 0.5 (14)	+16.0 ± 0.5 (5)
MS-BG[*]	*Alectoria sarmentosa*	St. John's	606	9.5	+6.3 ± 0.4 (15)	+6.2 ± 0.2 (5)
AG-214[♮]	*Cladonia sp.*	Western	374	5.8	+10.0 ± 0.8 (11)	+9.7 ± 0.5 (5)
AG-017[♮]	*Cladonia sp.*	Avalon Peninsula	426	6.5	+5.3 ± 0.5 (13)	+4.2 ± 0.5 (5)

Note:

1 S concentration in the lichen, determined by ion chromatography analysis.

2 S amount used per CF-lichen analysis.

3 Numbers in parentheses represent the number of replicates. Analytical errors are based on standard deviations (1σ).

[#] Sampling, and ion chromatography and DI analyses were conducted by Nowotczynski (1998).

[*] Sampling (from Botanical Garden, MUN), and ion chromatography and DI analyses were conducted by the author.

[♮] Samples collected by Blake (1998), and analyzed by Gollop (1998) using ion chromatography and DI analyses.

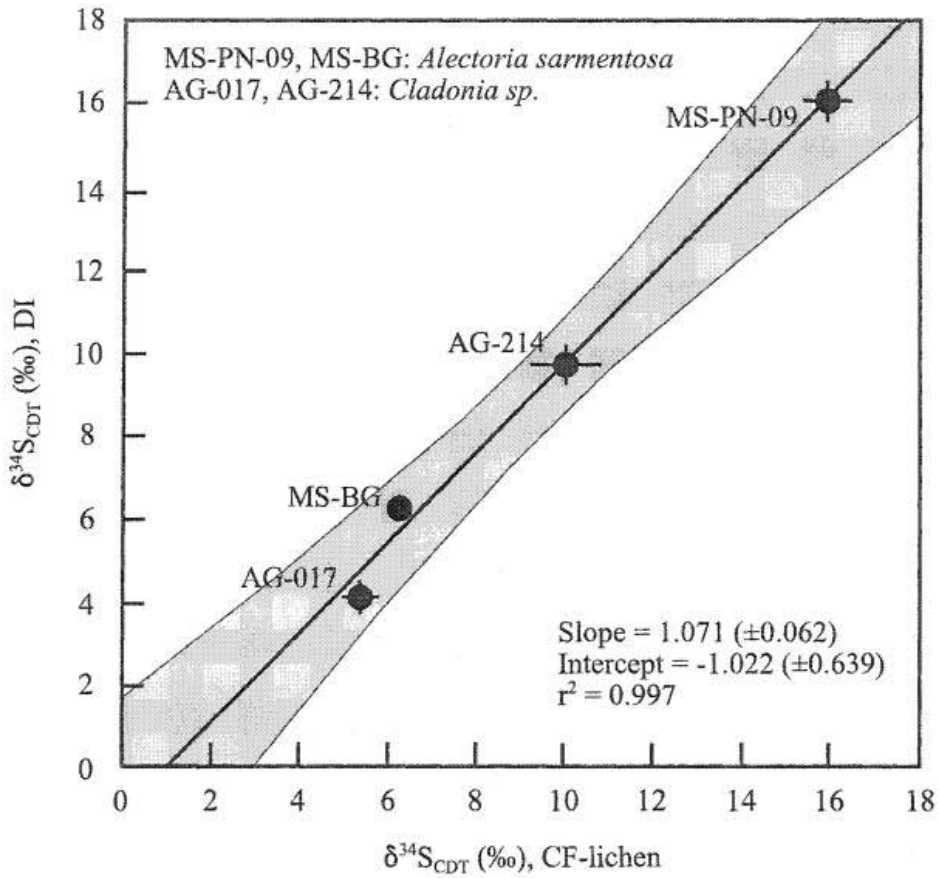

Figure 4-8. Comparison of $\delta^{34}S_{CDT}$ values of four different lichen samples measured by CF-lichen and DI methods. The solid line represents the linear regression and the shaded area represents the 95% confidence interval of the regression. Error bars are based on standard deviations (1σ). Errors are smaller than that symbols when they are not shown.

The analytical precisions obtained by CF-lichen analyses are 0.3‰ (calibrated by sulphide standards) and 0.4‰ (calibrated by sulphate standards) (Table 4-3 and Figure 4-6). These precisions are not significantly different from those of the DI (0.2‰) and CF-$BaSO_4$ (0.3‰) methods at the 95% confidence level (F test), demonstrating that the on-line CF-lichen method can produce excellent precision comparable to those of the other two.

4.4 MINIMUM S AMOUNT

In the previous section, it was mentioned that analytical precision is a function of S concentration introduced into the system; precision becomes poorer with decrease in S concentration. Minimum S amount in this study is defined as the minimum S concentration required for an analysis to yield a specified precision around the δ-value. In order to determine the minimum S amount, analyses were performed on sample sizes representing various S concentrations. In some cases, single analyses were performed while for others several replicates were analyzed allowing the determination of analytical errors for each point.

4.4.1 Minimum S amount for mineral analysis

For CF-mineral analysis, minimum S amount was tested with a mineral standard, NBS-127. The S concentration tested ranged from 36 μg (corresponding 0.26 mg) to 8 μg (corresponding 0.06 mg). The results are presented in Figure 4-9.

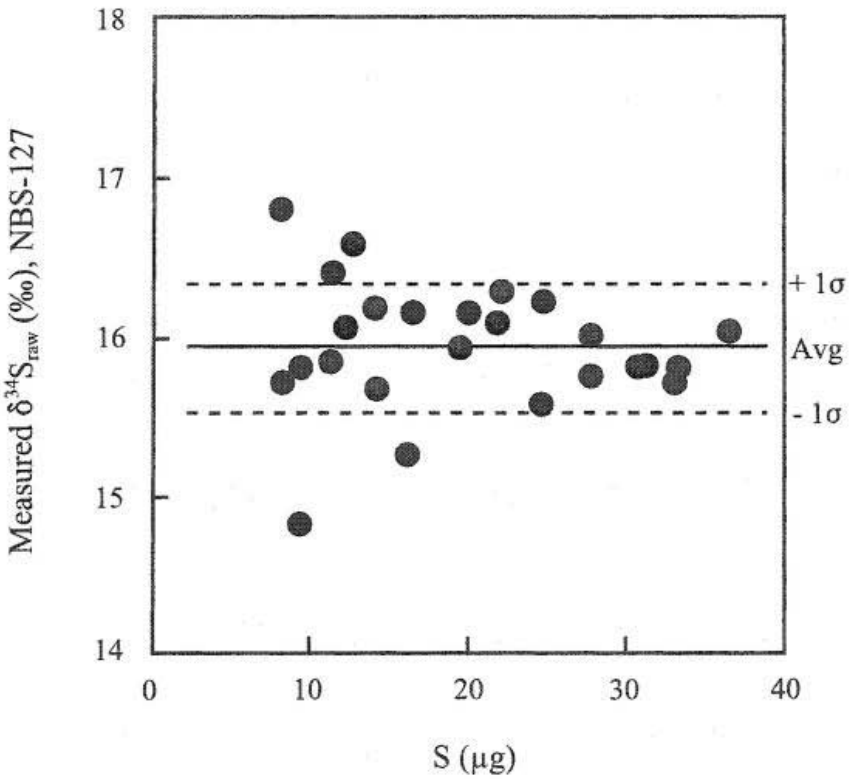

Figure 4-9. Variations of $\delta^{34}S_{raw}$ values with decreasing S amount for NBS-127. Each data point represents single analysis.

The mean $\delta^{34}S_{raw}$ value is +15.9‰ with standard deviation (1σ) of ±0.4‰ (n=25). The minimum S amount for CF-mineral technique estimated with NBS-127 is approximately 10 μg S (Figure 4-9). This result is consistent with that of Giesemann, et al., (1994) who reported that the minimum S amount necessary for on-line S-isotope analysis (using $BaSO_4$ and Ag_2S) was about 10 μg S. In addition, their reproducibility down to 20 μg S with $BaSO_4$ (0.2‰, n=15) shows an excellent agreement with that of NBS-127 (0.2‰, n=13) in this study.

4.4.2 Minimum S amount for lichen analysis

For the test of minimum S amount for lichen analysis, single lichen samples were analyzed, ranging from about 9 μg (corresponding to 15 mg of sample) to about 3 μg (corresponding to 5 mg of sample) (Figure 4-10). NBS-127 and $BaSO_4$ #10 were used as calibration standards.

The mean $\delta^{34}S_{CDT}$ value of these analyses is +6.5‰ with standard deviation (1σ) of ±0.5‰ (n=12). Lichen samples containing as little as 3 μg S were analyzed by the CF-lichen method (Figure 4-10).

To determine the analytical errors for different S amounts, several lichen replicate sets, with S amount ranging from 9.5 μg to 3.7 μg, were analyzed (Table 4-6). Each set consisted of fourteen or fifteen replicates and different calibration standard sets were used for different replicate sets. Lichen samples containing as little as 5.5 μg S yielded valid

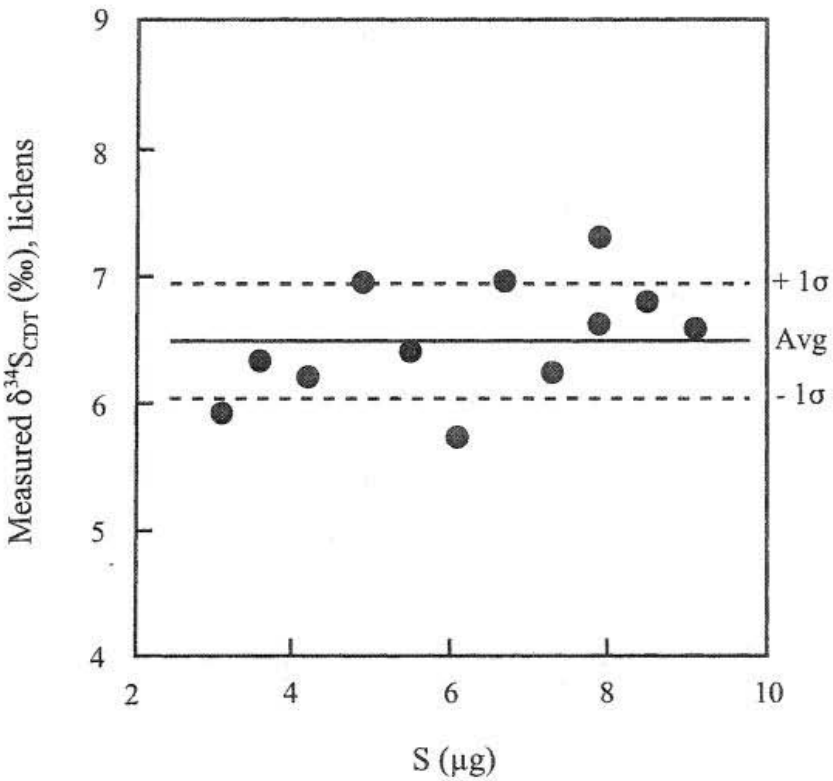

Figure 4-10. Variations of $\delta^{34}S_{CDT}$ values with decreasing S amount for lichens. Each data point represents single analysis.

Table 4-6. Average $\delta^{34}S_{CDT}$ values of untreated lichen sets with different sample size and calibration standards analyzed for each set.

Lichen (mg)	S (μg)	Calibration standards	n	$\delta^{34}S_{CDT}$ (‰)
15.6	9.5	NBS-127, $BaSO_4$ #10	15	+6.3 ± 0.4
13.0	7.9	NBS-123, MUN-Py	14	+6.5 ± 0.5
12.1	7.3	NBS-127, $BaSO_4$ #10	14	+6.6 ± 0.7
9.1	5.5	NBS-127, MUN-Py	14	+6.7 ± 0.6
6.1	3.7	NBS-127, $BaSO_4$ #10	14	+7.3 ± 1.1

Note:
n Number of replicates.
Analytical errors are based on standard deviations (1σ).

isotope measurements without a loss of precision. The same result was observed in Table 4-5 and Figure 4-8. Sample AG-214 containing 5.8 μg S showed excellent accuracy and precision compared to analysis by DI method. However, further reduction of sample size comes at the expense of precision (Table 4-6).

In Figure 4-11, the standard precision (1σ) data in Table 4-5 (open circles) and in Table 4-6 (solid circles) are plotted against their corresponding S amounts. This diagram provides insight on the precision surrounding δ-values reported for other studies associated with lichen analysis, once the S concentrations in lichen samples are determined.

4.5 MEMORY EFFECTS

Memory effects occur when an analysis is contaminated by the residual traces of the previous analyses. This is a particular problem for SO_2 analysis because of its "sticky" character. The problem can be overcome in DI-IRMS by heating the inlet system to improve the flow of gas or by allowing longer pumping times between samples. Although this problem can be reduced in the CF-IRMS system because the high flow of He carrier gas purges the capillary interface along which SO_2 gas is transported, inter-sample memory effects on mineral and lichen analyses were investigated in this study. This was done by alternating analyses of samples with widely differing isotopic compositions with the analysis order organized to maximize any potential memory effect.

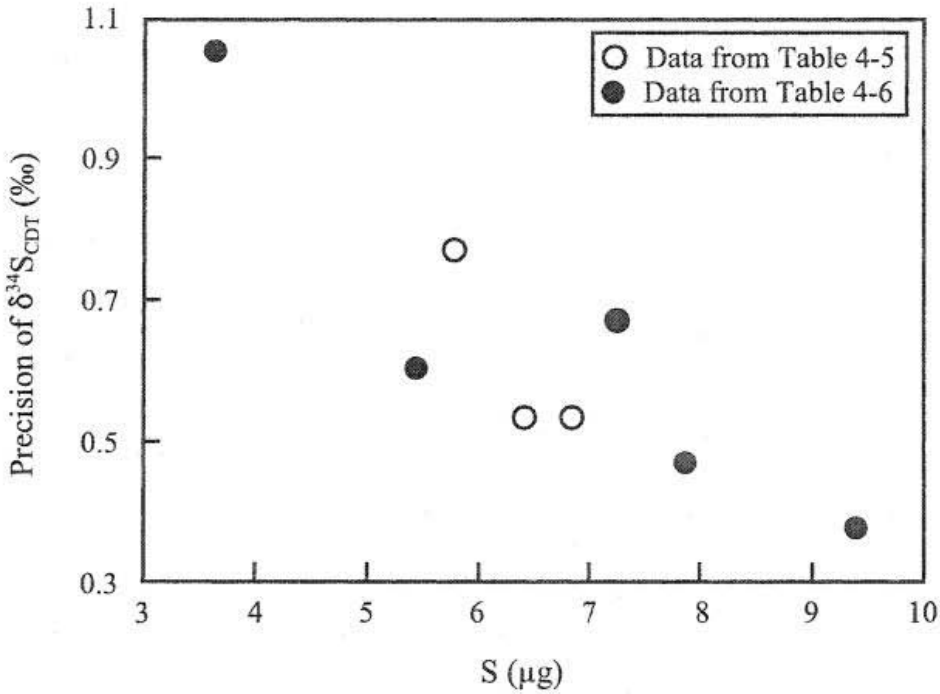

Figure 4-11. Correlation between precision of $\delta^{34}S_{CDT}$ and S concentration.

4.5.1 Memory effects on mineral analysis

The test of memory effects on mineral analysis was conducted with two mineral standards, NBS-123 and MUN-Py. The difference in $\delta^{34}S_{CDT}$ value for the two standards is approximately 16‰; +17.09 ± 0.31‰ for NBS-123 and +1.26 ± 0.40‰ for MUN-Py. Fourteen mineral samples (five NBS-123 and nine MUN-Py) were analyzed in series and the calibration standards used were NBS-127 and $BaSO_4$ #10.

As shown in Figure 4-12, no memory effects are observed. The mean and standard deviations (1σ) obtained are +17.5 ± 0.3‰ and +1.0 ± 0.2‰ for NBS-123 and MUN-Py, respectively. These values are in good agreement with their known values. In particular, precision for both standards are better than their reported precision.

4.5.2 Memory effects on lichen analysis

For lichen analysis, the memory effects were tested with two different lichen samples, MS-BG and MS-PN-09. The sample amounts used were about 11 mg (~6.5 μg S) for MS-BG and about 15 mg (~7 μg S) for MS-PN-09. The approximate difference in $\delta^{34}S_{CDT}$ value between the two lichen samples is 10‰, based on previous DI analysis; +6.2 ± 0.2‰ (n=5) for MS-BG and +16.0 ± 0.5‰ (n=5) for MS-PN-09. The DI analysis for MS-PN-09 was obtained by Nowotczynski (1998). A total of seventeen samples (nine MS-BG and eight MS-PN-09) were analyzed in series and NBS-127 and $BaSO_4$ #10 were used as calibration standards.

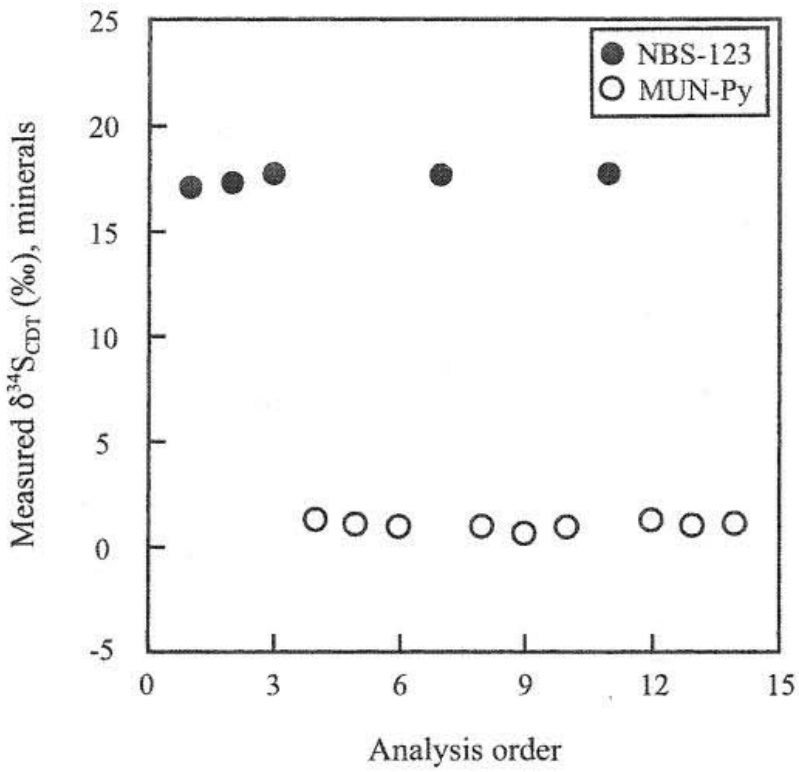

Figure 4-12. Memory effect test with minerals. Errors based on standard deviations (1σ) are smaller than the symbols.

As shown in Figure 4-13, there were no memory effects between the two lichen samples. The mean $\delta^{34}S_{CDT}$ value of MS-BG replicates is +6.8‰, with standard deviation (1σ) of ±0.5‰. For MS-PN-09 replicates, the mean is +15.7‰, with standard deviation (1σ) of ±0.7‰. Significant levels of differences between the values obtained by two methods were tested statistically: 99% and 95% (T and F tests, respectively) for MS-BG, and 95% (T and F tests), for MS-PN-09.

4.6 TIME AND S AMOUNT REQUIRED PER ANALYSIS

The total time required per analysis for the three analytical methods mainly depends on the number of sample preparation steps (see Figure 2.3). The required time per analysis of untreated lichen by CF-IRMS method has been reduced to approximately 15 minutes by eliminating chemical sample preparation steps, including $BaSO_4$ extraction by Parr Bomb™ oxidation and SO_2 extraction line. While about 18 hours are necessary for off-line method and about 13 hours for on-line method with $BaSO_4$ (Table 4-7). The time required for the physical pretreatment steps, such as air-drying, cleaning, grinding and homogenizing, was excluded for the total estimated time in Table 4-7.

The elimination of chemical sample preparation steps also reduces the amount of S required per analysis. The reasonable S amount per analysis is approximately 680 μg S for off-line method and, for on-line method with $BaSO_4$, about 35 μg S. However, for on-line method with untreated lichen, only 9 μg S is required (Table 4-7). This reduction in S

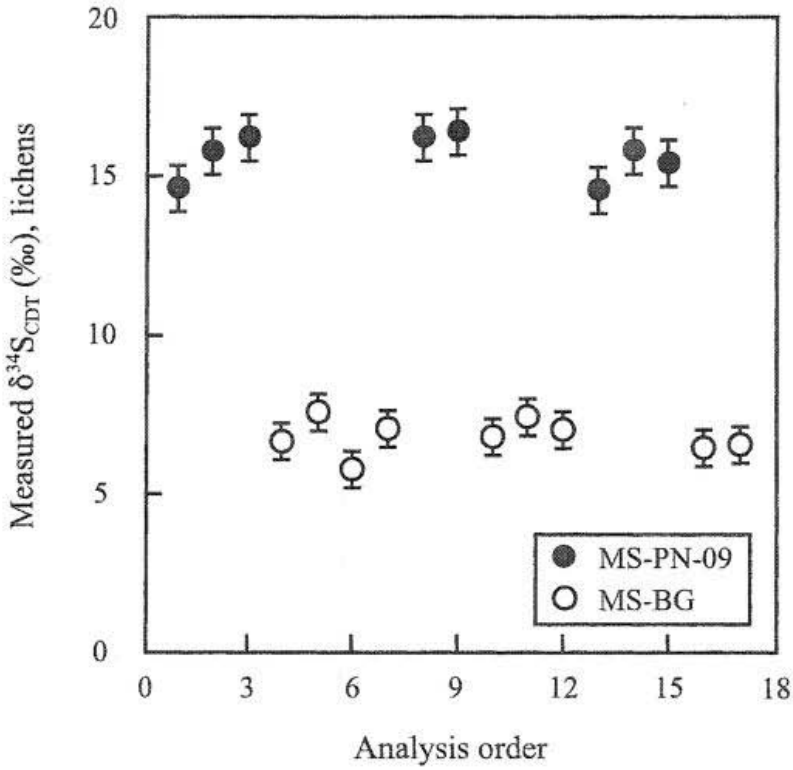

Figure 4-13. Memory effect test with lichens. Errors bars are based on standard deviations (1σ).

amount is a great advantage in a study requiring the analysis of very small samples, where the conventional off-line method cannot be applied.

Table 4-7. Comparison of total time and S amount required per analysis for the three isotope analysis methods.

Analytical methods	Time (min)	S (μg)
DI	1100	680
CF-$BaSO_4$	800	35
CF-lichen	15	9

Note:
Time of the physical pretreatments for the three methods is excluded.

CHAPTER 5

VARIATIONS OF S ISOTOPIC COMPOSITIONS IN A LICHEN STRAND

5.1 INTRODUCTION

During a previous study (Blake, 1998) it was determined that repeated off-line isotopic analysis of lichen samples (*Alectoria sarmentosa*) ground using a mortar and pestle yielded values with very high associated standard deviations, on the order of ±1.5‰. Since mechanical crushing, followed by sieving to uniform particle size improved standard deviations to ±0.5‰, the initial results were attributed to isotopic inhomogeneity in the sample itself. The technique developed in this thesis makes it possible to investigate the nature of isotopic inhomogeneity in lichen strands.

Fruticose lichens grow both centripetally and apically (Hale, 1973; Hale, 1974). In the early stages, most growth activity is funneled into increasing the surface area of the lichen thallus. Eventually, lateral transport of nutrients between the margin and center of the thallus is hampered and the older parts thicken somewhat or become folded, produce vegetative structures, or divert energy into the reproductive formation (Hale, 1974). Honnegger (1996) mentioned that, in adult parts, the fungal and algal cells are less active in their uptake of nutrients and other elements while, in new growing parts, the cells are highly active. Moreover, with age, the cortex becomes thicker and more compact, such that it prevents or impedes the penetration of SO_2 into the lichen strand (Wirth and Türk, 1974).

5.1.1 Sampling location: Come-By-Chance oil refinery

In order to maximize the possibility of observing $\delta^{34}S$ variation within lichen strands, they should be collected from an area where a change in atmospheric S composition has occurred within the lifetime of the lichen thallus. The oil refinery in Come-By-Chance (CBC), eastern Newfoundland is the largest point source of SO_2 in the province. It was established by Provincial Refining in October 1973, but financial problems caused the closure of the refinery in February 1976 (Smallwood and Pitt, 1981; Concord Environmental, 1993). The refinery was then reopened in the fall of 1987 by Newfoundland Processing and has been in operation ever since. Since anthropogenic S in Newfoundland is isotopically distinct from the natural background, the CBC site was deemed suitable for this application.

Based on the report by Concord Environmental (1993), the refinery charge rate in 1988 was 85,569 barrels per stream day (BPSD) and this rate has not been greatly changed since the reopen of the refinery. In Table 5-1, the refinery charge and total SO_2 emission among five oil refineries in Canada including CBC oil refinery are compared. CBC oil refinery had the highest SO_2 emissions, about six and a half times higher than Petro-Canada, which had the second highest emissions. Concord Environmental (1993) also reported that the oil refinery did not operate the Sulphur Recovery Unit (SRU) until the summer of 1993.

Table 5-1. Comparison of refinery charge and SO_2 emissions of CBC refinery with other refineries (Concord Environmental, 1993).

Refinery	Refinery Charge (m^3/CD)[#]	SO_2 (tonnes/yr)
Esso (Dartmouth, Nova Scotia)	11,944	3,858
Shell (Scotford, Alberta)	9,635	462
Petro-Canada (Oakville, Ontario)	10,054	5,712
Suncor (Sarnia, Ontario)	9,932	3,453
CBC[*] (CBC, Newfoundland)	**8,386**	**37,229** (~9,300)[♮]

Note:

[#] Cubic meters per calender day.

[*] Come-By-Chance data is for 1992. Other data is for 1988.

[♮] Total SO_2 emission without operating Sulphur Recovery Unit (SRU) by the refinery. The number in the parenthesis is total SO_2 emission estimated with 75% of recovery efficiency by SRU operation.

5.1.2 Previous studies of S in lichen in Newfoundland

The distribution of S concentration and isotopic composition of lichens in Newfoundland was studied by Evans (1996), Blake (1998), and Wadleigh and Blake (1999). Based on their studies, S concentrations in Newfoundland ranged from 262 to 787 ppm, with values exceeding 450 ppm in regions surrounding urban centers and point sources of S emissions. $\delta^{34}S_{CDT}$ values in Newfoundland range from +3.7 to +16.6‰ and show a general decrease from coastal areas to interior parts of the island (Figure 5-1). $\delta^{34}S_{CDT}$ values in coastal areas are generally +12.0 - +16.6‰, contributed by seasalt aerosols ($\delta^{34}S_{CDT}$ = +21‰) and/or sulphate or SO_2 derived from the oxidation of DMS ($\delta^{34}S_{CDT}$ = +16 - +21‰). Inland regions which are not near urban or industrial centers have lower $\delta^{34}S_{CDT}$ values (+9 - +11‰), contributed primarily by anthropogenic S compounds ($\delta^{34}S_{CDT}$ = +4 - +7‰) either transported from continental North America or from urban/industrial regions within Newfoundland such as the CBC refinery.

In the area of the CBC refinery, S concentrations range from 249 to 757 ppm and the majority of $\delta^{34}S_{CDT}$ values (Figure 5-2) range from +5.2 to +8.3‰. In general, lichens in the refinery area show high S concentrations and low $\delta^{34}S_{CDT}$ values typical of anthropogenic influence.

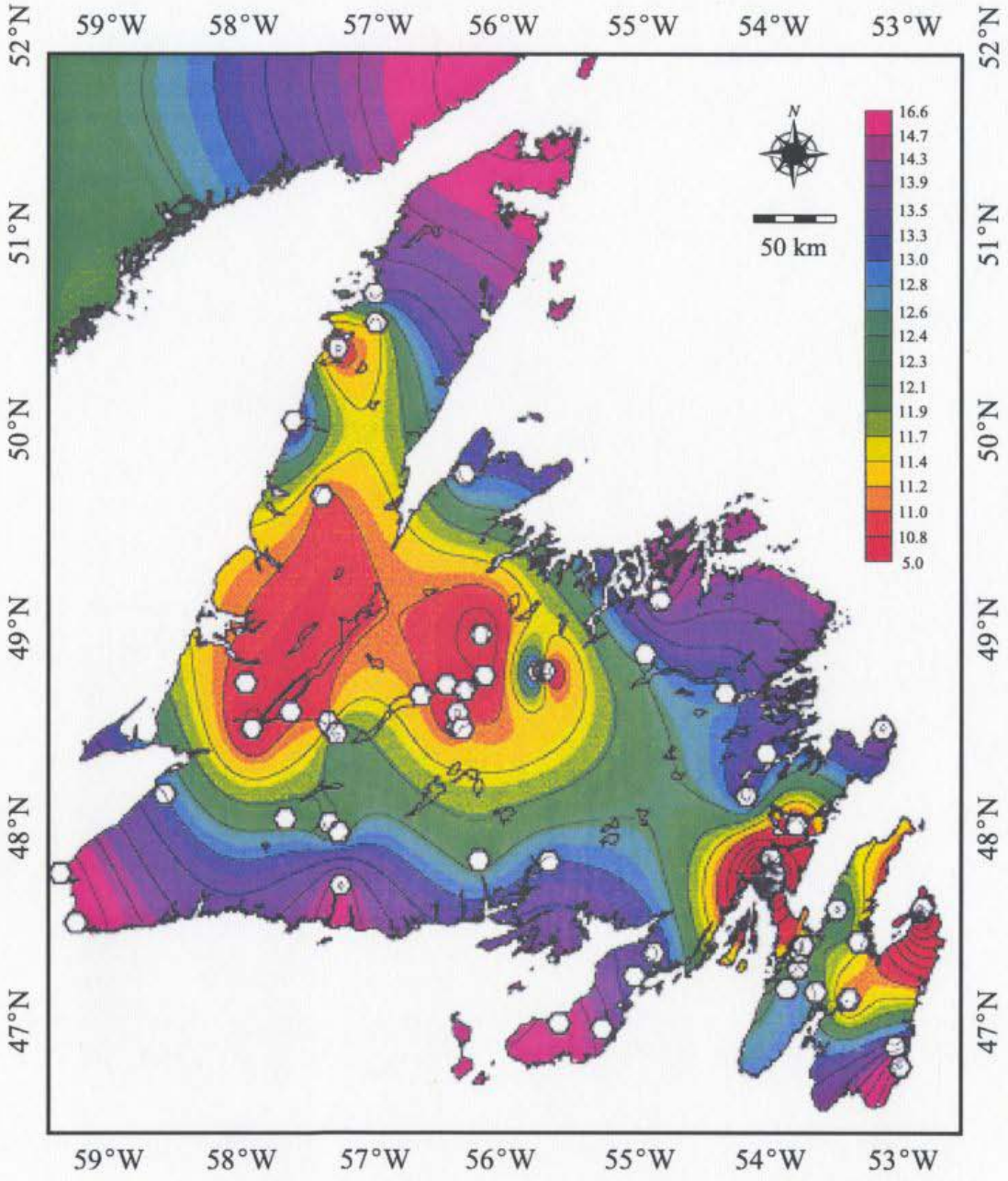

Figure 5-1. Contour map of S isotopic composition for Insular Newfoundland (from Wadleigh and Blake, 1999). All data in ‰ versus CDT.

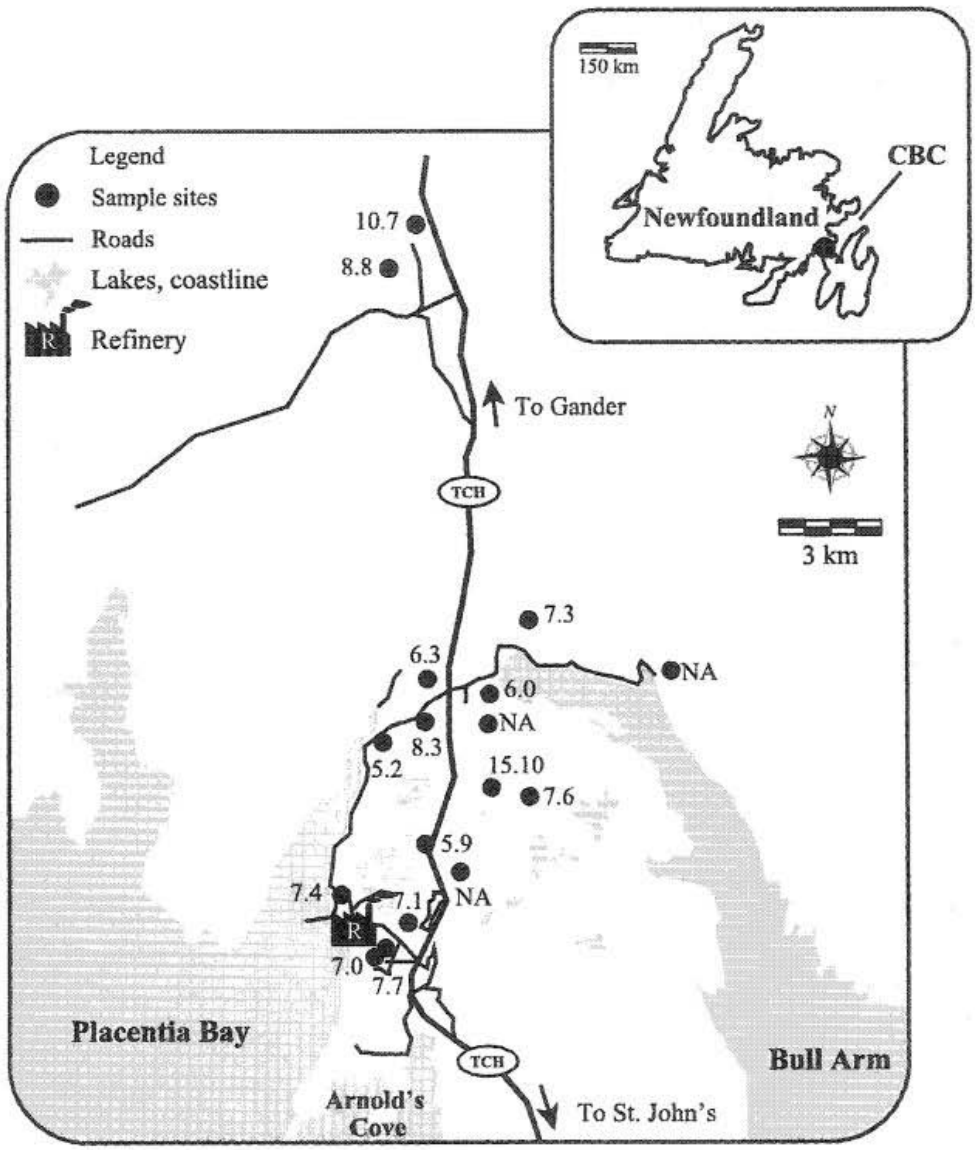

Figure 5-2. Distribution of S isotopic composition in Come-By-Chance (CBC) area, NF (modified from Blake, 1998). All data in ‰ in versus CDT. TCH represents Trans-Canada-Highway.

5.2 SAMPLING AND EXPERIMENTAL PROCEDURES

5.2.1 Sampling

Lichen samples (*Alectoria sarmentosa*) were collected from two sites, B and D near the refinery (Figure 5-3). Site-B is about 7 km north of the refinery close to the town of Come-By-Chance. Site-D is about 7 km northeast of the refinery, and east of Trans-Canada-Highway (TCH) and south of the town of Sunnyside. On an annual basis, the predominant direction of wind is from the southwest (see Figure 5-3), implying the S emissions from the refinery will blow towards the towns of CBC and Sunnyside. The sampling sites were selected at least 3 km away from the refinery because lichen samples collected within 2.5 km from the refinery may not directly reflect S from the refinery (Case and Krouse, 1980; Blake, 1998). Case and Krouse (1980) suggested that the lichens in this zone may release isotopically light S in response to the high atmospheric concentrations, therefore increasing the $\delta^{34}S$ of the remaining S in the lichen.

Several thalli were collected from sites-B and -D, respectively. Since the average growth rate of fruticose lichens is generally 1 cm or less per year (Hale, 1974; Richardson, 1992), lichen strands 25-35 cm in length were expected to include lichen growth pre-refinery (before 1973) to the present. One lichen thallus from each site was used for bulk analysis to measure average S concentration and $\delta^{34}S_{CDT}$ value. Sampling method was described in Section 2.1.1.

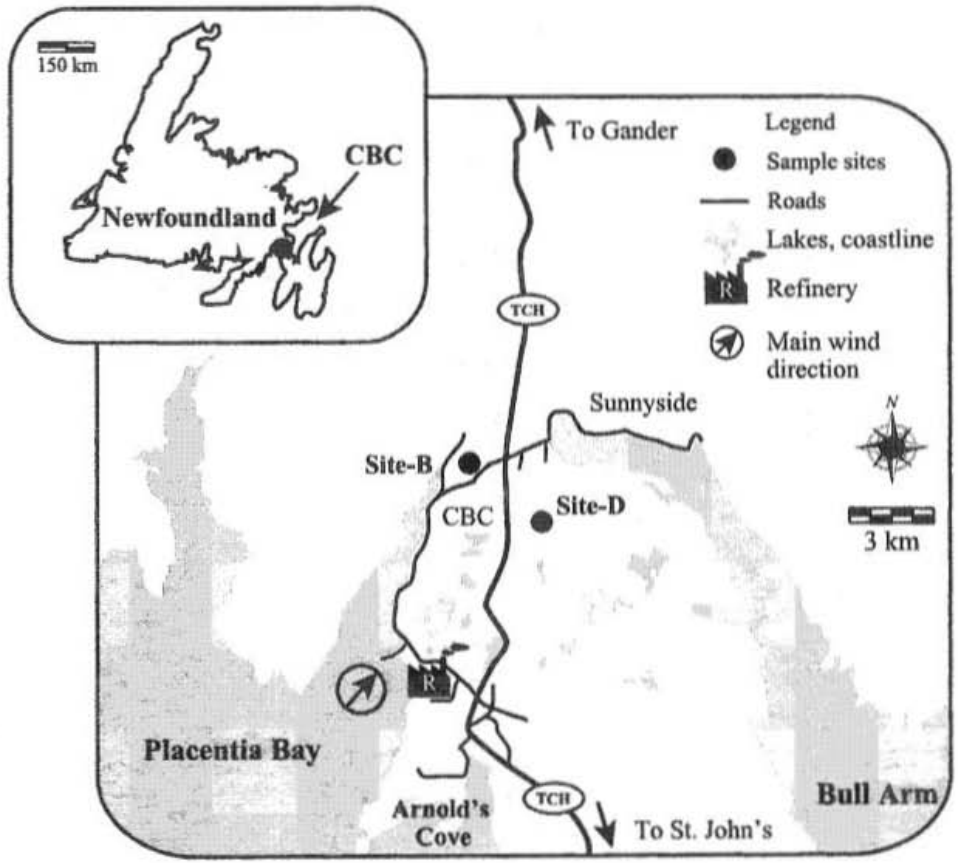

Figure 5-3. Map showing two sampling sites, Come-By-Chance (CBC), NF. TCH represents Trans-Canada-Highway.

5.2.2 Sample preparation

Figure 5-4 summarizes the sample preparation procedures. Upon arriving in the lab from the field, the lichen thalli were air dried for 3-5 days and cleaned by removing foreign materials in the same ways before in Section 2.1.2.

For end portion analyses (left flow in Figure 5-4), strands 25-35 cm in length were separated from the cleaned lichen thalli. Then, young and old portions were separated from each lichen strand. Only the end portions from these selected lichen strands were analyzed to maximize the possibility of $\delta^{34}S$ difference as illustrated in Figure 5-5. Clean stainless steel tweezers, unpowdered vinyl gloves and a magnifier with light were used for separation procedures. Extreme care was taken during the separation processes, not to lose any portions and to avoid contamination. Old portions were cut around 3 cm in length from an end (Figures 5-5a, b) and young portions were cut about 1-2 cm from the other end (Figures 5-5a, c). Since the young portions were hair-size in thickness, in order to supply enough sample amounts for the CF analysis, more young portions were separated from the strands than old portions (Figures 5-5a, c). The thickness of the old portions was variable: the old portions from site-D were mostly 2-3 mm in thickness while lichens from site-B were approximately 1 mm thick. Each portion was then ground separately in a mortar and pestle, after immersing in liquid nitrogen. The powder was oven dried at 80 °C for about 15 hrs prior to CF-IRMS analysis. In order to prevent possible sample inhomogeneities associated with grinding by the mortar and pestle, all of the ground sample was used for the analyses.

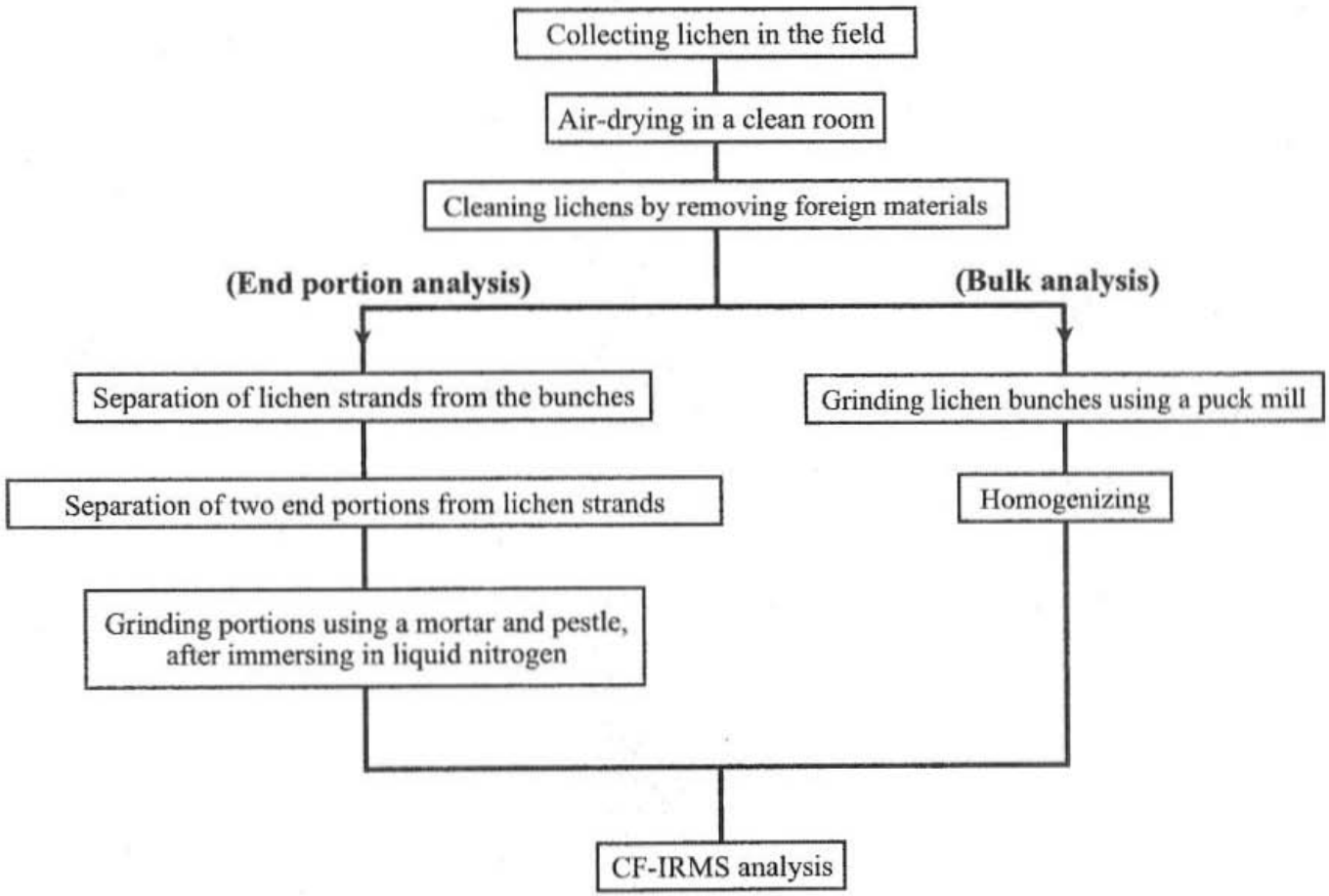

Figure 5-4. Flow chart showing sample preparation steps for end portion (left) and bulk (right) analyses.

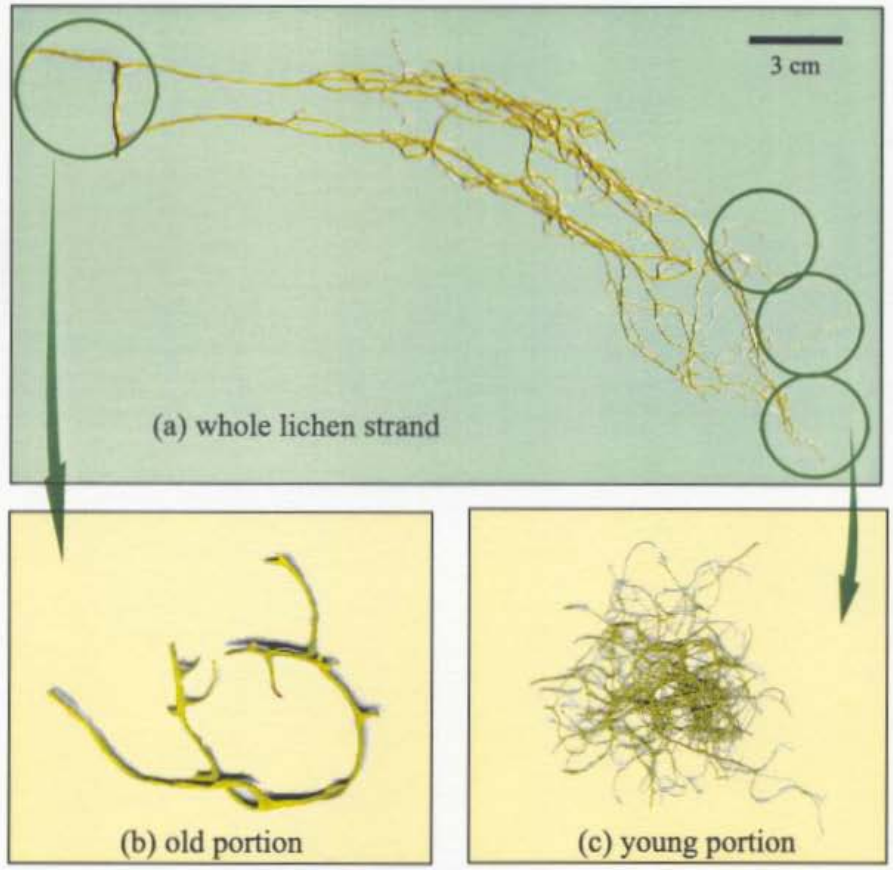

Figure 5-5. An example of the separated old and young portions from a lichen str
(a) whole lichen strand before separation (*Alectoria sarmentosa*), and
(b) and (c) separated old and young portions, repectively.

For bulk analyses (right flow in Figure 5-4), the lichen thalli from each site were ground using a puck mill and homogenized, followed by oven drying. For the details of analytical conditions, refer to Chapter 3.

5.3 RESULTS AND DISCUSSION

5.3.1 S concentrations

S concentrations of end portion and bulk lichen samples were roughly measured by CF-IRMS by analyzing an organic material with known S concentration (BBOT, $C_{26}H_{26}N_2O_2S$, with 7.45% S) and comparing the mass 64 peak areas of the samples with the average mass 64 peak area of replicate BBOT analyses. The detailed calculation procedure is provided with an example in Appendix IV and the calculated S concentrations (in ppm) are given in Appendix V.

These S concentrations are plotted in Figure 5-6. For both sites-B and -D, S concentrations of young portions are consistently higher than those of their corresponding old portions. This result suggests that input of atmospheric S has increased since the lichen strands started to grow, but not necessarily linearly, since S concentrations obtained by bulk analyses are not simply an average of the S concentrations obtained for end portions. In fact, average S concentrations from bulk analyses are closer to those of the old portions, consistent with a more recent increase of S. A similar pattern was found by Blake (1998). He separated strands of *Alectoria sarmentosa* from CBC refinery area into three 3 cm

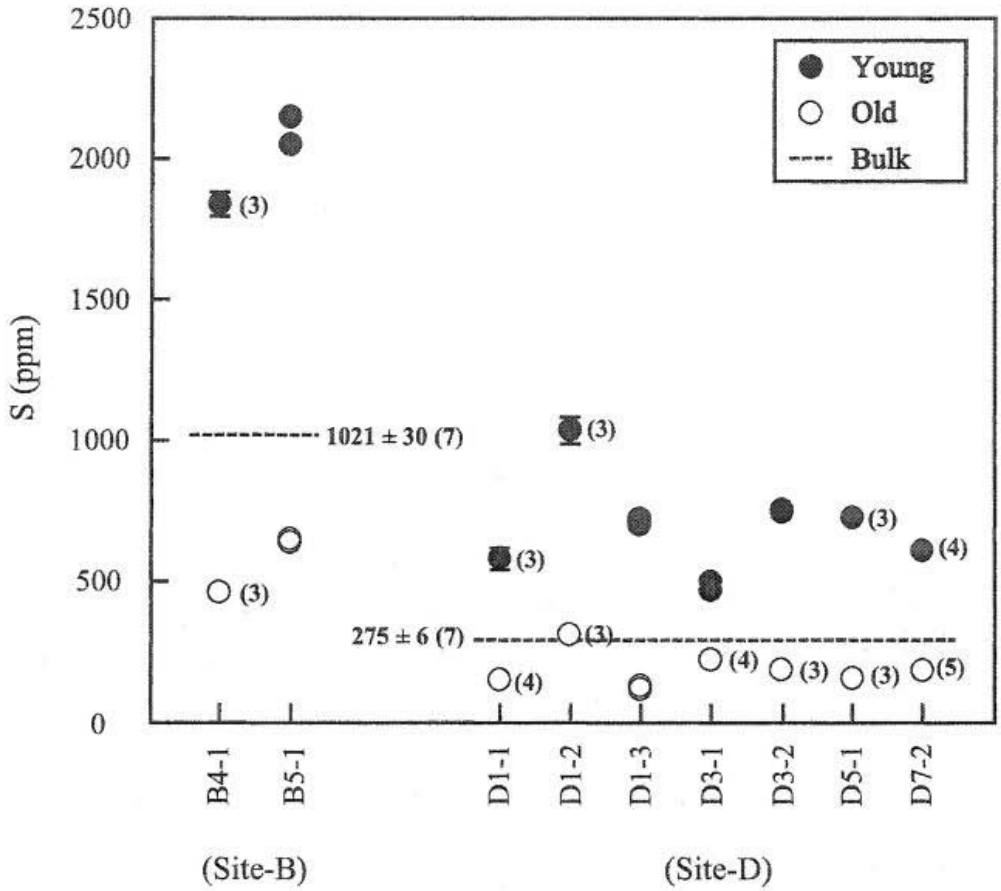

Figure 5-6. S concentrations of young (solid circles) and old (open circles) portions. Mean S concentrations of the bulk analyses are represented as dotted lines. Numbers in parentheses are replicate numbers and data points without replicate numbers are single analysis. Note the systematic difference in S concentration between young and old portions, and mean of bulk analyses plotting between them. Errors bars are based on standard deviations (1σ). Errors are smaller than the symbols when they are not shown.

segments and analyzed their S concentrations using Inductively Coupled Plasma-Optical Emission Spectrometry (ICP-OES). Concentrations decreased continuously with age, from 435 ppm S for the youngest, 384 ppm S for the middle and 366 ppm S for the oldest, with the mean of 395 ppm S. Both the mean S concentration (395 ppm) and the S concentration of the middle portion (384 ppm) are closer to that of old portion.

Although the length of lichen strands from both sites are similar (25-35 cm) and both sampling sites were almost at the same distance (~7 km) from the refinery, old portions from site-B have higher S concentrations than those from site-D (Figure 5-6). This may indicate that atmospheric S concentrations were higher when the lichen strands from site-B started to grow compared to those from site-D.

The difference in thickness of old portions (2-3 mm for old portions from site-D and ~1 mm for old portions from site-B) suggests the lichens from site-B are in fact younger than those from site-D and must have grown at a faster rate to achieve the same length as those from site-D. In other words, lichen strands from site-D record a longer time interval than those from site-B. Annual growth rates of lichens from the same area do not necessarily have to be uniform (Ahmadjian, 1967). Yearly increments may vary considerably according to the conditions of the growth environment such as moisture and temperature (Ahmadjian, 1967). Growth rates may vary within a single strand (Hale, 1954) and with the age of the strand (Frey, 1959; Phillips, 1963). Also, the heterogeneous composition (e.g. a fungus and an alga or a fungus and a cyanobacterium) and lack of physiological integration result in

growth that is usually irregular and unpredictable (Hayward and Grace, 1982; Armstrong, 1984). The more variable S concentrations of young portions in contrast to old portions even at the same sampling site (Figure 5-6) can also be explained by different growth rate, combined with the different sampling methods used for old and young portions (see Section 5.2.2).

It is interesting to note that the S concentrations of old portions from site-B are similar to those of young portions from site-D. This may indicate that the atmospheric S when the lichen strands from site-B started to grow was similar to that during the time of active S uptake by young portions from site-D.

5.3.2 S isotopic compositions

$\delta^{34}S_{CDT}$ values of end portion and bulk lichen samples are plotted in Figure 5-7, and the detailed results are summarized in Appendix V. For site-B, there is no difference between $\delta^{34}S_{CDT}$ values of old and young portions (range of +5.0 - +6.6‰). These values are consistent with anthropogenic S from the refinery operation being the dominant input throughout the lifetime of these lichens. The mean $\delta^{34}S_{CDT}$ value (+5.2 ± 0.4‰, n=7) measured by bulk analyses is similar to those $\delta^{34}S_{CDT}$ values of the end portions.

For site-D, there is a distinct difference in $\delta^{34}S_{CDT}$ between end portions (+6.2 to +10.9‰ for old portions and +5.1 to +8.2‰ for young portions), consistent with increasing anthropogenic input over the lifetime of the lichens. The mean $\delta^{34}S_{CDT}$ value (+6.6 ± 0.7‰,

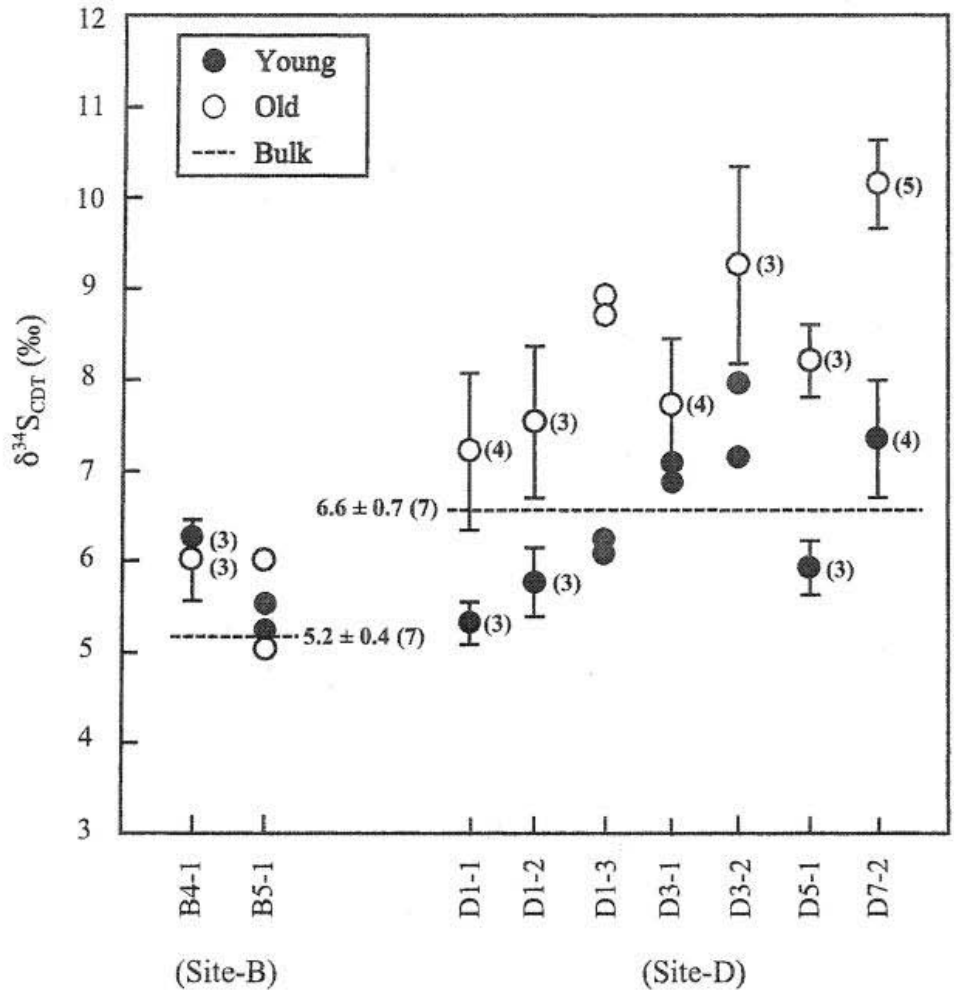

Figure 5-7. $\delta^{34}S_{CDT}$ values of young (solid circles) and old (open circles) portions, with mean $\delta^{34}S_{CDT}$ values of bulk analyses (dotted lines) from sites-B and -D. Numbers in parentheses are replicate numbers and data points without replicate numbers are single analysis. Note that there is a systematic difference in S isotopic compositions between young and old portions from site- D. Error bars are based on standard deviations (1σ).

n=7) measured by bulk analyses falls between the $\delta^{34}S_{CDT}$ values measured for end portions.

The total range of $\delta^{34}S_{CDT}$ values obtained from site-B (+5.0 to +6.6‰) is within the range obtained for young portions alone (+5.1 to +8.2‰) from site-D (Figure 5-7). It is also within the rage of $\delta^{34}S_{CDT}$ values previously reported for the CBC area (+4 to +8‰) (Evans, 1996; Blake, 1998). Old portions from site-D are similar in $\delta^{34}S_{CDT}$ range (+6.2 to +10.9‰) to that of inland regions (+9 to +11‰) which are not near urban or industrial centers (Blake, 1998). These data support the interpretation that the old portions from site-D preserve $\delta^{34}S_{CDT}$ values with lower anthropogenic S, and the young portions from site-D and both portions from site-B reflect $\delta^{34}S_{CDT}$ values with higher anthropogenic S contribution.

Figure 5-8 is a schematic diagram showing the possible correlations among S isotopic compositions, S concentration and time based on the history of refinery operation. Lichen strands from site-B represent the time period from Operation-I (1973-1976) to Operation-III (the present) while the lichen strands from site-D include the time period from Pre-refinery (before 1973) when there was less contribution of anthropogenic S to Operation-III (the present).

5.4 SUMMARY

In summary, the developed CF-lichen method reveals inhomogeneous distributions of S isotopic composition as well as S concentration along single lichen strands. However, more segment data between young and old portions are required to reveal detailed histories

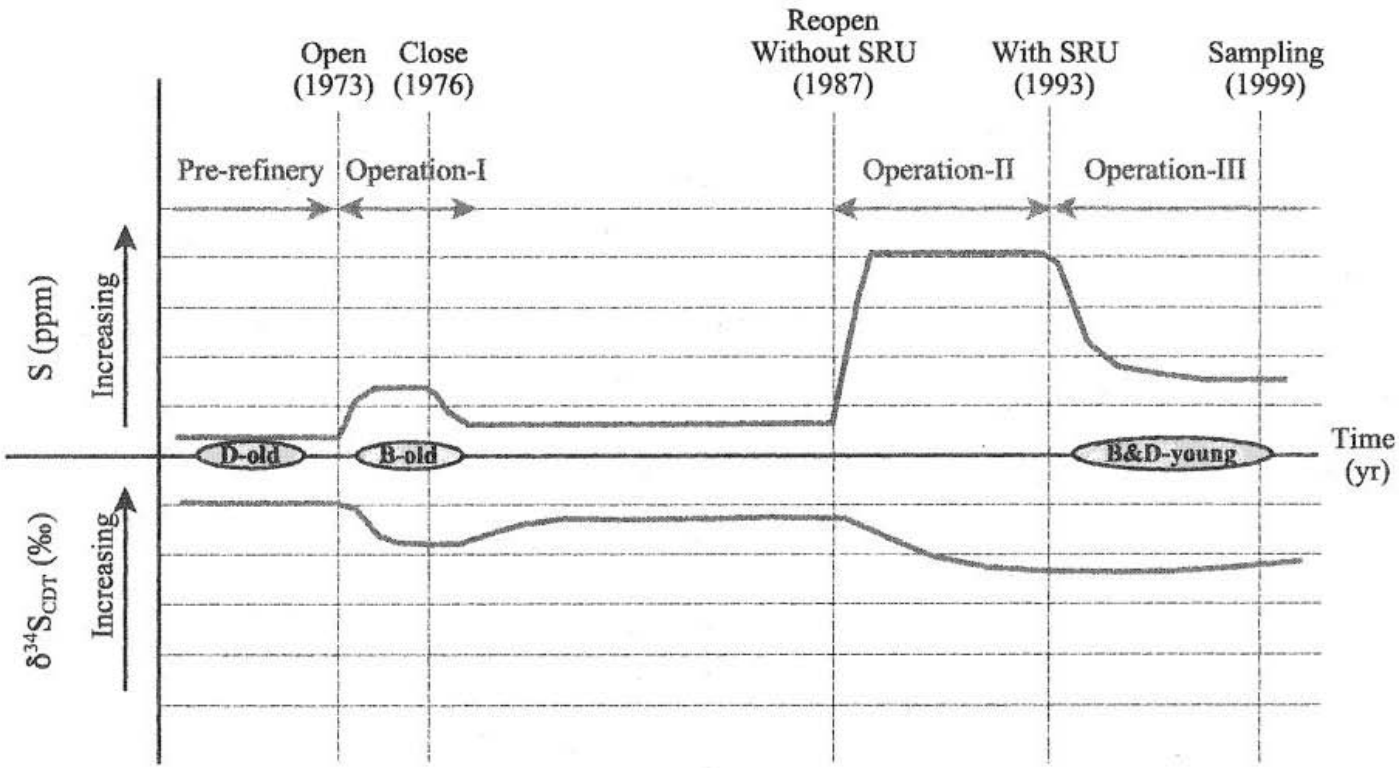

Figure 5-8. Schematic diagram showing the relationship of represented time, S concentration and S isotopic compositions of two end portions from both sites-B and -D. SRU represents Sulphur Recovery Unit.

of S concentration and $\delta^{34}S_{CDT}$ change. Through this application, it was demonstrated that the developed CF-lichen technique can successfully be applied to the analysis of very small amount of organic material with low S concentration. The micro analytical capability of this method is a great advantage for other studies which require very small amount of sample with low S concentration.

In addition, the fact that the distribution of S concentration and S isotopic compositions in lichen strands may not be homogeneous possibly explains the somewhat complicated distribution pattens of S concentration and S isotopic values in Newfoundland in general and CBC in particular reported in previous studies. Thus, the analyses of young portions only may reduce the amount of scatter in S concentration and S isotopic values that result from bulk analysis.

CHAPTER 6

CONCLUSIONS

An on-line analytical method has been developed for the routine measurement of S isotopic composition in lichens using continuous flow isotope ratio mass spectrometry (CF-IRMS). Analytical problems encountered that were attributed to incomplete combustion and subsequent blocking of gas flow because of low S concentration (~600 ppm) and high moisture content (~10 wt%) were solved by (i) oven-drying the lichen powder, (ii) increasing O_2 supply for combustion and, finally, (iii) increasing the sensitivity using a shorter GC column and decreasing GC oven temperature.

The analytical quality of CF-IRMS method with chemically untreated lichen is concluded below:

1. For two sets of replicate analyses of a lichen sample (*Alectoria sarmentosa*) collected from the Botanical Garden of Memorial University of Newfoundland mean $\delta^{34}S_{CDT}$ values, +6.3 ± 0.4‰ (calibrated by sulphates) and +6.1 ± 0.3‰ (calibrated by sulphides), were compared to those by DI (+6.2 ± 0.2‰) and CF-$BaSO_4$ (+5.9 ± 0.3‰) methods, resulting in excellent accuracy and precision for the technique.

2. For four different lichen sample sets with the $\delta^{34}S_{CDT}$ range of +4 - +16‰, collected from various locations in Newfoundland, mean $\delta^{34}S_{CDT}$ values were compared to those by DI method, also showing excellent accuracy and precision for the range of $\delta^{34}S_{CDT}$.

3. Lichen samples containing as little as 5-6 μg S (approximately 9 mg lichen) could be successfully analyzed without a loss of precision.

4. There were no memory effects observed over the $\delta^{34}S_{CDT}$ value range in lichen of +6 - +16‰.

5. Analytical time and reasonable S amount required per analysis are reduced greatly over conventional techniques to 15 mins and 9 μg S, respectively.

Using the developed CF-lichen method, old and young portions of lichen strands collected from Come-By-Chance oil refinery area, eastern Newfoundland, were analyzed in order to investigate variations of S isotopic composition along the lichen strands with time. There was a systematic variation in S isotope signatures ($\delta^{34}S_{CDT}$) observed between old (+6.2 to +10.9‰) and young portions (+5.1 to +8.2‰), demonstrating that the old portions represent the atmospheric S of pre-refinery, which is characterized by less contribution of anthropogenic S from the refinery operation while those of the young portions represent the present atmospheric S with more contribution of anthropogenic S. The micro analytical capability of the developed CF-lichen method may be applied to other studies which require the analysis of very small amount of organic materials containing low S concentration.

REFERENCES

Ahmadjian, V., 1967. *The Lichen Symbiosis.* Blaisdell Publishing Company, Massachusetts.

Ahmadjian, V., 1993. *The Lichen Symbiosis.* John Wiley & Sons, New York.

Andreae, M. O., 1985. **The Emission of Sulfur to the Remote Atmosphere.** In *The Biogeochemical Cycling of Sulfur and Nitrogen in the Remote Atmosphere*, (eds.) J. N. Galloway, R. J. Charlson, M. O. Andreae and H. Rodhe. D. Reidel Publishing Company, Dordrecht, The Netherlands.

Armstrong, R. A., 1984. **Growth of Experimentally Reconstructed Thalli of the Lichen *Parmelia conspersa*.** New Phytologist 98: 497-502.

Barrie, A. and Prosser, J., 1996. **Automated Analysis of Light-Element Stable Isotopes by Isotope Ratio Mass Spectrometry.** In *Mass Spectrometry of Soils*, (eds.) T. W. Boutton and S. I. Yamasaki. Marcel Dekker, New York.

Berresheim, H. and Jaeschke, W., 1983. **The Contribution of Volcanoes to the Global Atmospheric Sulfur Budget.** J. Geophy. Res. 88: 3732-3740.

Blake, D. M., 1998. **Atmospheric Sulphur Deposition Monitoring in Newfoundland Using Lichens.** Unpublished M. Sc. thesis, Memorial University of Newfoundland, Canada.

Blum, O. B., 1973. **Water Relations.** In *The Lichens*, (eds.) V. Ahmadjian and M. E. Hale. Academic Press, New York.

Brenna, J. T., Corso, T. N., Tobias, H. J. and Caimi, R. J., 1997. **High-Precision Continuous-Flow Isotope Mass Spectrometry.** Mass Spectrometry Reviews 16: 227-258.

Brimblecombe, P., Hammer, C., Rodhe, H., Ryaboshapko, A. and Boutrov, C. F., 1989. **Human Influence on the Sulphur Cycle.** In *Evolution of the Global Biogeochemical Sulphur Cycle, SCOPE 39*, (eds.) P. Brimblecombe and A. Yu. Lein. John Wiley & Sons, New York.

Caimi, R. J., 1995. **The Development and Application of Liquid Chromatography-Combustion-High Precision Isotope Ratio Mass Spectrometry (LCC-IRMS).** Unpublished Ph. D. thesis, Cornell University, U. S. A.

Carlo Erba® Instruments. **Instruction Manual of NA 1500.**

Case, J. W. and Krouse, H. R., 1980. **Variations in Sulphur Content and Stable Sulphur Isotope Composition of Vegetation Near a SO_2 Source at Fox Creek, Alberta, Canada.** Oecologia 44: 248-257.

Castleman, A. W. Jr, Munkelwitz, H. R. and Manowitz, B., 1974. **Isotopic Studies of the Sulfur Component of the Stratospheric Aerosol Layer.** Tellus, 26; 222-234.

Charlson, R. J., Anderson, T. L. and McDuff, R. E., 1992. **The Sulfur Cycle.** In *Global Biogeochemical Cycles* (eds.) S. S. Butchur, R. J. Charlson, G. H. Orians and G. V. Wolfe. Academic Press, San Diego.

Concord Environmental, 1993. **On Stream Inspection and Air Contaminant Emission Estimate Come By Chance Refinery/Prepared for Government of Newfoundland and Labrador, Department of Environment and Lands, Industrial Environment Engineering Division.** Concord Environment, Ontario.

Cortecci, G and Longinelli, A., 1970. **Isotopic Composition of Sulfate in rain water, Pisa, Italy.** Earth Planet. Sci. Lett., 8: 36-40.

Dequasi, H. L. and Grey, D. C., 1970. **Stable Isotopes Applied to Pollution Studies.** Amer. Lab. Dec., 19-27.

Dugan, G., 1977. **Automatic Carbon, Hydrogen, Nitrogen, Sulfur Analyzer: Chemistry of Sulfur Reactions.** Analytical Letters 10: 639-657.

Ehleringer, J. R. and Rundel, P. W., 1988. **Stable Isotopes: History, Units, and Instrumentation.** In *Stable Isotope in Ecological Research*, (eds.) P. W. Rundel, J. R. Ehleringer and K. A. Nagy. Springer-Verlag, New York.

Eriksen, J. and Johansen, H. S., 1994. **Correction Factors in the Determination of Natural Abundance of Stable S Isotopes in Soil.** Appl. Radiat. Isot. 45: 889-893.

Eriksen, J., 1996. **Measuring Natural Abundance of Stable S Isotopes in Soil by Isotope Ratio Mass Spectrometry.** Commun. Soil Sci. Plant Anal. 27: 1251-1264.

Eriksson, E., 1963. **The Yearly Circulation of Sulphur in Nature.** J. Geophys. Res. 68: 4001-4008.

Evans, A. N. G., 1996. **Characterizing Atmospheric Sulphur Using Lichen and Rain in Eastern Newfoundland.** Unpublished B. Sc. (Hons.) thesis, Memorial University of Newfoundland, Canada.

Finnigan® MAT, 1996. **Elemental Analyzer-IRMS Interface.**

Finnigan® MAT Application Flash Report No. G25, 1997. **$^{34}S/^{32}S$ in Micrograms of S in Pine Needles by Direct Combustion.**

Finnigan® MAT 252 **Operator Course Note**, Nov. 17-25, 1997.

Frey, E., 1959. **Die Flechtenflora und-Vegetation des Nationalparks im Unterengadin II.** Die Entwicklung der Flechtenvegetation auf photogrammetrisch kontrollierten Dauerflächen 41: 241-319.

Fry, B., Garritt, R., Tholke, K., Neill, C., Michener, R. H., Mersch, F. J. and Brand, W., 1996. **Cryoflow: Cryofocusing Nanomole Amounts of CO_2, N_2, and SO_2 from an Elemental Analyzer for Stable Isotopic Analysis.** Rapid Communications in Mass Spectrometry 10: 953-958.

Giesemann, A., Jager, H. J., Norman, A. L., Krouse, H. R. and Brand, W. A., 1994. **On-Line Sulfur-Isotope Determination Using an Elemental Analyzer Coupled to a Mass Spectrometer.** Anal. Chem. 66: 2816-2819.

Gollop, A. J., 1998. **Measuring the Isotopic Composition of Atmospheric Sulphur Using the Epiphytic Lichen, *Cladonia sp.*.** Unpublished B. Sc. (Hons.) thesis, Memorial University of Newfoundland, Canada.

Granat, L., Rodhe, H. and Hallberg, R. O., 1976. **The Global Sulphur Cycle.** In *Nitrogen, Phosphorus and Sulphur-Global Cycles, SCOPE Report 7*, (eds.) B. H. Svenson and R. Söderlund, Ecol. Bull. (Stockholm) 22: 89-134.

Grey, D. C. and Jensen, M. L., 1972. **Bacteriogenic Sulphur in Air Pollution.** Science (Wash. D. C.), 177: 1099-1100.

Gries, C., 1996. **Lichens as Indicators of Air Pollution.** In *Lichen Biology*, (eds.) T. H. Nash III. Cambridge University Press, Cambridge.

Hale, M. E., 1954. **First Report on Lichen Growth Rate and Succession at Aton Forest, Connecticut.** Bryologist 57: 244-247.

Hale, M. E., 1973. **Growth.** In *The Lichens*, (eds.) V. Ahmadjian and M. E. Hale. Academic Press, New York.

Hale, M. E., 1974. *The Biology of Lichens.* Edward Arnord. London.

Hawksworth, D. L. and Rose, F., 1976. *Lichens as Pollution Monitors.* Edward Arnold, London.

Hayward, B. W. and R. V. Grace, 1982. **Lichen Growth and Grazers. Five Years of Monitoring Lichen Quadrats at Kawerua.** Journal of the Aukland University Field Club 28: 187-197.

Hoefs, J., 1997. *Stable Isotope Geochemistry.* Springer, New York.

Holt, B. D., Engelkemeir, A. G. and Venters, A., 1972. **Variations of Sulfur Isotope Ratios in Samples of Water and Air near Chicago.** Environ. Sci. Technol., 6: 338-341.

Honegger, R., 1996. **Morphogenesis.** In *Lichen Biology* (eds.) T. H. Nash III. Cambridge University Press, Cambridge.

Ivanov, M. V., 1983. **Major Flux of the Global Biogeochemical Cyclo of Sulphur.** In *The Global Biogeochemical Sulphur Cycle, SCOPE 19*, (eds.) M. V. Ivanov and J. R. Freney. John Wiley & Sons, New York.

Jamieson, R. E., 1996. **A Stable Isotopic Study of Natural and Anthropogenic Sulphur in Precipitation in Eastern Canada.** Unpublished M. Sc. thesis, Memorial University of Newfoundland, Canada.

Jensen, M. L. and Nakai, N., 1961. **Sources and Isotopic Composition of Atmospheric Sulphur.** Science (Wash. D. C.), 134: 2102-2104.

Kellogg, W. W., Cadle, R. D., Allen, E. R., Lazrus, A. L. and Martell, E. A., 1972. **The Sulphur Cycle.** Science 175: 587-596.

Kendall, C. and Caldwell, E. A., 1998. **Fundamentals of Isotope Geochemistry.** In *Isotope Tracers in Catchment Hydrology* (eds.) C. Kendall and J. J. McDonnell. Elsevier Science, New York.

Krouse, H. R., 1977. **Sulphur Isotope Abundance Elucidate Uptake of Atmospheric Sulphur Emissions by Vegetation.** Nature 265: 45-46.

Krouse, H. R., 1980. **Sulphur Isotopes in Our Environment.** In *Handbook of Environmental Isotope Geochemistry: Volume 1-The Terrestrial Environment A,* (eds.) P. Fritz and J. Ch. Fontes. Elsevier Scientific Publishing Company, New York.

Krouse, H. R., Legge, A. H. and Brown, H. M., 1984. **Sulphur Gas Emissions in the Boreal Forest: the West Whitecourt Case Study - V. Stable Sulphur Isotopes.** Water, Air, and Soil Pollution 22: 321-347.

Krouse, H. R., 1988. **Sulfur Isotope Studies of the Pedosphere and Biosphere.** In *Stable Isotope in Ecological Research*, (eds.) P. W. Rundel, J. R. Ehleringer and K. A. Nagy. Springer-Verlag, New York.

Krouse, H. R., 1991. **Sulphur Isotope Tracing of the Fate of Emissions from Sour Gas Processing in Alberta, Canada (Section 8.2).** In *Stable Isotopes in the Assessment of Natural and Anthropogenic Sulphur in the Environment, SCOPE 43*, (eds.) H. R. Krouse and V. A. Grinenko. John Wiley & Sons, New York.

Krouse, H. R., Mayer, B. and Schoenau, J. J., 1996. **Applications of Stable Isotope Techniques to Soil Sulfur Cycling.** In *Mass Spectrometry of Soils*, (eds.) T. W. Boutton and S. I. Yamasaki. Marcel Dekker, New York.

Ludwig, F. L., 1976. **Sulfur Isotope Ratios and the Origins of the Aerosols and Cloud Droplets in California Stratus.** Tellus, 28: 427-433.

McKinney, C. R., McCrea, J. M., Epstein, S., Allen, H. A. and Urey, H. C., 1950. **Improvements in Mass Spectrometers for the Measurement of Small Differences in Isotope Abundance Ratios.** The Review of Scientific Instruments 21: 724-730.

Micromass®, 1996. **Isotopic Sulphur Determination by Continuous-Flow IRMS (CF-IRMS).**

Mitchell, M. J., Krouse, H. R., Mayer, B., Stam, A. C. and Zhang, Y., 1998. **Use of Stable Isotopes in Evaluating Sulfur Biogeochemistry of Forest Ecosystems.** In *Isotope Tracers in Catchment Hydrology* (eds.) C. Kendall and J. J. McDonnell. Elsevier Science, New York.

Nash III, T. H., 1996. **Nutrients, Elemental Accumulation and Mineral Cycling.** In *Lichen Biology* (eds.) T. H. Nash III. Cambridge University Press, Cambridge.

Newman, L., Krouse, H. R. and Grinenko, V. A., 1991. **Sulphur Isotope Variations in the Atmosphere.** In *Stable Isotopes in the Assessment of Natural and Anthropogenic Sulphur in the Environment*, (eds.) H. R. Krouse and V. A. Grinenko. John Wiley & Sons, New York.

Nieboer, E., Richardson, D. H. S. and Tomassini, F. D., 1978. **Mineral Uptake and Release by Lichens: An Overview.** The Bryologist 81(2): 226-246.

Nowotczynski, P. A., 1998. **Characterizing Atmospheric Sulphur of the Burin Peninsula Using Epiphytic Lichens.** Unpublished B. Sc. (Hons.) thesis, Memorial University of Newfoundland, Canada.

Nriagu, J. O., Coker, R. D. and Barrie, L. A., 1991. **Origin of Sulphur in Canadian Arctic Haze from Isotope Measurements.** Nature 349: 142-145.

Parker, S. P. (ed. in chief), 1993. *McGraw-Hill Encyclopedia of Chemistry (2nd ed.).* McGraw-Hill, Inc., New York.

Phillips, H. C., 1963. **Growth Rate of *Parmelia isidiosa* (Müll. Arg.) Hale.** J. Tennessee Acad. Sci. 38: 95-96.

Potts, P. J., 1987. **Gas Source Mass Spectrometry.** In *A Handbook of Silicate Rock Analysis.* Blackie, New York.

Rees, C. E., 1973. **A Steady-state Model for Sulphur Isotope Fractionation in Bacterial Reduction Processes.** Geochimica et Cosmochimica Acta 37: 1141-1162.

Richardson, D. H. S. and Nieboer, E., 1981. **Lichens and Pollution Monitoring.** Endeavour, New Series 5: 127-133.

Richardson, D. H. S., 1992. *Pollution Monitoring with Lichens.* Richmond Publishing Co. Ltd.

Rittner, R. C. and Culmo, R., 1966. **Simultaneous Microdeterminations of Carbon, Hydrogen, and Sulfur.** Microchemical Journal 11: 269-276.

Ryaboshapko, A. G., 1983. **The Atmospheric Sulphur Cycle.** In *The Global Biogeochemical Sulphur Cycle, SCOPE 19*, (eds.) M. V. Ivanov and J. R. Freney. John Wiley & Sons, New York.

Smallwood, J. R. and Pitt, R. D. W. (eds.), 1981. *Encyclopedia of Newfoundland and Labrador - Vol. I.* Newfoundland Book Publishers (1967) Limited, St. John's, NF.

Taiz, L. and Zeiger, E., 1991. *Plant Physiology.* The Benjamin/Cummings Publishing Company Inc., California.

Thode, H. G., 1991. **Sulphur Isotopes in Nature and the Environment: An Overview.** In *Stable Isotopes in the Assessment of Natural and Anthropogenic Sulphur in the Environment, SCOPE 43,* (eds.) H. R. Krouse and V. A. Grinenko. John Wiley & Sons, New York.

Trust, B. A. and Fry, B., 1992. **Stable Sulphur Isotopes in Plants: a Review.** Plant. Cell and Environment 15: 1105-1110.

Ueda, A. and Krouse, H. R., 1986. **Direct Conversion of Sulphide and Sulphate Minerals to SO_2 for Isotope Analyses.** Geochemical Journal 20: 209-212.

Wadleigh, M. A., Schwarcz, H. P. and Kramer, J. R., 1994. **Sulphur Isotope Tests of Seasalt Correction Factors in Precipitation: Nova Scotia, Canada.** Water, Air and Pollution 77: 1-16.

Wadleigh, M. A., Schwarcz, H. P. and Kramer, J. R., 1996. **Isotopic Evidence for the Origin of Sulphate in Coastal Rain.** Tellus 48: 44-59.

Wadleigh, M. A. and Blake, D. M., 1999. **Tracing Sources of Atmospheric Sulphur using Epiphytic Lichens.** Environmental Pollution 106: 265-271.

Whelpdale, D. M., 1992. **An Overview of the Atmospheric Sulphur Cycle.** In *Sulphur Cycling on the Continents, SCOPE 48*, (eds.) R. W. Howarth, J. W. B. Stewart and M. V. Ivanov. John Wiley & Sons, New York.

White, F. A. and Wood, G. M., 1986. *Mass Spectrometry: Applications in Science and Engineering.* John Wiley & Sons, New York.

Winner, W. E., Smith, C. L., Koch, G. W., Mooney, H. A., Bewley, J. D. and Krouse, H. R., 1981. **Rates of Emission of Hs from Plants and Patters of Stable Sulphur Isotope Fractionation.** Nature 289: 672-673.

Wirth, V. and Türk, R., 1974. **Über die SO_2-resistenz von Flechten und die mit ihr interferierenden Faktoren.** Verhandlungen der Gesellschaft fürr Ökologie.

Yanagisawa, F. and Sakai, H., 1983. **Thermal Decomposition of Barium-Vanadium Pentaoxide-Silica Glass Mixtures for Preparation of Sulfur Dioxide In Sulfur Isotope Ratio Measurements.** Analytical Chemistry 55: 985-987.

APPENDIX I

CALCULATION OF S CONCENTRATION IN LICHENS

Example: sample MS-1 of Table III-1, Appendix III

I Total amount of lichen powder combusted by Parr Bomb™ oxidation: 4.2405 g
II The volume diluted from the washing solution of Parr Bomb™ oxidation for ion chromatography analysis: 0.50 L
III Sulphate concentration obtained from ion chromatography analysis: 17.62 ppm
IV Percentage of sulphur in a sulphate molecule: 33.4%

$$\frac{17.62\ mg}{1\ L} = \frac{X\ mg}{0.50\ L}$$

X = 8.81 mg of sulphate in 0.50 L solution

$$\frac{8.81\ mg}{0.0042405\ Kg} = \frac{Y\ mg}{1\ Kg}$$

Y = 2078 ppm of sulphate in total lichen

Therefore, sulphur concentration in total lichen
= 2078 ppm × 0.334 = 694 ppm

APPENDIX II

CALIBRATION PROCEDURE OF CF-IRMS METHOD

Example:

I $\delta^{34}S_{raw}$ and Known $\delta^{34}S_{CDT}$ of calibration standards (NBS-127 and $BaSO_4$ $\#_{10}$).

Standards	$\delta^{34}S_{raw}$	Known $\delta^{34}S_{CDT}$
NBS-127	+14.6	+20.32 ± 0.36
NBS-127	+14.2	+20.32 ± 0.36
NBS-127	+14.6	+20.32 ± 0.36
NBS-127	+14.5	+20.32 ± 0.36
$BaSO_4$ #10	+0.4	+2.07 ± 0.40
$BaSO_4$ #10	+0.3	+2.07 ± 0.40
$BaSO_4$ #10	+0.3	+2.07 ± 0.40
$BaSO_4$ #10	+0.2	+2.07 ± 0.40
$BaSO_4$ #10	+0.3	+2.07 ± 0.40

II Calibration line produced from the relationship between the obtained $\delta^{34}S_{raw}$ and the known $\delta^{34}S_{CDT}$ of the calibration standards.

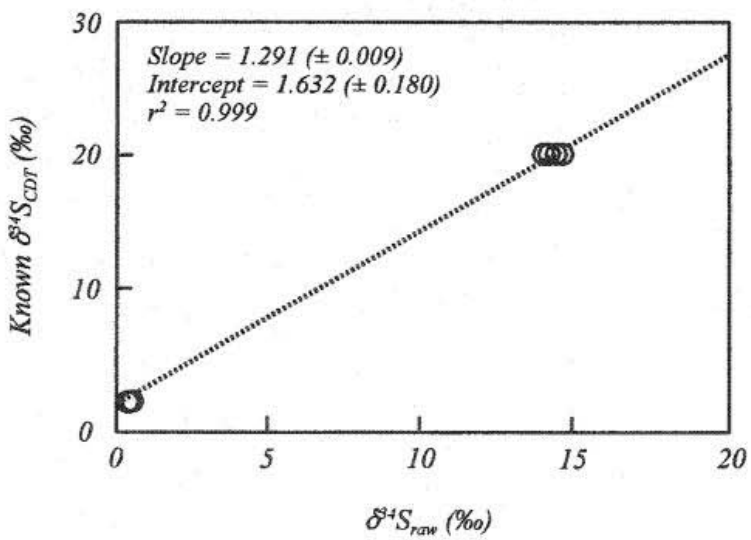

III Using the slope above, $\delta^{34}S_{CDT}$ of lichens can be calculated by applying the obtained $\delta^{34}S_{raw}$ of lichens to X axis. An example is shown below. If the $\delta^{34}S_{raw}$ of lichen is +3.4 ‰,

$$Known\ \delta^{34}S_{CDT} = 1.291 \times \delta^{34}S_{raw} + 1.632$$
$$= 1.291 \times 3.4 + 1.632 = 6.0\ ‰$$

APPENDIX III

RESULTS OF THE TESTS IN CHAPTER 4

Table III-1. S concentration measured by ion chromatography.

Samples	Weight (mg)	$BaSO_4$ (mg)[1]	SO_4^{2-} (ppm)[2]	S (ppm)[3]
MS-1	4.24	15.7	17.62	694
MS-2	4.28	15.8	16.78	655
MS-3	4.46	16.7	16.57	595
MS-4	4.25	12.6	12.30	480
Avg ± stds				**606 ± 93**

Note:

1 $BaSO_4$ prepared with lichen by Parr Bomb™ oxidation.

2 SO_4^{2-} concentration measured by ion chromatography.

3 S concentration calculated with SO_4^{2-} (see Appendix I).

Error is based on standard deviation (1σ).

Table III-2. V_2O_5 effect test on mineral analysis (NBS-127).

Samples	Weight (mg)	V_2O_5 (mg)	$\delta^{34}S_{raw}$ (‰)	$\delta^{34}S_{CDT}$ (‰)
NBS-127	0.261	No	+15.1	+20.9
NBS-127	0.260	No	+14.5	+20.1
NBS-127	0.262	No	+15.1	+21.0
NBS-127	0.261	No	+15.2	+21.1
NBS-127	0.261	No	+14.6	+20.2
NBS-127	0.260	No	+14.4	+20.0
Avg ± stds	**0.261 ± 0.001**	**No**	**+14.8 ± 0.4**	**+20.5 ± 0.5**
NBS-127	0.260	0.100	+14.9	+19.6
NBS-127	0.261	0.100	+15.3	+20.1
NBS-127	0.260	0.101	+15.5	+20.3
NBS-127	0.260	0.101	+15.0	+19.7
NBS-127	0.262	0.100	+15.5	+20.4
NBS-127	0.259	0.100	+15.1	+19.8
Avg ± stds	**0.260 ± 0.001**	**0.100 ± 0.001**	**+15.2 ± 0.3**	**+20.0 ± 0.3**
NBS-127	0.261	0.200	+15.4	+20.1
NBS-127	0.260	0.201	+15.4	+20.2
NBS-127	0.261	0.201	+15.4	+20.1
NBS-127	0.260	0.202	+15.4	+20.1
NBS-127	0.260	0.202	+15.6	+20.3
NBS-127	0.259	0.200	+15.7	+20.4
Avg ± stds	**0.260 ± 0.001**	**0.201 ± 0.001**	**+15.5 ± 0.1**	**+20.2 ± 0.1**

Note:

Sulphide standards (NBS-123, MUN-Py) were used as calibration standards.

The same amount of V_2O_5 added to samples was added to the calibration standards.

Errors are based on standard deviations (1σ).

Table III-3. V_2O_5 effect test on lichen analysis.

Samples	Weight (mg)	V_2O_5 (mg)	$\delta^{34}S_{raw}$ (‰)	$\delta^{34}S_{CDT}$ (‰)
MS-BG	15.062	No	+4.0	+7.0
MS-BG	15.111	No	+3.7	+6.6
MS-BG	15.017	No	+3.8	+6.8
MS-BG	15.033	No	+3.3	+6.2
MS-BG	15.110	No	+3.2	+5.9
MS-BG	15.122	No	+4.1	+7.1
Avg ± stds	**15.076 ± 0.045**	**No**	**+3.7 ± 0.4**	**+6.6 ± 0.5**
MS-BG	15.000	0.201	+3.6	+6.5
MS-BG	15.094	0.220	+4.1	+7.2
MS-BG	15.013	0.201	+4.0	+7.1
MS-BG	15.078	0.213	+3.5	+6.4
MS-BG	15.086	0.201	+3.8	+6.8
MS-BG	15.079	0.200	+3.7	+6.6
Avg ± stds	**15.058 ± 0.041**	**0.206 ± 0.008**	**+3.8 ± 0.2**	**+6.8 ± 0.3**

Note:

Sulphate standards (NBS-127, $BaSO_4$ #10) were used as calibration standards.

0.15-0.200 mg of V_2O_5 was added to the working standards.

Errors are based on standard deviations (1σ).

Table III-4. Test of calibration standard selection.

Standards	Weight (mg)	S (μg)	$\delta^{34}S_{raw}$ (‰)
NBS-127	0.462	64.17	+15.9
NBS-127	0.437	60.69	+15.1
NBS-127	0.386	53.61	+15.4
$BaSO_4$ #10	0.574	79.72	+0.2
$BaSO_4$ #10	0.459	63.75	+0.3
$BaSO_4$ #10	0.770	106.94	+0.6
CdS	0.226	51.36	+7.6
CdS	0.232	52.73	+7.9
MUN-Py	0.117	65.00	-0.4
MUN-Py	0.104	57.78	-0.3
MUN-Py	0.091	50.56	-0.3
NBS-123	0.162	54.00	+13.1
NBS-123	0.185	61.67	+13.2
NBS-123	0.172	57.33	+13.1

Table III-5. DI-IRMS analysis.

Samples	$\delta^{34}S_{CDT}$ (‰)
MS-1-DI	+6.6
MS-2-DI	+6.4
MS-3-DI	+5.9
MS-4-DI	+6.2
MS-5-DI	+6.2
Avg ± stds	**+6.2 ± 0.2**

Note:

MUN-Py was used as a reference gas.

Error is based on standard deviation (1σ).

Table III-6. CF-IRMS analysis with $BaSO_4$.

Samples	Weight (mg)	S (μg)	$\delta^{34}S_{raw}$ (‰)	$\delta^{34}S_{CDT}$ (‰)
MS-1-CF	0.194	26.94	+3.6	+5.7
MS-2-CF	0.194	26.94	+3.6	+5.8
MS-3-CF	0.193	26.81	+3.5	+5.6
MS-4-CF	0.190	26.39	+3.5	+5.6
MS-5-CF	0.189	26.25	+3.5	+5.7
MS-6-CF	0.191	26.53	+3.3	+5.3
MS-7-CF	0.185	25.69	+3.8	+6.0
MS-8-CF	0.189	26.25	+3.9	+6.1
MS-9-CF	0.183	25.42	+3.5	+5.6
MS-10-CF	0.184	25.56	+3.5	+5.6
MS-11-CF	0.184	25.56	+4.3	+6.7
MS-12-CF	0.215	29.86	+4.1	+6.4
MS-13-CF	0.184	25.56	+4.0	+6.3
MS-14-CF	0.194	26.94	+4.0	+6.2
MS-15-CF	0.203	28.19	+3.2	+5.3
MS-16-CF	0.191	26.53	+3.6	+5.7
MS-17-CF	0.203	28.19	+3.7	+5.9
MS-18-CF	0.193	26.81	+3.7	+5.9
MS-19-CF	0.213	29.58	+3.6	+5.8
MS-20-CF	0.192	26.67	+3.8	+6.0
MS-21-CF	0.218	30.28	+3.9	+6.2
MS-22-CF	0.204	28.33	+3.6	+5.8
MS-23-CF	0.194	26.94	+3.7	+5.9
MS-24-CF	0.202	28.06	+3.8	+6.0
MS-25-CF	0.188	26.11	+4.1	+6.4
MS-26-CF	0.187	25.97	+3.8	+6.1

(Table III-6 continued)

MS-27-CF	0.183	25.42	+4.1	+6.4
MS-28-CF	0.190	26.39	+4.0	+6.3
MS-29-CF	0.196	27.22	+3.6	+5.7
MS-30-CF	0.175	24.31	+3.8	+6.0
Avg ± stds	**0.193 ± 0.010**	**26.86 ± 1.38**	**+3.7 ± 0.3**	**+5.9 ± 0.3**

Note:

Sulphate standards (NBS-127, $BaSO_4$ #10) were used as calibration standards.

Errors are based on standard deviations (1σ).

Table III-7. CF-IRMS analysis with lichens, calibrated by sulphates (NBS-127 and $BaSO_4$ #10) standards.

Samples	Weight (mg)	S (µg)	$\delta^{34}S_{raw}$ (‰)	$\delta^{34}S_{CDT}$ (‰)
MS-BG	15.348	9.30	+3.4	+6.0
MS-BG	15.514	9.40	+3.6	+6.2
MS-BG	15.585	9.45	+3.6	+6.2
MS-BG	15.431	9.35	+3.5	+6.2
MS-BG	15.587	9.45	+3.6	+6.2
MS-BG	15.632	9.47	+3.4	+6.0
MS-BG	15.483	9.38	+3.2	+5.8
MS-BG	15.595	9.45	+3.3	+5.9
MS-BG	15.575	9.48	+3.3	+5.9
MS-BG	15.672	9.50	+4.1	+6.9
MS-BG	15.886	9.63	+4.1	+7.0
MS-BG	15.661	9.49	+4.1	+6.9
MS-BG	15.600	9.45	+3.7	+6.4
MS-BG	15.545	9.42	+3.6	+6.3
MS-BG	15.624	9.47	+3.6	+6.2
Avg ± stds	**15.583 ± 0.121**	**9.44 ± 0.07**	**+3.6 ± 0.3**	**+6.3 ± 0.4**
MS-BG	12.106	7.34	+4.3	+6.9
MS-BG	12.098	7.33	+3.6	+6.0
MS-BG	12.176	7.38	+4.4	+7.1
MS-BG	12.055	7.31	+4.6	+7.3
MS-BG	12.068	7.31	+3.5	+5.9
MS-BG	12.144	7.36	+3.3	+5.6
MS-BG	12.095	7.33	+3.6	+6.0
MS-BG	12.024	7.29	+3.6	+6.0

(Table III-7 continued)

MS-BG	12.099	7.33	+4.9	+7.7
MS-BG	12.060	7.31	+4.1	+6.6
MS-BG	12.114	7.34	+4.8	+7.5
MS-BG	12.105	7.34	+4.0	+6.6
MS-BG	12.086	7.32	+3.9	+6.4
MS-BG	12.026	7.29	+4.6	+7.3
Avg ± stds	**12.090 ± 0.042**	**7.33 ± 0.03**	**+4.1 ± 0.5**	**+6.6 ± 0.7**
MS-BG	6.150	3.73	+4.1	+7.1
MS-BG	5.926	3.59	+5.0	+8.3
MS-BG	6.073	3.68	+4.5	+7.6
MS-BG	6.160	3.73	+3.9	+6.8
MS-BG	6.027	3.65	+2.8	+5.4
MS-BG	6.109	3.70	+5.2	+8.6
MS-BG	6.068	3.68	+5.2	+8.6
MS-BG	6.143	3.72	+4.2	+7.3
MS-BG	6.179	3.74	+4.8	+8.1
MS-BG	6.044	3.66	+3.3	+6.1
MS-BG	5.936	3.60	+4.2	+7.3
MS-BG	5.942	3.60	+3.0	+5.8
MS-BG	6.353	3.85	+3.5	+6.4
MS-BG	6.008	3.64	+5.1	+8.3
Avg ± stds	**6.080 ± 0.115**	**3.68 ± 0.07**	**+4.2 ± 0.8**	**+7.3 ± 1.1**

Note:

Errors are based on standard deviations (1σ).

Table III-8. CF-IRMS analysis with lichens, calibrated by sulphides (NBS-123 and MUN-Py) standards.

Samples	Weight (mg)	S (µg)	$\delta^{34}S_{raw}$ (‰)	$\delta^{34}S_{CDT}$ (‰)
MS-BG	15.337	9.29	+4.5	+6.7
MS-BG	15.357	9.31	+4.2	+6.2
MS-BG	15.198	9.21	+4.3	+6.3
MS-BG	15.251	9.24	+4.1	+6.1
MS-BG	15.226	9.23	+4.6	+6.8
MS-BG	15.253	9.24	+4.3	+6.4
MS-BG	15.241	9.24	+4.0	+6.0
MS-BG	15.285	9.26	+3.8	+5.7
MS-BG	15.098	9.15	+4.3	+6.3
MS-BG	15.039	9.11	+3.9	+5.8
MS-BG	15.172	9.19	+3.8	+5.7
MS-BG	15.050	9.12	+3.9	+5.9
MS-BG	15.246	9.24	+4.3	+6.3
MS-BG	15.175	9.20	+4.1	+6.1
MS-BG	15.242	9.24	+3.8	+5.7
Avg ± stds	**15.211 ±0.093**	**9.22 ± 0.06**	**+4.1 ± 0.3**	**+6.1 ± 0.3**
MS-BG	13.014	7.89	+3.4	+6.1
MS-BG	13.034	7.90	+4.6	+7.6
MS-BG	13.085	7.93	+4.0	+6.8
MS-BG	13.075	7.92	+3.5	+6.2
MS-BG	13.039	7.90	+3.9	+6.7
MS-BG	13.031	7.90	+3.8	+6.6
MS-BG	13.020	7.89	+4.1	+7.0
MS-BG	13.011	7.88	+3.6	+6.3
MS-BG	13.006	7.88	+3.6	+6.3

(Table III-8 continued)

MS-BG	13.052	7.91	+3.7	+6.5
MS-BG	13.062	7.92	+3.6	+6.4
MS-BG	13.034	7.90	+4.2	+7.1
MS-BG	13.011	7.89	+3.2	+5.8
MS-BG	13.038	7.90	+3.4	+6.1
Avg ± stds	**13.037 ± 0.024**	**7.90 ± 0.02**	**+3.8 ± 0.4**	**+6.5 ± 0.5**

Note:

Errors are based on standard deviations (1σ).

Table III-9. CF-IRMS analysis with lichens, calibrated by sulphate (NBS-127) and sulphide (MUN-Py) standards.

Samples	Weight (mg)	S (µg)	$\delta^{34}S_{raw}$ (‰)	$\delta^{34}S_{CDT}$ (‰)
MS-BG	9.030	5.47	+3.6	+6.4
MS-BG	9.045	5.48	+4.4	+7.4
MS-BG	9.038	5.48	+4.2	+7.1
MS-BG	9.041	5.48	+3.9	+6.8
MS-BG	9.061	5.49	+3.2	+5.8
MS-BG	9.083	5.50	+3.5	+6.3
MS-BG	9.069	5.50	+3.7	+6.5
MS-BG	9.035	5.48	+4.4	+7.3
MS-BG	9.036	5.48	+3.6	+6.4
MS-BG	9.091	5.51	+4.1	+7.0
MS-BG	9.084	5.50	+3.5	+6.2
MS-BG	9.049	5.48	+4.2	+7.1
MS-BG	9.073	5.50	+3.2	+5.9
MS-BG	9.007	5.46	+4.8	+7.8
Avg ± stds	**9.053 ± 0.024**	**5.49 ± 0.02**	**+3.9 ± 0.5**	**+6.7 ± 0.6**

Note:

Errors are based on standard deviations (1σ).

Table III-10. CF-lichen analysis applied to different lichen species.

Sample	Weight (mg)	S (µg)	$\delta^{34}S_{raw}$ (‰)	$\delta^{34}S_{CDT}$ (‰)
MS-PN-09	14.967	6.95	+12.5	+16.6
MS-PN-09	14.846	6.89	+12.4	+16.4
MS-PN-09	14.835	6.89	+11.9	+15.8
MS-PN-09	14.372	6.67	+11.8	+15.7
MS-PN-09	14.944	6.94	+12.5	+16.6
MS-PN-09	14.750	6.85	+11.9	+15.8
MS-PN-09	14.943	6.94	+12.0	+15.9
MS-PN-09	14.887	6.91	+12.3	+16.3
MS-PN-09	14.828	6.88	+12.0	+15.9
MS-PN-09	14.944	6.94	+12.4	+16.4
MS-PN-09	14.670	6.81	+12.1	+16.0
MS-PN-09	14.689	6.82	+11.0	+14.7
MS-PN-09	14.985	6.96	+11.8	+15.7
MS-PN-09	14.915	6.93	+11.4	+15.2
Avg ± stds	**14.827 ± 0.165**	**6.88 ± 0.08**	**+12.0 ± 0.4**	**+15.9 ± 0.5**
AG-214	15.632	5.84	+7.8	+10.6
AG-214	15.559	5.82	+7.9	+10.7
AG-214	15.412	5.76	+7.1	+9.8
AG-214	15.433	5.77	+7.0	+9.7
AG-214	15.597	5.83	+7.6	+10.3
AG-214	15.251	5.70	+7.1	+9.8
AG-214	15.413	5.76	+7.0	+9.7
AG-214	15.503	5.80	+7.7	+10.5
AG-214	15.363	5.74	+6.5	+9.0
AG-214	15.613	5.84	+8.4	+11.4

(Table III-10 continued)

AG-214	15.572	5.82	+6.4	+8.9
Avg ± stds	**15.486 ± 0.121**	**5.79 ± 0.05**	**+7.3 ± 0.6**	**+10.0 ± 0.8**
AG-017	15.018	6.39	+3.9	+5.8
AG-017	15.017	6.39	+4.0	+5.8
AG-017	15.219	6.48	+3.3	+5.0
AG-017	15.173	6.46	+2.7	+4.2
AG-017	15.103	6.43	+4.0	+5.9
AG-017	15.173	6.46	+3.5	+5.2
AG-017	15.113	6.43	+2.8	+4.4
AG-017	15.025	6.39	+3.7	+5.5
AG-017	15.220	6.48	+3.8	+5.7
AG-017	15.270	6.50	+3.9	+5.7
AG-017	15.050	6.41	+3.4	+5.2
AG-017	15.152	6.45	+3.4	+5.1
AG-017	15.192	6.47	+3.9	+5.7
Avg ± stds	**15.133 ± 0.085**	**6.44 ± 0.04**	**+3.5 ± 0.4**	**+5.3 ± 0.5**

Note:

Sulphate standards (NBS-127, $BaSO_4$ #10) were used as calibration standards.

Errors are based on standard deviations (1σ).

Table III-11. Minimum S amount for CF-mineral analysis (single analysis).

Sample	Weight (mg)	S (µg)	$\delta^{34}S_{raw}$ (‰)
NBS-127	0.263	36.53	+16.0
NBS-127	0.238	33.06	+15.7
NBS-127	0.240	33.33	+15.8
NBS-127	0.222	30.83	+15.8
NBS-127	0.221	30.69	+15.8
NBS-127	0.200	27.78	+15.8
NBS-127	0.200	27.78	+16.0
NBS-127	0.179	24.86	+16.2
NBS-127	0.178	24.72	+15.6
NBS-127	0.158	21.94	+16.1
NBS-127	0.160	22.22	+16.3
NBS-127	0.145	20.14	+16.2
NBS-127	0.141	19.58	+15.9
NBS-127	0.117	16.25	+15.3
NBS-127	0.119	16.53	+16.2
NBS-127	0.102	14.17	+16.2
NBS-127	0.103	14.31	+15.7
NBS-127	0.089	12.36	+16.1
NBS-127	0.092	12.78	+16.6
NBS-127	0.082	11.39	+15.8
NBS-127	0.083	11.53	+16.4
NBS-127	0.068	9.44	+14.8
NBS-127	0.068	9.44	+15.8
NBS-127	0.060	8.33	+15.7
NBS-127	0.059	8.19	+16.8
Avg ± stds			**+15.9 ± 0.4**

Note:

Error is based on standard deviation (1σ).

Table III-12. Minimum S amount for CF-lichen analysis (single analysis).

Sample	Weight (mg)	S (µg)	$\delta^{34}S_{raw}$ (‰)	$\delta^{34}S_{CDT}$ (‰)
MS-BG	15.094	9.15	+3.9	+6.6
MS-BG	14.175	8.53	+4.1	+6.8
MS-BG	13.059	7.91	+4.5	+7.3
MS-BG	13.039	7.90	+3.9	+6.6
MS-BG	12.100	7.33	+3.6	+6.2
MS-BG	11.036	6.69	+4.2	+7.0
MS-BG	10.075	6.11	+3.2	+5.7
MS-BG	9.024	5.47	+3.7	+6.4
MS-BG	8.031	4.87	+4.2	+6.9
MS-BG	7.045	4.27	+3.6	+6.2
MS-BG	6.033	3.66	+3.7	+6.3
MS-BG	5.070	3.07	+3.4	+5.9
Avg ± stds			**+3.8 ± 0.4**	**+6.5 ± 0.5**

Note:

Errors are based on standard deviations (1σ).

Table III-13. Memory effect test on mineral analysis.

Sample	Weight (mg)	S (µg)	$\delta^{34}S_{raw}$ (‰)	$\delta^{34}S_{CDT}$ (‰)
NBS-123	0.116	38.67	+12.7	+17.1
NBS-123	0.120	40.00	+12.8	+17.3
NBS-123	0.115	38.33	+13.1	+17.7
MUN-Py	0.091	50.56	+0.2	+1.3
MUN-Py	0.081	45.00	0.0	+1.1
MUN-Py	0.096	53.33	-0.1	+1.0
NBS-123	0.112	37.33	+13.1	+17.6
MUN-Py	0.084	46.67	-0.1	+0.9
MUN-Py	0.094	52.22	-0.3	+0.6
MUN-Py	0.084	46.67	-0.1	+0.9
NBS-123	0.107	35.67	+13.2	+17.7
MUN-Py	0.083	46.11	+0.1	+1.2
MUN-Py	0.078	43.33	-0.0	+1.0
MUN-Py	0.096	53.33	0.0	+1.1

Note:

Sulphate standards (NBS-127, $BaSO_4$ #10) were used as calibration standards.

Table III-14. Memory effect test on lichen analysis.

Sample	Weight (mg)	S (µg)	$\delta^{34}S_{raw}$ (‰)	$\delta^{34}S_{CDT}$ (‰)
MS-PN-09	14.773	6.86	+10.0	+14.6
MS-PN-09	14.910	6.92	+10.9	+15.8
MS-PN-09	14.909	6.92	+11.3	+16.2
MS-BG	11.014	6.67	+3.7	+6.7
MS-BG	11.081	6.72	+4.4	+7.6
MS-BG	10.993	6.66	+3.0	+5.8
MS-BG	11.039	6.69	+4.0	+7.1
MS-PN-09	14.776	6.86	+11.3	+16.3
MS-PN-09	14.774	6.86	+11.4	+16.4
MS-BG	11.089	6.72	+3.8	+6.8
MS-BG	11.108	6.73	+4.3	+7.4
MS-BG	11.092	6.72	+4.0	+7.0
MS-PN-09	14.830	6.88	+10.0	+14.6
MS-PN-09	14.615	6.78	+10.9	+15.8
MS-PN-09	14.639	6.79	+10.6	+15.5
MS-BG	10.979	6.65	+3.6	+6.5
MS-BG	11.036	6.69	+3.6	+6.6

Note:

Sulphate standards (NBS-127, $BaSO_4$ #10) were used as calibration standards.

APPENDIX IV

CALCULATION OF S CONCENTRATION IN OLD/YOUNG PORTIONS OF LICHEN STRANDS

Example: sample CBC-D1-2 of Table V-2, Appendix V

I Calculation of the S concentrations in BBOT samples.

Samples	Weight (mg)	Peak area (Vs)[2]	S (μg)[3]
BBOT[1]	0.668	33.69	49.76
BBOT	0.639	32.95	47.60
BBOT	0.626	32.24	46.78
Avg ± stds[4]		**32.96 ± 0.73**	**48.05 ± 1.54**

Note:

1 BBOT ($C_{26}H_{26}N_2O_2S$) is an organic material with 7.45% S.
The molecular weight of BBOT is 430.56 g.

2 Peak area of mass 64. Vs = voltage × second.

3 S concentration in BBOT samples (in μg)

$$= (wt.\ of\ sample,\ mg) \times (0.0745) \times (\frac{1000\ \mu g}{1\ mg})$$

4 Errors are based on standard deviations (1σ).

II Calculation of the S concentrations in old and young portion samples.

Sample	Weight (mg)	Peak area (Vs)[2]	S (μg)[3]	S (ppm)[4]	Avg ± stds (ppm)[5]
CBC-D1-2-O[1]	15.152	3.24	4.72	311.74	
CBC-D1-2-O	15.053	3.09	4.50	299.26	
CBC-D1-2-O	15.309	3.27	4.77	311.39	**307.46 ± 7.11**
CBC-D1-2-Y[1]	15.030	10.18	14.84	987.41	
CBC-D1-2-Y	15.247	10.90	15.89	1042.20	
CBC-D1-2-Y	15.183	11.30	16.47	1085.00	**1038.21 ± 48.92**

Note:

1 O and Y represent old and young portion, respectively.

2 Peak area of mass 64. Vs = voltage × second.

3 S concentration of old and young portion samples (in μg)[3]

$$= \frac{(\textit{Avg. S concentration of BBOT, } \mu g) \times (\textit{peak area of lichen portion sample, Vs})}{(\textit{Avg. peak area of BBOT, Vs})}$$

$$= \frac{(48.05\ \mu g) \times (\textit{peak area of lichen portion sample, Vs})}{(32.96\ \textit{Vs})}$$

4 S concentration of old and young portion samples (in ppm)

$$= \frac{(\textit{S concentration of lichen portion sample, } \mu g) \times (1000\ \textit{mg})}{(\textit{wt. of lichen portion sample, mg}) \times (1\ \textit{g})}$$

5 Errors are based on standard deviations (1σ).

APPENDIX V

DATA SUMMARY OF CHAPTER 5

Table V-1. Old/young portion and bulk analyses (site-B, CBC).

Sample	Weight (mg)	S (ppm)[1]	$\delta^{34}S_{raw}$ (‰)	$\delta^{34}S_{CDT}$ (‰)
B4-1-O#	15.485	490.81	+4.3	+6.6
B4-1-O	15.561	452.72	+3.6	+5.7
B4-1-O	12.162	430.23	+3.7	+5.8
Avg ± stds	**14.403 ± 1.941**	**457.92 ± 30.62**	**+3.8 ± 0.4**	**+6.0 ± 0.5**
B4-1-Y#	15.155	1887.36	+4.0	+6.2
B4-1-Y	15.521	1824.03	+4.2	+6.5
B4-1-Y	15.226	1811.37	+3.9	+6.1
Avg ± stds	**15.301 ± 0.194**	**1840.92 ± 40.72**	**+4.0 ± 0.2**	**+6.3 ± 0.2**
B5-1-O	15.542	636.65	+3.8	+6.0
B5-1-O	15.528	638.17	+3.1	+5.0
B5-1-Y	15.295	2044.01	+3.2	+5.2
B5-1-Y	15.319	2152.43	+3.4	+5.5
B-Bulk	15.054	1063.63	+2.7	+5.0
B-Bulk	15.126	1055.78	+3.0	+5.4
B-Bulk	15.069	1026.22	+3.1	+5.5
B-Bulk	15.225	1015.70	+2.6	+4.9
B-Bulk	15.095	1009.56	+2.8	+5.2
B-Bulk	15.135	992.05	+2.3	+4.6
B-Bulk	15.087	984.03	+3.1	+5.6
Avg ± stds	**15.113 ± 0.057**	**1020.64 ± 30.04**	**+2.8 ± 0.3**	**+5.2 ± 0.4**

Note:

Sulphate standards (NBS-127, $BaSO_4$ #10) were used as calibration standards.

O and Y represent old and young portions, respectively.

1 S concentration calculated by analyzing an organic material with known S concentration (BBOT, 7.45% S) by CF-IRMS and comparing the mass 64 peak area of the sample with the average mass 64 peak area of replicate BBOT analyses (see Appendix IV). Errors are based on standard deviations (1σ).

Table V-2. Old/young portion and bulk analyses (site-D, CBC).

Sample	Weight (mg)	S (ppm)[1]	$\delta^{34}S_{raw}$ (‰)	$\delta^{34}S_{CDT}$ (‰)
D1-1-O#	15.361	159.44	+4.8	+6.9
D1-1-O	15.024	150.40	+5.8	+8.1
D1-1-O	15.056	139.43	+5.4	+7.7
D1-1-O	15.368	139.45	+4.2	+6.2
Avg ± stds	**15.202 ± 0.188**	**147.18 ± 9.67**	**+5.0 ± 0.7**	**+7.2 ± 0.9**
D1-1-Y#	15.180	538.77	+3.6	+5.5
D1-1-Y	15.072	587.12	+3.6	+5.4
D1-1-Y	15.163	611.48	+3.3	+5.1
Avg ± stds	**15.138 ± 0.058**	**579.12 ± 37.01**	**+3.5 ± 0.2**	**+5.3 ± 0.2**
D1-2-O	15.152	311.74	+5.8	+8.1
D1-2-O	15.053	299.26	+4.5	+6.6
D1-2-O	15.309	311.39	+5.6	+7.9
Avg ± stds	**15.171 ± 0.129**	**307.46 ± 7.11**	**+5.3 ± 0.7**	**+7.6 ± 0.8**
D1-2-Y	15.030	987.41	+3.6	+5.4
D1-2-Y	15.247	1042.20	+3.9	+5.8
D1-2-Y	15.183	1085.00	+4.2	+6.1
Avg ± stds	**15.153 ± 0.112**	**1038.21 ± 48.92**	**+3.9 ± 0.3**	**+5.8 ± 0.4**
D1-3-O	15.165	145.16	+6.2	+8.7
D1-3-O	15.058	133.60	+6.4	+8.9
D1-3-Y	15.140	692.33	+4.2	+6.2
D1-3-Y	15.454	709.39	+4.1	+6.1

(Table V-2 continued)

D3-1-O	15.092	231.83	+6.3	+8.7
D3-1-O	15.230	201.97	+5.6	+7.9
D3-1-O	15.226	218.30	+5.1	+7.3
D3-1-O	15.374	222.84	+5.0	+7.2
Avg ± stds	**15.231 ± 0.115**	**218.74 ± 12.51**	**+5.5 ± 0.6**	**+7.8 ± 0.7**
D3-1-Y	15.205	467.89	+4.8	+6.9
D3-1-Y	15.085	496.74	+5.0	+7.1
D3-2-O	15.264	189.11	+6.8	+9.4
D3-2-O	15.227	180.95	+5.8	+8.1
D3-2-O	15.472	179.97	+7.5	+10.3
Avg ± stds	**15.321 ± 0.132**	**183.34 ± 5.02**	**+6.7 ± 0.9**	**+9.3 ± 1.1**
D3-2-Y	15.017	749.45	+5.0	+7.1
D3-2-Y	12.396	755.03	+5.7	+8.0
D5-1-O	15.542	171.15	+5.2	+7.8
D5-1-O	15.551	141.92	+5.9	+8.6
D5-1-O	15.580	144.47	+5.6	+8.3
Avg ± stds	**15.558 ± 0.020**	**152.51 ± 16.19**	**+5.6 ± 0.3**	**+8.2 ± 0.4**
D5-1-Y	15.076	702.87	+4.0	+6.3
D5-1-Y	15.309	739.90	+3.7	+5.9
D5-1-Y	15.641	738.22	+3.6	+5.7
Avg ± stds	**15.342 ± 0.284**	**727.00 ± 20.91**	**+3.8 ± 0.2**	**+5.9 ± 0.3**
D7-2-O	15.056	211.63	+6.8	+9.8
D7-2-O	15.062	172.73	+6.7	+9.7
D7-2-O	15.407	178.34	+7.0	+10.1
D7-2-O	15.529	169.41	+7.6	+10.9
D7-2-O	15.658	169.89	+7.3	+10.5
Avg ± stds	**15.342 ± 0.274**	**180.40 ± 17.81**	**+7.1 ± 0.4**	**+10.2 ± 0.5**

(Table V-2 continued)

D7-2-Y	15.632	585.30	+5.0	+7.5
D7-2-Y	15.100	584.63	+5.5	+8.2
D7-2-Y	14.977	618.71	+4.3	+6.7
D7-2-Y	15.034	638.72	+4.6	+7.1
Avg ± stds	**15.186 ± 0.302**	**606.84 ± 26.55**	**+4.9 ± 0.5**	**+7.4 ± 0.7**
D-Bulk	15.538	284.43	+3.9	+6.4
D-Bulk	15.547	269.10	+4.1	+6.6
D-Bulk	15.558	267.97	+4.4	+7.0
D-Bulk	15.481	268.35	+4.8	+7.6
D-Bulk	15.443	275.69	+3.8	+6.3
D-Bulk	15.415	279.05	+4.1	+6.7
D-Bulk	15.454	278.35	+3.1	+5.3
Avg ± stds	**15.491 ± 0.057**	**274.70 ± 6.39**	**+4.0 ± 0.5**	**+6.6 ± 0.7**

Note:

Sulphate standards (NBS-127, $BaSO_4$ #10) were used as calibration standards.

[#] O and Y represent old and young portions, respectively.

1 S concentration calculated by analyzing an organic material with known S concentration (BBOT, 7.45% S) by CF-IRMS and comparing the mass 64 peak area of the sample with the average mass 64 peak area of replicate BBOT analyses (see Appendix IV). Errors are based on standard deviations (1σ).